THE EFFECT OF NON-UNIFORM FLOW ON HEAT TRANSFER COEFFICIENT OF A CYLINDER WALL

A Thesis
Submitted to the College of Engineering
of AL-Nahrain University in partial
Fulfillment
of the Requirements for the
Degree of Master of Science
In Mechanical Engineering

By

Fady Sabah Al-kuraishy

(B.Sc. in Mechanical Engineering 2001)

Rajab	**1425**
September	**2004**

Abstract

The present study has been carried out to investigate the problem of heat transfer by force convection as unsteady state conduction ((i.e. lumped-capacitance system)) from the out side surface of horizontal cylinder in cross flow of air was studied. Experimental works were involved for this purpose. The cylinder is closed ended and heat insulated, circular in cross-section and its internal surface dissipates heat uniformly (constant heat flux).

The cylinder is placed in rectangular wind tunnel that was used for the experimental tests having length equal to (244 cm) with inlet and outlet cross- section areas equal to (6.25*12.5 cm) and (6.25*25 cm) respectively and Reynold's number is ($Re = 6*10^5$). The section area of the wind tunnel diverges downstream from the inlet position at a distance equals to (160 cm) from its entery. One cylinder of aluminum for different cylinder positions were used, di [illegible] cylinder length is 6.7 cm and thickness o [illegible] placed at 6.5 cm from the discontinuous wall.

Ten sets of reference temperature (T_o) were used for each cylinder position (Y =3.7, 7.75, 15.25, 19 cm). From Appendix (A), one of fife test section at (θ =90) is used and one node of twelve thermocouple nodes at ($\theta = 90$) on the cylinder to measure surface temperature were used.

The experimental results were made in the form of temperature vs time interval (t). The computational results were made by a package program (MATLAP 6.1) from the experimental results in this study. This package is focused on calculating heat transfer coefficient, Nusselt number, Temperature ratio, time ratio.

It was concluded that the rate of decreasing in surface temperature of cylinder (T) with time interval (t) will be increased as reference temperature (T_o =150, 140, 130, 120, 110, 100, 90, 80, 70, 60 C^o) is increased and cylinder position (Y=3.7, 7.75, 15.25, 19 cm) is decreased. At some reference temperature (T_o =150, 140, 130, 120, 110, 100, 90, 80, 70, 60 C^o) and cylinder position (Y=3.7, 7.75, 15.25, 19 cm), heat transfer coefficient and Nusselt number was found to increase with time interval (t). Finally, heat transfer coefficient and Nusselt number will be increased as cylinder position (Y=3.7, 7.75, 15.25, 19 cm) is decreased.

Chapter One

Introduction

1.1 Introduction

Heat transfer between solid and a surrounding fluid will be investigated under unsteady state conditions. Experimental data will be collected for aluminum cylinder heated or cooled by forced or natural convection. If a solid body is suddenly subjected to a change in environment, some time must elapse before an equilibrium temperature condition will prevail in the body. The equilibrium condition was referred as the steady state and calculated the temperature distribution and heat transfer by methods described in Chaps. 2 and 3.In the transient heating or cooling process which takes place in the interim period before equilibrium is established. The analysis must be modified to take into account the change in internal energy of the body with time, and the boundary condition must b [illegible] situation which is apparent in the unst [illegible] Unsteady-state transfer analysis is obviously of significant practical interest because of the large number of heating and cooling process, which must be calculated, in industrial application [1]. The data will be analyzed to estimate heat transfer coefficient and thermal conductivity of aluminum cylinder. If the rate of heat flow and the temperature at any point of a system change with time, the conduction is termed “unsteady state”. The temperature may vary both in time and space. However, in general only consider with temperature that vary in one space dimension. The heat equation for one dimensional unsteady conduction in Cartesian coordinate with uniform thermal conductivity is

$$\frac{\partial^2 T}{\partial x^2} = \frac{1}{\alpha}\frac{\partial T}{\partial t}$$

There is experience in math courses on how to solve this system for simple boundary conduction. However, these solutions are cumbersome and require infinite series. There are two engineering shortcuts often used to get around using such heavy math. They are

1. Lumped capacitance simplification ($\partial / \partial x = 0$)
2. Solution table for simple shapes

When a heated (or cooled) substance is immersed in a bath having different temperature, heat transfer takes place. Heat is conducted throughout the substance, and convection occurs at the surface. There are different ways to model this unsteady problem, depending on the relative magnitude of the convection coefficient and the thermal conductivity of the material. In this experiment, unsteady temperature versus time is measured for a material, and the convection coefficient is calculated. The results are then used with Heisler chart in order to predict the expected temperature, and the results are compared. Continue discussion of transi[illegible] [illegible] which may be considered unifo[illegible] analysis is called the lumped-heat-capacity method. Such systems are obviously idealized because a temperature gradient must exist in a material if heat is to be conducted into or out of the material. In general, the smaller the physical size of the body is the more realistic is the assumption of a uniform temperature throughout; in the limit a differential volume could be employed as in the derivation of the general heat-conduction equation. For many systems the thermal conductivity resistance is low compared to other resistance in the system. Consider the cooling of a metal bar by a jet of air. Intuitive understanding of heat transfer was known so far that the upstream side will be hotter than the downstream side. More importantly, that the inside will be hotter than the outside. Many industrial problems of heat transmission come under this class of heat flow. One familiar example is the flow of heat through a building wall during the daily twenty-four hours heating and cooling cycle. Other examples include the annealing of casting burning of bricks and the heating and cooling of slabs and furnace wall sections.

1.2 Objective

1. The objective of the present work is to carry out a experimental analysis for the heat transfer coefficient from cylinder wall at a range of reference temperatures (To) and for different cylinder position to obtain the results shall be illustrated in chart form to explain transient conduction (i.e. unsteady state conduction).
2. The air flow behavior on the variation of heat transfer coefficient and rate of heat transfer with time and cylinder position from cylinder wall.
3. In future, this research will give more information for the students who they work in the same direction [illegible] boundary condition.

Chapter Two

Literature Survey

2.1 Introduction

As mention in the introduction the published work on heat transfer by transient zone duct in from outside surface of cylinder and different shapes to air flow is limited. A summary of this work is given here.

2.2 Previous Work

Remn-Min Guo [4] studied a two-dimensional transient thermal behavior of work rolls in rolling process. In rolling process, large amount of heat generated in the roll bite transfers to work rolls and strip. Work rolls are cooled by cooling medium in both entry and exit sides of the mill. Transient cooling behavior of the roll affects temperature distribution and thermal profile. This article proposes a semi-analytical solution to solve temperature field of the work roll, which is subjected [illegible] boundary conditions. Lap lace and inverse [illegible] the unsteady solution for one boundary condition. The complete solution for various boundary conditions is superimposed by related Individual solutions using Duhamel's rule. Case studies as demonstrated show versatility of the developed model. They concluded theta two-dimension transient model has been introduced to solve thermal characteristics of the work roll in rolling process. Lap lace transform, Cauchy's residual theory, and Duhamel's rule are applied to achieve the analytical solution. Boundary conditions are considered to embrace all combinations of current mill operations. The model was designed not only for theoretical investigation but also for future on-line control. Practical application requires identifying the roll-bite heat equation, which is a function of rolling force, mill speed, forward slip, and strip material. Case studies as demonstrated in the article show that the heat generated in the roll bite could penetrate into the roll center before the roll reaches the steady state. In cycles of rolling and idling processes, a critical line in the radial direction separates transient temperature field into two zones. The inner zone, which has the majority of the radius, exhibits continuous temperature gain. The thin-layer outer zone has a temperature fluctuation. As mentioned before, if the temperature field is not of importance in the real-time application, thermal profiles can be calculated directly bypassing the lengthy calculation of temperature field. Hence this two-dimensional solution may provide better accuracy with acceptable computing time. The future research work should concentrate on improvement of computing efficiency and determination of the roll-bite heat Equation. It is interesting to compare the results produced by various methods such as one dimensional model, finite difference model, and this two dimensional model. Accuracy and computing time are two key factors.

M. [illegible]ka & [illegible] inverse heat conduction method for high [illegible] inverse heat conduction task was developed. The task uses classical minimization method in combination with optimization method. The method was developed for the very steep changes of the measured temperature and the demand on precise results. Typical industrial applications are in decaling (removing oxides from steel surface by high energetic spray). The minimization method is used as a basic method. The precision of this method is improved in the area of big temperature gradients by combination with optimization method. The peaks of HTC of heat flux are computed precisely afterwards. They concluded that the combination of two numerical methods allows increasing precision of inverse calculation. The results of minimization method using several forward time steps are improved by optimization method in area of sharp changes of heat transfer coefficient. The method allows evaluating long temperature records. Optimization method is applied only locally. The new investigative approach does not have the negative impact on stability of inverse task.

A. F. Emery [6] studied the transient and steady state free convection from a horizontal cylinder. Estimating parameters in steady state, homogeneous a system is a well-developed process, usually involving the least squares technique or the Bayesian statistical approach. The Forward Variable method was developed to estimate time varying surface fluxes for inverse heat conduction problems. Electrical and systems engineers tend to utilize the Kalman filter approach in such situations. The two approaches have much in common and the Kalman filter can often be applied to conduction/convection problems. It is particularly useful when multiple parameters vary with time. They described the application of both methods to the problem of transient and steady state free convection from a horizontal cylinder. The problem involves noisy data [illegible] time variation of the heat transfer coefficien[illegible] and compare the resulting estimates of the parameters. They compared the use of the forward variable approach [1] with the extended Kalman filter method in the estimation of the convective heat transfer coefficient for free convection from a horizontal cylinder. They concluded that the use of the Kalman filter made it possible to track the history of the uncertainties and to determine the times when the heat transfer coefficient was most poorly estimated. By then expanding the state variables to include losses and imprecision in the estimate of the stored energy we were able to that the difficult was most probably due to interfacial resistance. When the resistance was reduced, substantially better results were obtained. The Kalman filter approach is not a total panacea for problems like this. In analyzing the results and predicting the History of h, both the forward variable and Kalman filter approaches estimated the temperature history of the cylinder very well as Evidenced by the very small values of σT, being in the order of 0.05C. In this case, the results of the cfd simulation and the correlation make it clear that the inverse estimation of the first experiment, and even that of the second at early times, is significantly in error. Once again reinforcing the idea that one must know much about the problem and must design the experiment carefully before conducting it.

Wing [7] have carried out blow down tests and presented results which showed the histories of pressure, surface temperature and heat transfer coefficient. The surface temperature results indicated that as long as nucleate boiling is established on the rod surface, the thermal properties of the material in the test rod are unimportant, because the heat transfer coefficient due to nucleate boiling on the rod surface is larger compared to th[illegible] gap conducted and thermal conductance of the test rod material.

[illegible] R. [illegible], R.C.S. [illegible] [illegible] [8] carried out The evaluation [illegible] temperature thermo resistive Sensor based feedback circuit, excited by a pulse width modulated (PWM) waveform is done by a way of simulation studies in PSPICE environment and compared with that of a circuit excited by an analog voltage (continuous time domain). For a thermo resistive sensor with an intrinsic time Constant much larger than the period of the PWM waveform, the degradation the response time of the PWM circuit is negligible and they concluded that The evaluation of response time of constant temperature feed-back circuits employing a thermo resistive sensor has been done for two different circuit configurations, one operating in con-tenuous time domain and other employing a PWM voltage to heat the sensor. The simulation studies done in the PSPICE environment show that for given parameters, the settling time in the discrete time circuit increases as the PWM frequency decreases.

The results also show that the discrete CTC be-comes Unstable when PWM period approaches the sensor in-transitive constant. The introduction of the pulse width modulator in the feedback loop linearizes the input-output transfer characteristics, but the circuit complexity is increased. The use of digital circuits to generate the PWM waveform gives versatility to the measure-men instrument. To reduce the circuit's complexity, a fast comparator may replace the operational amplifier and the A/D converter and a digital control algorithm implemented by software in an inexpensive micro controller.

Donea [9] discussed three numerical integration schemes connected with a FE solution to the transient heat conduction problems. The main emphasis was on the achievable accuracy. He conducted that if only initial and final states are considered in time region, the Galarkin process provide a convenient scheme for time integration of fast-varying heat conduction problems. When the high frequency com[illegible] Crank-Nicholson scheme should be used to [illegible] time accuracy. Since both schemes differ only by numerical coefficients branching from one scheme to the other is an easy matter.

Brush Jr. and Zyroloski [10] used a finite Weighted Residual process to solve Transient linear and non-linear to dimensional heat conduction require constant parameters over entire solution domain, and isoperimetric element can be used. Furthermore, the method is easily programmed, stable, computationally fast, and convergence to the exact solution.

Sparrow et at [11] treated the inverse problem using the lap lace transform technique; a solution for the transformed temperature is obtained in convenient manner. In turn the two constant of integration may be eliminated by thermal symmetry requirement in recent with solids, and the internal response. At this stage the resultant temperature expression cannot be inverted, consequently a special g-function is introduced for this purpose, but unfortunately, the integral must be evaluated numerically.

Imber and Khan [12] tried to solve a non-dimensional IHC, using a measured data from several interior thermocouples, and making an extrapolation to the surface by a curve- fitting procedure. Clearly this method is undesired since for large surface the temperature gradient are significant in the vicinity of the boundary and the curve-fit cannot affect this behavior.

Burggraf [13] their found the exact solution for the instantaneous surface heat flux for a given continuous temperature and heat flux histories at given internal point. When Burggraf's equation is utilized with discrete or experimental data, the results are also approximate.

Osman and Beck [14] used Sequential future information Method (SFIM) for solving non-linear two-dimensional inverse heat transfer coefficient problem (IHTCP). He suggested that the estimation of the [illegible] at a time [illegible] must depended not only on the data up to t[illegible] steps. The use of temperature future information and least squares is sable for the solution of IHCP.

Beck [15] used the function specification Method (FSM) for solving the time inverse problems. The FSM has two such features that it lets problems that are parabolic remain almost parabolic and that linear problem remains linear. Furthermore, this method can be used for convolution integral equation and various inverse boundary or volumetric source problems in diffusion that are formulated using partial differential equation.

Beck [16] used the FDM to present a suitable method for treating problems with non-linear thermal problems. He assumed that the material properties during a very small time interval is constant, also his method depends upon the number of data (temperature or heat flux) measurements.

Majeed [17] introduced a comprehensive FE package, which is capable to analyze both steady and transient heat conduction problems. This package has been used to solve thee dimensional, two dimensional and ax symmetrical heat conduction problems. The influence of composite material, the heat generation, and the nonlinearity of material properties has been taken in consideration while construction his package. He also discusses the general definition of the inverse method using FE analysis.

Martin et al [18] uses the inverse boundary element method procedure to determine the unknown heat transfer coefficient on the surface of arbitrary shaped solids. The procedure that he used is non-iterative and cost effective, involving only a simple modification to any existing steady-state heat conduction BEM algorithm.

Jafar.M.H [19] designed an experimental system and installed in the reactor building, to investigation the depressurization effects in an annular test section. Liquid Freon 113 was chosen [illegible] transfer occurring in light water nuclear rea[illegible] used with maximum operation pressure pf 193.9 kN/m^2 and the test condition covers a range of initial circulation velocities up to .55 m/sec. The maximum value of electrical heat supply to the test section was 1800 watt. Continuous recording were made of pressure, temperature at the test section during a sudden pressure reduction process. Thermodynamic non-equilibrium was found experimentally from measuring both the pressure and temperature of the coolant at the outlet of the test section during the blow down. The local heat transfer coefficient was found to increase throughout the blow down. The local surface temperature of the inner heated rod of the annular test section decreased during the transient mainly due to the agitation and turbulence in the bulk of the flowing Liquid as a result of bubble formation.

Nabras.H.G [20] investigated for the calculation of the temperature and heat flux distribution effect for the steady and transient case for a rocket engine case. This is done by using two numerical methods, Finite Element method and boundary element method. The use of these two methods were classified into two parts, in the first one the domain of the rocket engine case was treated as a direct problem in which all the boundary condition are known, while in the second one the domain was treated again but with consideration it as an inverse problem, where the temperature measurements are made at the outer surface of the rocket engine so as to predict the inner wall condition. The inverse technique was also used to predict the heat transfer and physical properties such as the heat transfer coefficient, thermal conductivity of the material. The results showed that the boundary Element method algorithm is more accurate in most cases than finite Element method. Comparison of the studied cases with exact and published results showed good agreement.

Foots [21] used the approximate i[illegible] theory in fluid dynamics to obtain information a heat conduction problems involving a moving two-dimensional solidification front. The sample treated in his investigation is solidification of a uniform prism having a square cross sectional and filled with liquid initially at its fusion temperature. His results about the location and time history of the front are in good agreement with other published results.

Beaubouef [22] analyzed the freezing of the solid phase from fluid flowing past a cold surface. The time dependent local solid layer thickness and the time dependent temperature distribution in the solid phase were determine as a function of pertinent physical properties, the surface temperature and the surface convection heat flux. The latter may be a function of stream wise coordinate. He uses a numerical solution to solve the problem.

Stephan [23] calculated the solidification in flowing liquids along a plane wall pr through a pipe, with the assumption of finite ambient heat transfer, and an imposed or known heat flux to the solid-liquid interface. Very good approximate was obtained of in the solid phase a parabolic temperature distribution was is assumed which satisfies all boundary condition and agrees with energy equation only at the solid fluid interface.

Bekermann [24] studied the effect of a solid sub cooling on natural convection melting of a pure metal. He found that the solid sub cooling significantly reduces the melting rate when compared to melting with the solid at fusion temperature of, because when the cooled wall is below the fusion temperature of the metal, the solid-liquid interface eventually reaches the stationary position.

Nazar [25] numerical solution using enthalpy method with body fitted coordinate system was used for solving three-dimensional transient heat transfer [illegible] solution [illegible] ice thickness with time around three ve[illegible] insulated bath in addition to temperature distribution in solid and liquid phases. Also this solution was used to study the effect of boundary conditions on the shape and thickness of formatted ice with time. Experimental work involves building an apparatuses of three vertical circular cylinder located at staggered form in square insulated bath; ice thickness and temperature distribution with time in solid and liquid phases around each cylinder was measured.

Vick [26] studied freezing and melting with multiple phase fronts along the outside of a tube. The fluid temperature at the tube inlet cycles above and below the freezing temperature of the phase change material (PCM). Boundary element method is used to obtain a transient solution in each axial segment. Axial conduction is neglected and the problem is discredited into axial segments.

2.3 Summery

As mentioned above, there is a decrease in the information of heat transfer from cylinder wall as unsteady state conduction when the pressure inside a duct is changed, then the aim of this work is adding many information for this project.

Chapter Three

Theory

3.1 Introduction

There are two states of heat transfer from out side surface of cylinder, steady state and unsteady state. In this work, the unsteady state conduction will be studied but the steady state will be explained briefly as the following: -

While the engineer may frequently be interested in the heat-transfer characteristics of flow system inside tubes or over flat plates, equal importance must be placed on the heat transfer which may be achieved by a cylinder in cross flow, as shown in figure (3.1). When a body is held immersed in a flowing liquid, a thin layer of the liquid will [illegible] is fixed to the boundary of the body. But if the immersed body is a curved or angular one, the boundary layer does not s[illegible] of the body. The boundary layer leaves the [illegible] This phenomenon is known as boundary layer separation. The point, where the boundary layer gets separated from the surface of the body, is known as point of separation. Prandtl, after publishing his boundary layer theory, conducted series of experiments on boundary layer separation also. He held a cylinder in flowing liquid and sprinkled small particles of aluminum on the surface of the liquid. He allowed the liquid to flow around the cylinder, and found that the boundary layer has adhered to the surface of the cylinder throughout. The liquid also flowed in streamlines around the cylinder as shown in fig 12.6 (a). After this, he went on gradually increasing the velocity of liquid. After certain velocity, he found the streamlines at D started becomes irregular. On further increasing the velocity of liquid, he found that the boundary has separated from the surface on both sides of D and vortices have started to from as shown in fig 12.6 (b). He further went on increasing the velocity of liquid and found that the separation of boundary layer is taking place earlier and earlier; forming more pronounced vortices. After this, a stage came, when the separation of boundary layer took place at A and B as shown in fig 12.6 (c) [3].

Unsteady state conduction in a solid body suddenly to a change in environment has been extensively and thoroughly treated in Holman, heat transfer, McGraw Hill, 1986, chapter 4.See also chapters 6and 7 for heat transfer by forced and natural convection [1].

There are Three cases of transient conduction: -

Case 1:

Transient conduction in solid bodies with negligible internal resistance (lumped capacitance system).

Case 2:

[illegible] a semi-infini[illegible]

Case 3:

Transient conduction in infinite solid.

In this search, case one of transient conduction in solid bodies with negligible internal resistance (Lumped capacitance system) will be studied.

If a hot aluminum cylinder were immersed in a cool pan of air, the lumped-heat-capacity method of analysis might be used if an assumption of uniform cylinder temperature was justified during the cooling process. Clearly, the temperature distribution in the cylinder would depend on the thermal conductivity of the cylinder material and the heat-transfer condition from the surface of the cylinder to the surrounding fluid, i.e., the surface-convection heat-transfer coefficient. A reasonable uniform temperature distribution in the cylinder would be obtained if the resistance to heat transfer by conduction were small compared with the convection resistance at the surface, so that the major temperature gradient would occur through the fluid layer at the surface. The lumped-heat-capacity analysis, then, is one, which assumes that the internal resistance of the body is negligible in comparison with the external resistance [1].

3.2 Problem Description

The convection heat loss from a body is evidenced as a decrease in the internal energy of the body, as shown in Figure (3.2). Thus

$$q = hA(T - T\infty) = -c\rho V \frac{dT}{dt}$$

Where A is the surface area, for convection and V is the volume, the

initial condition is

$T = T_o$ at $t=0$

so that the solution is

$$\frac{T - T\infty}{T_o - T\infty} = e^{-[hA/\rho cV]\,t}$$

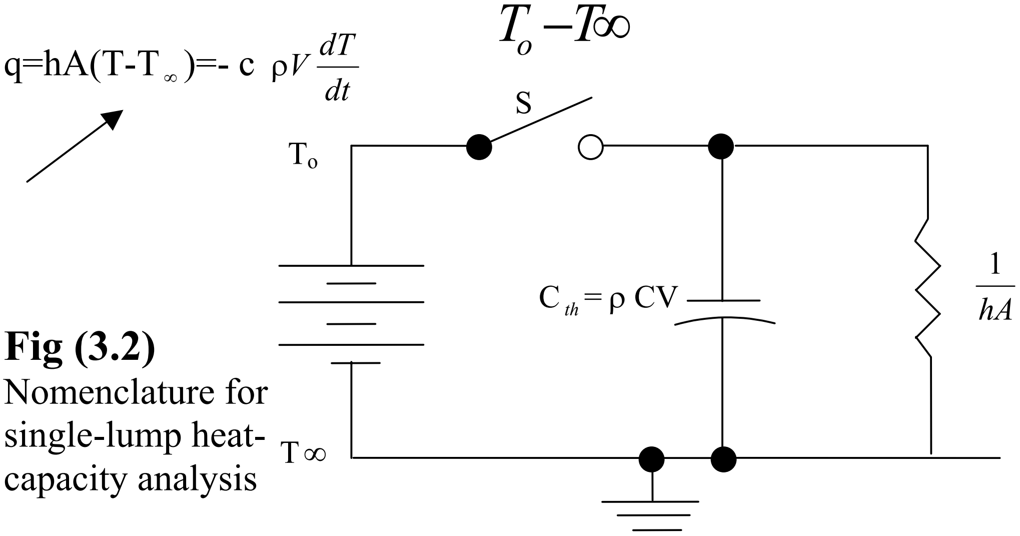

Fig (3.2)
Nomenclature for single-lump heat-capacity analysis

Where T∞ is the temperature of the convection environment. The thermal network for the single-capacity system is shown in Fig (3-2). In this network the thermal capacity of the system is "charged" initially at the potential to by closing the switch S. Then, when the switch is opened, the energy stored in the thermal capacitance is dissipated through the resistance 1/hA. The analogy between this thermal system and an electric system is apparent, and an electric system was constructed, which would behave exactly like the thermal system as long as the ratio was made

$$\frac{hA}{\rho\ cV} = \frac{1}{R_{th}C_{th}} \qquad R_{th} = \frac{1}{hA} \qquad C_{th} = \rho\ cV$$

Equal to $1/R_e C_e$, where R_e and the electric resistance and capacitance, respectively. In the thermal system, energy was stored, while in the electric system we store electric charge. The flow of energy in the thermal system is called heat, and the flow of charge is called electric current. The quantity [illegible] V/hA is called the time constant of [illegible] dimensions of time [illegible] when

$$\tau = \frac{c\rho\ V}{hA}$$

It is noted that the temperature difference T-T∞ has a value of 36.8 percent of the initial different T_o- T∞. We have already noted that the lumped-capacity type of analysis assumes a uniform temperature distribution throughout the solid body and that the assumption is equivalent to saying that the surface-convection resistance is large compared with the internal-conduction resistance. Such an analysis may be expected to yield reasonable estimates within about 5 percent when the following condition is met

$$\frac{h(V/A)}{k} < 0.1$$

Where k is the thermal conductivity of the solid. In section which we examine those situations for which this condition does not apply. We shall see that the lumped-capacity analysis has a direct relationship to the numerical methods discussed in Sec. (4-7). If one consider the ratio V/A=S as a characteristic dimension of the solid, the dimensionless group is called the Biot number

$$\frac{hS}{k} = \text{Biot number} = \text{Bi}$$

The reader should recognize that there are many practical cases where the lumped-capacity method may yield good result. Uncertainties in the knowledge of the convection coefficient of ± 25 percent are quite common, so that the condition Bi=h (V/A)/k<0.1 should allow for some leeway in [illegible] simplicity. Because of uncertainties in the convection coefficient, it may not be necessary to use more elaborate analysis techniques. If the temperature [illegible] the coo[illegible] [illegible] of the unsteady bulk temperature of the cylinder should be written [1]. In this case simple have

$$E_{in} = E_{store}$$

The rate of energy in is simply the amount of heat transfer by convection, so we use Newton's law of cooling E_{in}=hA ($T\infty$-T). The rate of heat stored is equal to the rate of change of internal energy that the thermal mass of the solid $\rho\, cV$ by the time derivation of temperature. This gives

$$hA\,(T\infty - T) = \rho\, cV \frac{\partial T}{\partial t}$$

If θ was used as define previously ($\theta = T - T\infty$), it follows that θ_o, the initial temperature difference is $\theta_o = T_o - T\infty$. Then a solution for unsteady bulk temperature would be written

$$\frac{\theta}{\theta_o} = e^{-hAt/\rho cV}$$

If it further writes $\tau = \rho cV / hA$ this becomes

$$\frac{\theta}{\theta_o} = e^{-t/\tau}$$

This definition of τ is interesting in that it contains the thermal convection resistance 1/hA and the heat capacity of the solid "thermal capacitance". Now one more re-write of the unsteady lumped capacitance can be done to give a second dimensionless time. If the equation was written

$$\frac{\theta}{\theta_o} = e^{-Bi.Fo}$$

It follow that this new variable Fo is defined as

$$Fo = \alpha t / L^2$$

This is time made dimensionless with the thermal diffusivity and a characteristic length scale. It could be called the Fourier number.

Chapter Four

Experimental Work

4.1 Description of Apparatus

At the beginning, from Appendix (A), configuration of experimental system becomes convenient to the requirements of a present study, only one of five test sections at ($\theta = 90$) is used in this work [2]. A schematic diagram and a photograph of the experiment set-up of the apparatus are shown in figs (4-1, 4-2) respectively. It consists essentially of an aluminum cylinder (2) of out side diameter (D_0) and thickness (t_c) and length (L) placed horizontally in cross flow of air with ends closed by plate of the same material. The inside surface of the cylinder is electrically heated by means of a [illegible] wire (8) (heater) of 1mm diameter, 500W (heat capacity) and 60cm length. The wire is electrically insulated by [illegible] placed uniformly along the cylinder length [illegible] the inside surface of cylinder by ceramic beads that is placed around the wire to give uniform heat flux.

Chromal-Alume thermocouples (1), referred to as type k. This type can be used in the temperature range of -200 to 1300 C^o. The thermocouple position in the wall of the cylinder was drilled with diameter of (1mm) and (3mm) deep and the thermocouples were embedded in the wall of the cylinder as shown in fig (4-1, 4-2), to measure the out side surface temperature of the cylinder at the center of length around the cylinder.

The number of thermocouples used and their position are listed in table (4-1).

The duct was slotted vertically to put the cylinder in slot position by screw that connecting to the cylinder view nut then the heater on both ends was bounded around screw, which bounded to electric source which give electric power that was required to the heater. The cylinder placed horizontally in a duct which is contains of a cross flow air on the cylinder and its heating insulated on both end by (Mica) and fixed on both ends by nut as shown in fig (4-1, 4-2). This slot was allowed a cylinder to move up or down at different positions then temperature measurement was taken.

The numbers of cylinder positions are listed in table (4-2).

4.2 Instrumentation & Measuring Devices

4.2.1 Power Supply to the Heater:

The necessary electric current was taken from the 220-v mains. The heat generated by the heater could be known by measuring the current and the voltage across the heater. The electric circu [illegible]

4.2.2 Temperature Measurement:

As mentioned before Chromal-Alume thermocouples were used to measure the temperature. They were made of 0.1mm glass covered wires. The junctions were made by fusing the ends of two wires together by means of an electric spark in an atmosphere free from oxygen. To measure the temperature of the out side surface of the cylinder, a digital thermometer was used. Selector switch connected the thermocouples to the digital thermometer. One of the junctions was connected to the selector and the other was embedded in the out side surface of the cylinder. The percent error of temperature and time measurement is 1.5%, and 5% respectively. The digital thermometer, thermocouples and selector circuit is shown in fig (4-3).

4.3 Sample of Calculation

Position of cylinder	(1), at Y=3.7cm
Diameter of cylinder	D_o=49.6mm =0.0496m
Length of cylinder	L=67mm =0.067m
The temperature of convection	T_∞=32.7C°
Initial Temperature	T_o =150C°
Attention Temperature	T =50C°
Thickness of cylinder	t_c =5mm =0.005m
The weight of cylinder	m =125gm =0.125kg
The inner diameter of cylinder (D_{in}): -	D_{in}= D_o-2t= 49.62(5)=39.6mm
The volume of cylinder (V): -	$V = \frac{\pi(D_o^2 - D_{in}^2)}{4} L$

$= \frac{\pi}{4}((0.0496)^2 - (0.0396)^2)0.067$

The density of cylinder (ρ): -

$\frac{\;}{V} \quad 0.000046938533$

$= 2663.05707 kg/m^3$

From Appendix (D-1) at (ρ=2663.05707), the specific heat (C) was found by applying the interpolation methods: -

$$\frac{2787 - 2659}{2787 - 2663.05707} = \frac{0.883 - 0.863}{0.883 - C} \Rightarrow C = 0.8675 kj/kg.C$$

Then: -

$$A = \pi D_o L = \pi\,(0.0496)(0.067) = 0.01044 m^2$$

$$c = \frac{A}{\rho C V} = \frac{0.01044}{(2663.05707)(0.8675)(0.00004693853)} = 0.0001028$$

The slop between two near points was found: -

$$S = \frac{y_2 - y_1}{t_2 - t_1}$$

y2 at T=50 C°

y1 at T=150 C°

$$y_2 = \ln\frac{T_2 - T_\infty}{T_i - T_\infty} = \ln\frac{50-32.7}{150-32.7} = -1.914$$

$$y_1 = \ln\frac{T_1 - T_\infty}{T_i - T_\infty} = 0$$

t_1=0 at T=130 C°, t_2=309 at T=50 C°

$$\therefore \quad S = \frac{y_2 - y_1}{t_2 - t_1} = \frac{-1.914-0}{309-0} = -0.006194$$

-hc= slop =-0.006194

-h (0.00018028) =-0.006194

h=60.2529w/m^2.C^{o}

From Appendix (D-2) at (T_∞=32.7 C^o), the thermal conductivity of air was found by applying the interpolation method:-

$$\frac{350-300}{350-305.85} = \frac{.03003-.02624}{.03003-K} \Rightarrow K = .0266843w/m^2.c^o$$

$\therefore Nu = \frac{hD}{K} = $ [illegible] $= 11.9982$

Table (4-1) Thermocouple Position

No	Cylinder (degree)
1	$\vartheta=0$
2	$\vartheta=30$
3	$\vartheta=60$
4	$\vartheta=90$
5	$\vartheta=120$
6	$\vartheta=150$
7	$\vartheta=180$
8	$\vartheta=210$
9	$\vartheta=240$
10	$\vartheta=27$[illegible]
11	$\vartheta=$[illegible]
12	$\vartheta=330$

Table (4.2) Cylinder Positions

No of position	(cm)
1	3.7
2	7.75
3	11.5
4	15.25
5	19

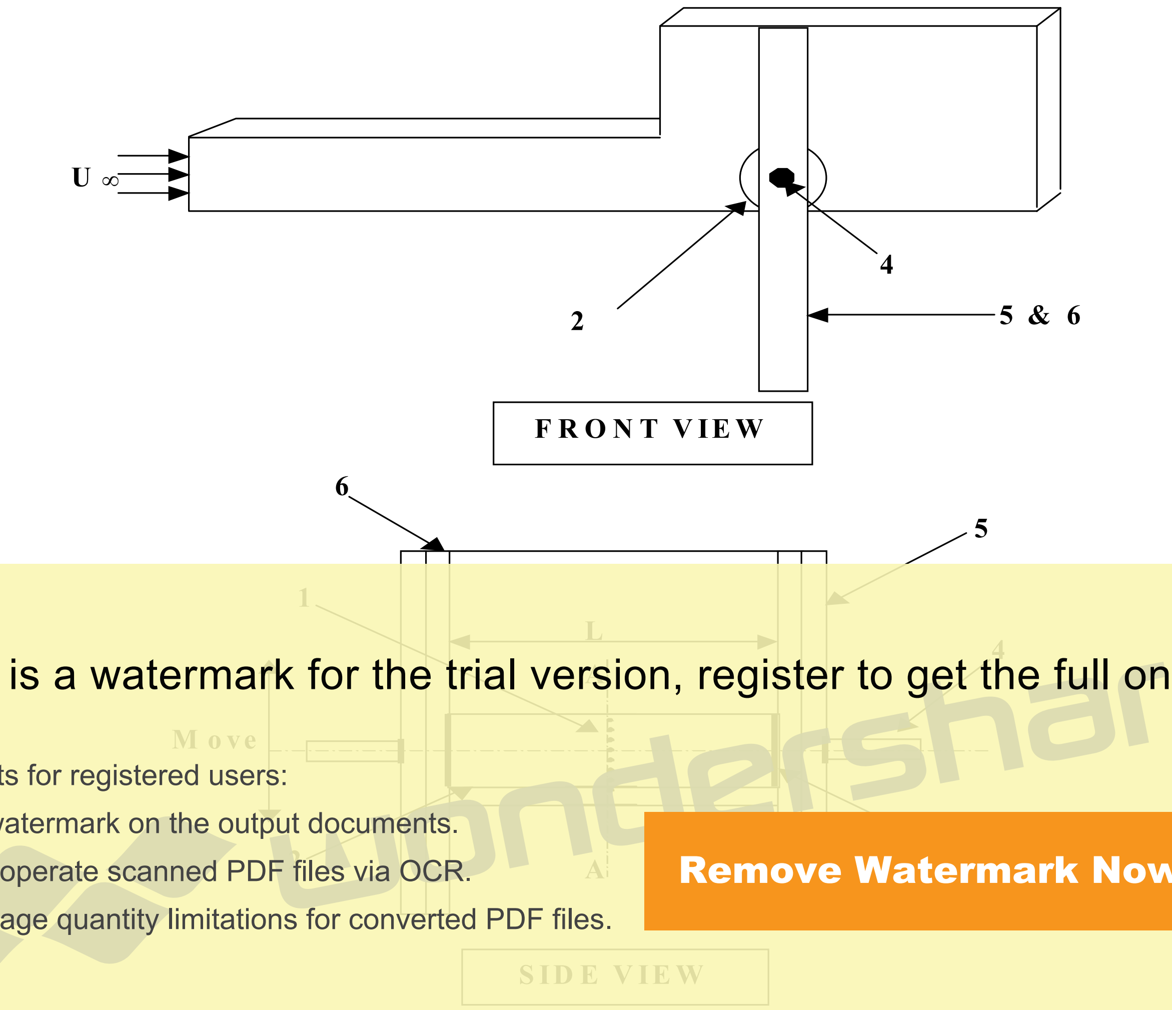

4-1-a

1. Chromal-Alume thermocouple position.
2. Aluminum cylinder of thickness (tc= 5 mm), diameter (Do=49.6mm) and length (L= 67 mm).
3. Ceramic bead.
4. Screw and net.
5. Glass wool.
6. Glass wool.
7. Fiber glass.
8. Heater.
9. Diameter of the thermocouple position in the cylinder (d =1 mm).
10. Deep of the thermocouple position in the cylinder (ℓ=3.5mm).
11. The plate of the same material.

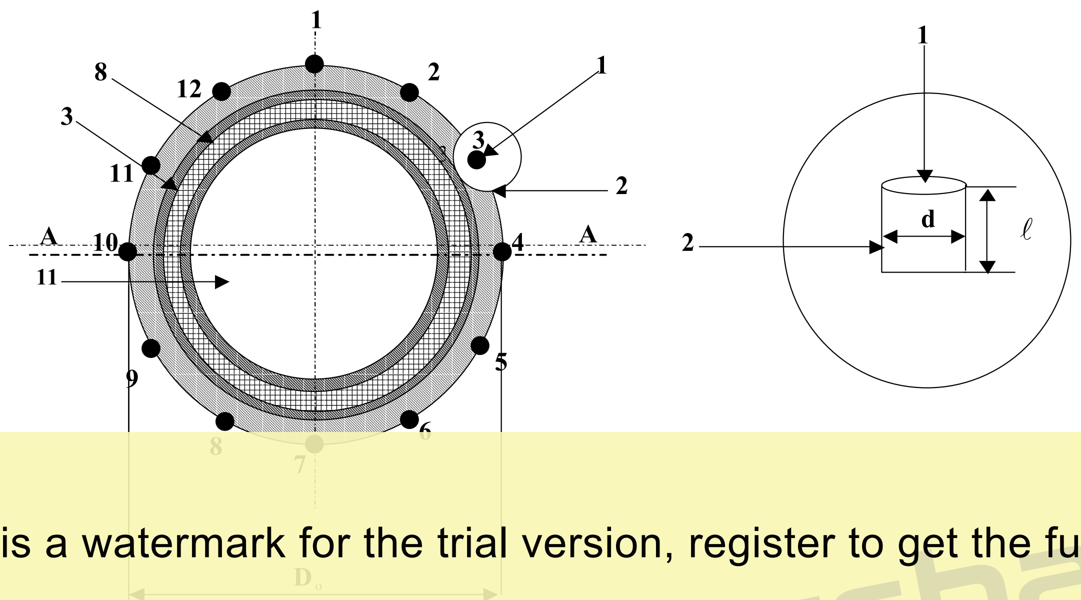

4-1-b

Figure (4-1): Schematic illustration

1. Chromal-Alume thermocouple position.
2. Aluminum cylinder of thickness (t_c= 5 mm), diameter (D_o=49.6mm) and length (L= 67 mm).
3. Ceramic bead.
4. Screw and net.
5. Glass wool.
6. Glass wool.
7. Fiber glass.
8. Heater.
9. Diameter of the thermocouple position in the cylinder (d =1 mm).
10. Deep of the thermocouple position in the cylinder (ℓ=3.5mm).
11. The plate of the same material.

Table (D-1)

Property values for metals[1]

Metal	Properties at 20°C ρ, kg/m^3	c_p, kJ/kg·°C	k, W/m·°C	$\alpha \times 10^5$, m^2/s	Thermal conductivity k, W/m·°C −100°C −148°F	0°C 32°F	100°C 212°F	200°C 392°F	300°C 572°F	400°C 752°F	600°C 1112°F	800°C 1472°F	1000°C 1832°F	1200°C 2192°F
Aluminum:														
Pure	2,707	0.896	204	8.418	215	202	206	215	228	249				
Al-Cu (Duralumin), 94–96% Al, 3–5% Cu, trace Mg	2,787	0.883	164	6.676	[illegible]	159	182	194						
Al-Si (Silumin, copper-bearing), 86.5% Al, 1% Cu	2,659	0.867	137	5.933	119	137	144	152	161					
Al-Si (Alusil), 78–80% Al, 20–22% Si	2,627	0.854	161	7.172	144	157	168	175	178					
Al-Mg-Si, 97% Al, 1% Mg, 1% Si, 1% Mn	2,707	0.892	177	7.311		175	189	204						
Lead	11,373	0.130	35	2.343	36.9	35.1	33.4	31.5	29.8					
Iron:														
Pure	7,897	0.452	73	2.034	[illegible]	73	67	62	55	48	40	36	35	36
Wrought iron, 0.5% C	7,849	0.46	59	1.626	[illegible]	59	57	52	48	45	36	33	33	33
Steel (C max ≈ 1.5%): Carbon steel														
C ≈ 0.5%	7,833	0.465	54	1.474		55	52	48	45	42	35	31	29	31
1.0%	7,801	0.473	43	1.172		43	43	42	40	36	33	29	28	29
1.5%	7,753	0.486	36	0.970		36	36	36	35	33	31	28	28	29

Table (D-2)

Properties of air at atmospheric pressure†

The values of μ, k, c_p, and Pr are not strongly pressure-dependent and may be used over a fairly wide range of pressures.

T, K	ρ kg/m^3	c_p, kJ/kg · °C	$\mu \times 10^5$, kg/m · s	$\nu \times 10^6$, m^2/s	k, W/m · °C	$\alpha \times 10^4$, m^2/s	Pr
100	3.6010	1.0266	0.6924	1.923	0.009246	0.02501	0.770
150	2.3675	1.0099	1.0283	4.343	0.013735	0.05745	0.753
200	1.7684	1.0061	1.3289	7.490	0.01809	0.10165	0.739
250	1.4128	1.0053	1.5990	11.31	0.02227	0.15675	0.722
300	1.1774	1.0057	1.8462	15.69	0.02624	0.22160	0.708
350	0.9980	1.0090	2.075	20.76	0.03003	0.2983	0.697
400	0.8826	1.0140	2.286	25.90	0.03365	0.3760	0.689
450	0.7833	1.0207	2.484	31.71	0.03707	0.4222	0.683
500	0.7048	1.0295	2.671	37.90	0.04038	0.5564	0.680
550	0.6423	1.0392	2.848	44.34	0.04360	0.6532	0.680
600	0.5879	1.0551	3.018	51.34	0.04659	0.7512	0.680
650	0.5430	1.0635	3.177	58.51	0.04953	0.8578	0.682
700	0.5030	1.0752	3.332	66.25	0.05230	0.9672	0.684
750	[illegible]	[illegible]	[illegible]	[illegible]	[illegible]	[illegible]	[illegible]
800	0.4405	1.0978	3.625	82.29	0.05779	[illegible]	[illegible]
850	0.4149	1.1095	3.765	[illegible]	[illegible]	[illegible]	[illegible]
900	[illegible]	1.1212	3.899	[illegible]	[illegible]	[illegible]	0.696
950	0.3716	1.1321	[illegible]	[illegible]	[illegible]	[illegible]	[illegible]
[illegible]	[illegible]	[illegible]	[illegible]	[illegible]	[illegible]	[illegible]	[illegible]
[illegible]	[illegible]	[illegible]	[illegible]	[illegible]	[illegible]	[illegible]	[illegible]
[illegible]	[illegible]	[illegible]	[illegible]	[illegible]	[illegible]	[illegible]	[illegible]
1300	0.2707	1.197	4.93	182.1	0.0837	2.583	0.705
1400	0.2515	1.214	5.17	205.5	0.0891	2.920	0.705
1500	0.2355	1.230	5.40	229.1	0.0946	3.262	0.705
1600	0.2211	1.248	5.63	254.5	0.100	3.609	0.705
1700	0.2082	1.267	5.85	280.5	0.105	3.977	0.705
1800	0.1970	1.287	6.07	308.1	0.111	4.379	0.704
1900	0.1858	1.309	6.29	338.5	0.117	4.811	0.704
2000	0.1762	1.338	6.50	369.0	0.124	5.260	0.702
2100	0.1682	1.372	6.72	399.6	0.131	5.715	0.700
2200	0.1602	1.419	6.93	432.6	0.139	6.120	0.707
2300	0.1538	1.482	7.14	464.0	0.149	6.540	0.710
2400	0.1458	1.574	7.35	504.0	0.161	7.020	0.718
2500	0.1394	1.688	7.57	543.5	0.175	7.441	0.730

†From *Natl. Bur. Stand. (U.S.) Circ.* 564, 1955.

Certification

I certify that this thesis titled" **study the effect of non-uniform flow on heat transfer coefficient of a cylinder wall"** was prepared by **Fady Sabah Al-kuraishy** under my supervision at Al-Nahrain University, College of Engineering, in partial fulfillment of the requirements for the degree of Master of Science in Mechanical Engineering.

Signat

Name: **Prof. Dr. K. A. Ismael**
(Supervisor)
Date: 19 / 9 / 2004

Signature:

Name: **Prof. Dr. H. Tawfiq**
(Head of Department)
Date: / / 2004

Certificate

We certify, as an examining committee, that we have read the thesis titled "**study the effect of non-uniform flow on heat transfer coefficient of a cylinder wall"** and examined the student **Fady Sabah Al-Kuraishy** and found that the thesis meets the standard for the degree of Master of Science in Mechanical Engineering.

Signature:

Name: **Prof. Dr. K. A. Ismael**
(Supervisor)

Date: 19 / 10 / 2004

Signature:

Name: **Dr. A. A. AL- Qalamchi**
(Member)

Date: 19 / 10 / 2004

Signature:

Name: Assist. Prof.
Dr. Asaad T. AL- Omran
(Member)

Date: 22 / 10 / 2004

Signature:

N[illegible]
Khalil. E. J. AL- Jumaily
(Chairman)

Date: 20 / 10 / 2004

Approval of the College of Engineering

Signature:

Name: **Prof. Dr. Fawzi M. AL- Naima**
(Dean of College of Engineering)

Date: / /

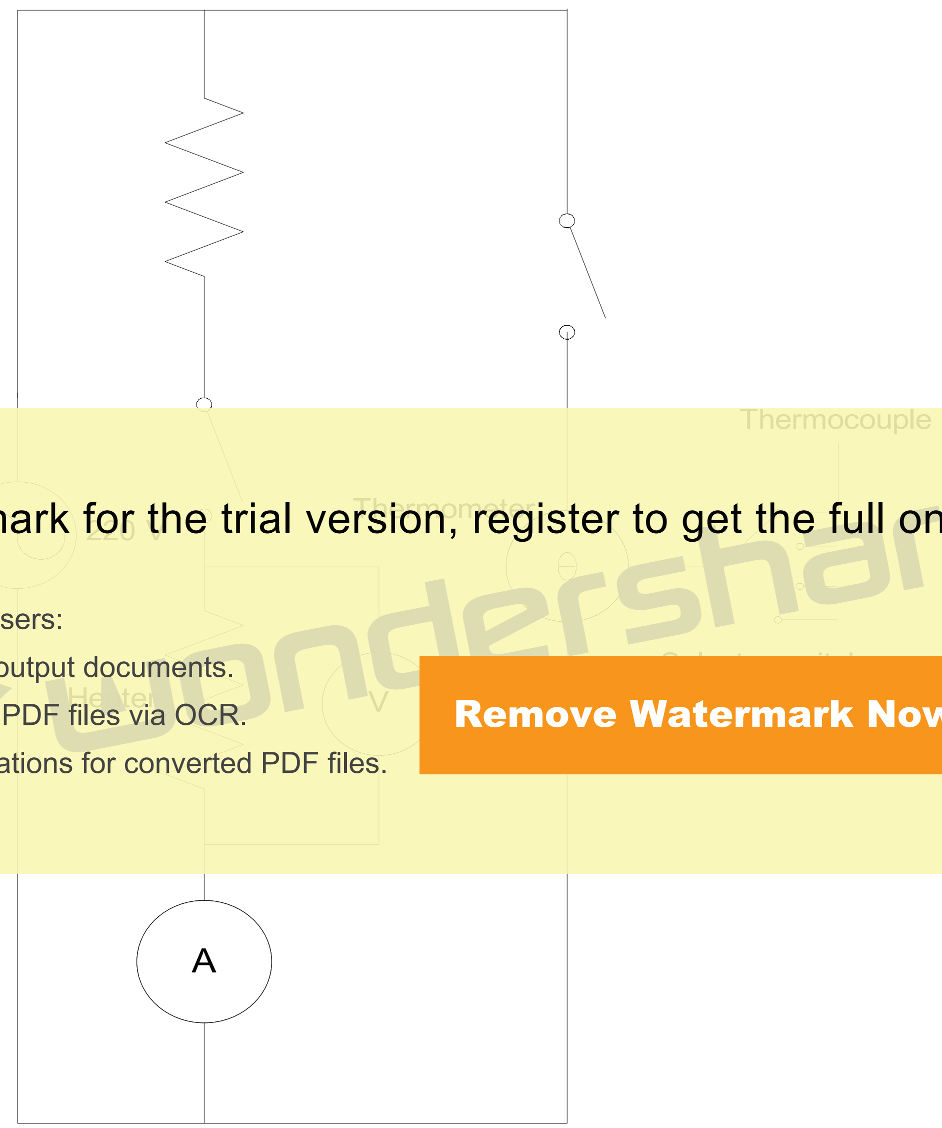

Figure (4-3): The circuit of the digital thermometer, thermocouples and selector.

Flow Chart of Work Procedure

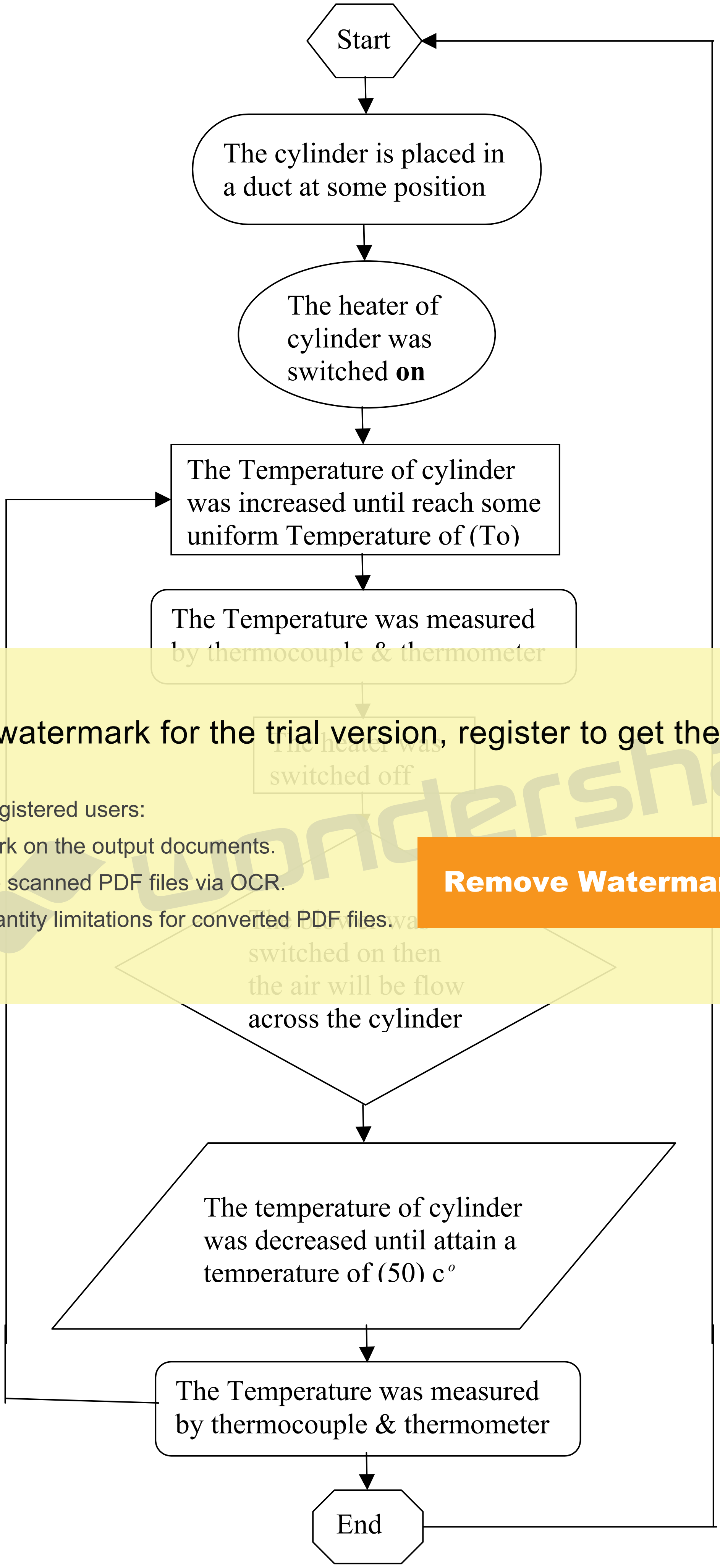

Chapter Five

Results and Discussion

5.1 Introduction

This chapter will include an investigation for the experimental and computational result, which observed in this study.

5.2 Experimental Work

The experimental results shown in this chapter are obtained for four-cylinder position with different reference temperature by using MATLAP 6.1 computer program. Results for one test section are repeated for four-cylinder position according to each value of reference temperature (T_o), which is supplied at the cylinder. These results are divided into four groups:

a- Determination for the variation of tem[illegible]

b- Determination for the variation of ($\ln (T-T_\infty)/(T_o-T_\infty)$) with time interval.

c- Determination for the variation of temperature with time interval at some reference temperature (T_o) and with different cylinder position.

d- Determination for the variation of temperature ratio of (T/T_{max}) with time ratio of (t/t_{max}).

5.2.1 Variation of surface temperature with time interval:

The measured surface temperature of the cylinder is plotted against time interval as shown in figures (5.1-5.4) for different cylinder positions

(Y=3.7, 7.75, 15.25,19 cm). The variation of (ln $(T-T_{\infty})/(T_o-T_{\infty})$) with time is shown in figures (5.5-5.44). It is shown that this variation is linear with time with decreasing slope. From figures (5.1-5.4) the variation of temperature ratio (T/T_{max}) against time ratio (t/t_{max}) will be obtained as shown in figures (5.55-5.58). The heat capacity of the material of a cylinder will be increased and also temperature difference will be increased as reference temperature (To) is increased, by the way the temperature difference depend on transient conduction equation that will be effected on the rate of heat transfer that means the rate of heat transfer will be increased as (To) is increased, because all of these, the rate of decreasing in temperature with time will be increased as (To) increased. As can be seen [illegible] figure (5.59). In (a b) region the temperature decrease rapidly along the curve and spanned little time comparing with region of (b c) that spanned much time and the temperature in the region (b c) decrease gradually [illegible] difference (T-50) in the region (a b) is high then the rate of heat transfer will be very quickly but at the region (b c) the temperature difference is low then the rate of heat transfer will be very slow. The pattern flow on each cylinder position was show in figures (5.60-5.63). At some reference temperature (T_o) with different cylinder position, the measured surface temperature of the cylinder is plotted against time at that moment shown in figures (5.45-5.54). At each figures the rate of decreasing in temperature with time at that moment will be increased as cylinder position is increased because of cylinder position associated will air flow that means, cylinder position (Y=3.7,7.75 cm) is placed in front of airflow in duct but cylinder position (Y=15.25 cm) is placed in front of discontinues region and the cylinder position (Y=19 cm) is placed in a dead zone that effected on the

the Rate of heat transfer from each cylinder is decreased as cylinder position is increased.

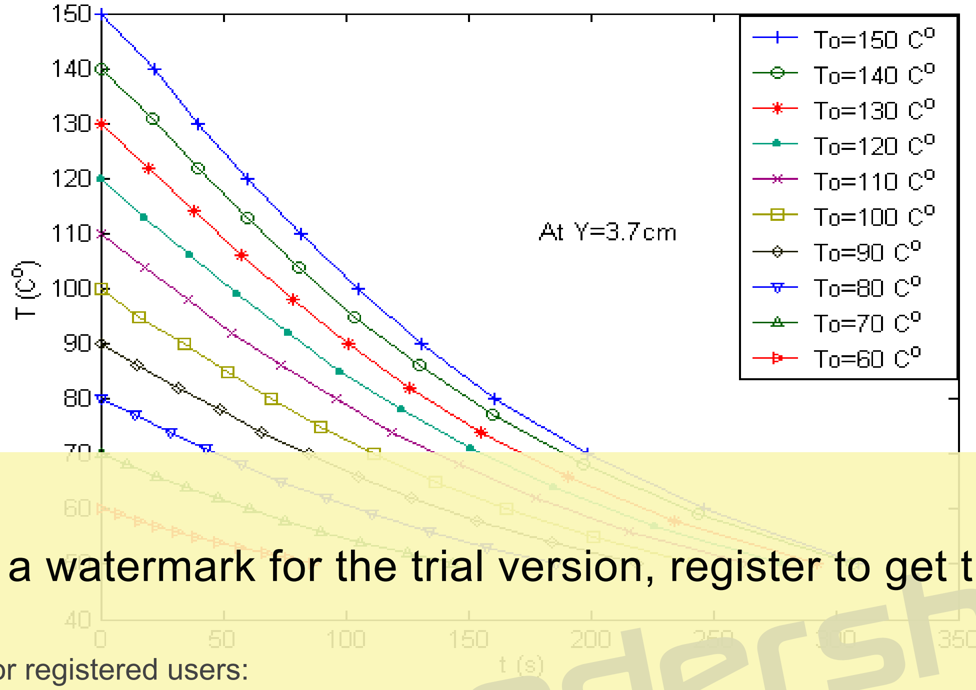

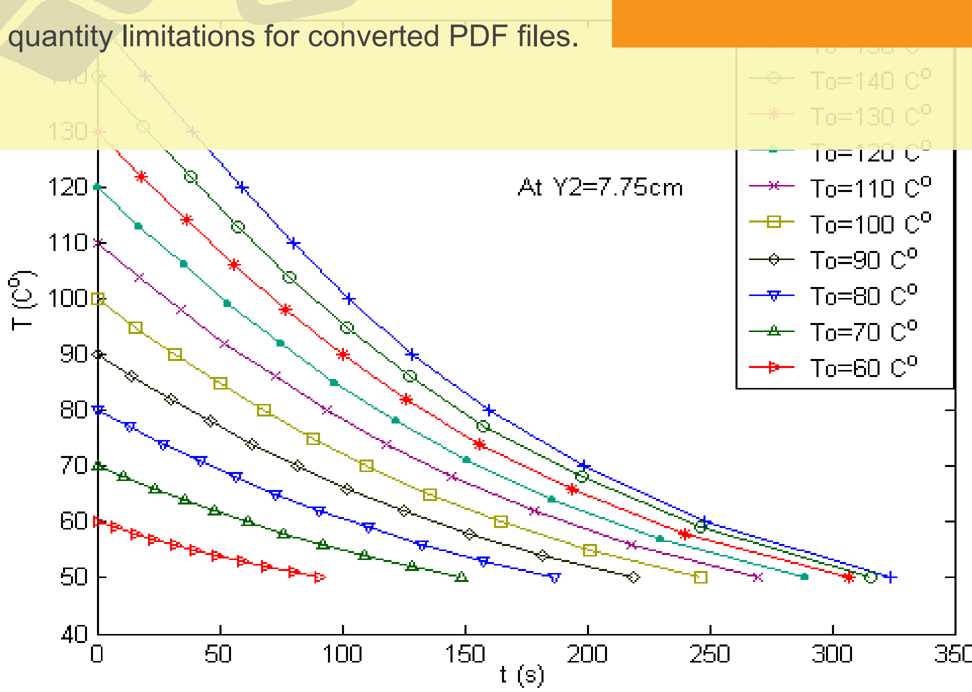

Figure (5.2) the variation of surface temperature against time interval.

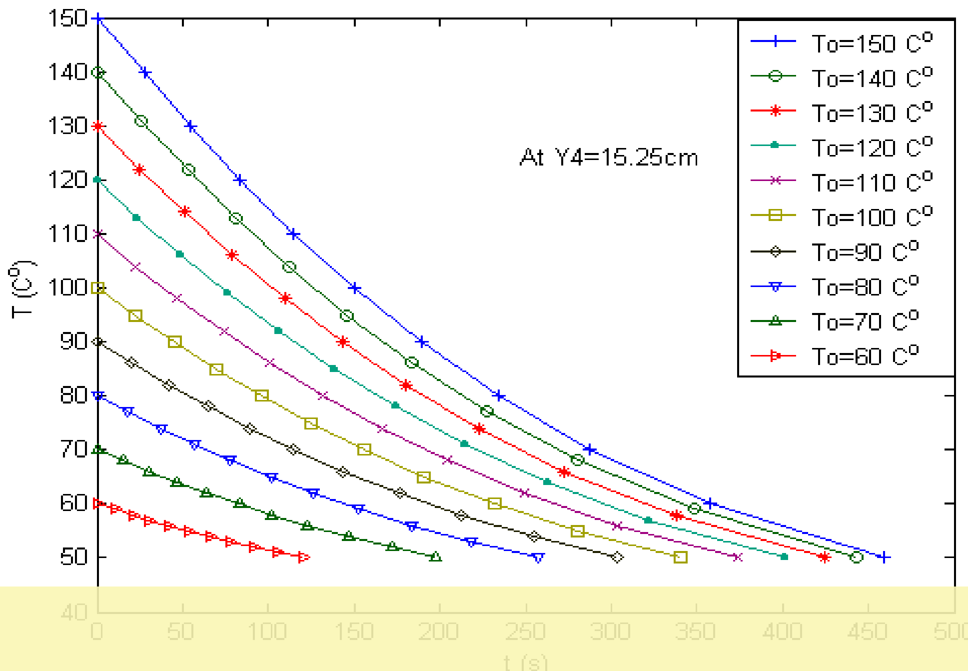

Figure (5.3) the variation of surface temperature against time interval.

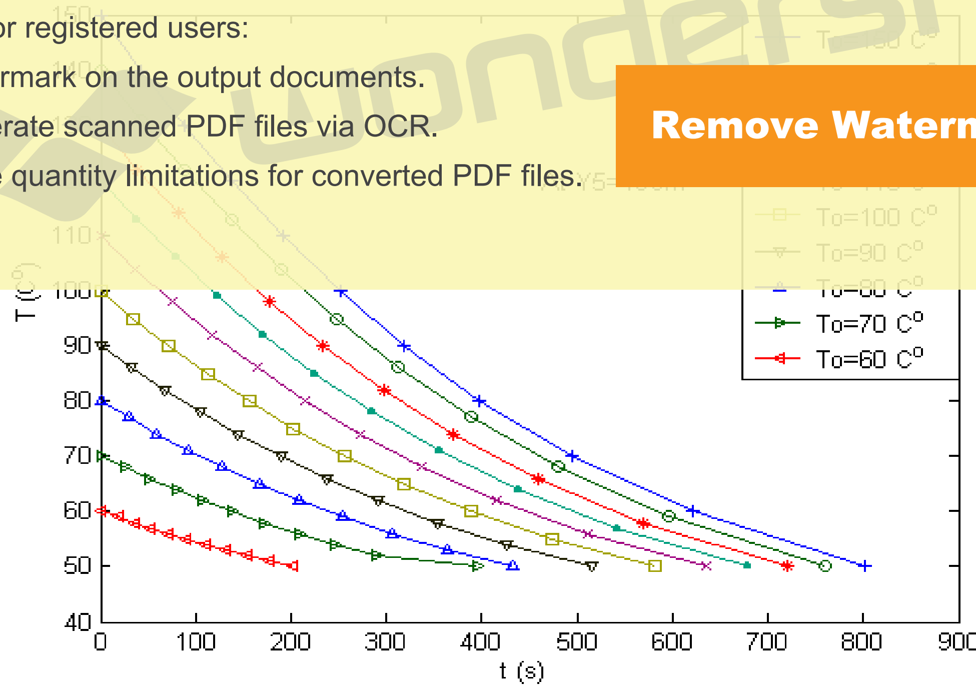

Figure (5.4) the variation of surface temperature against time interval.

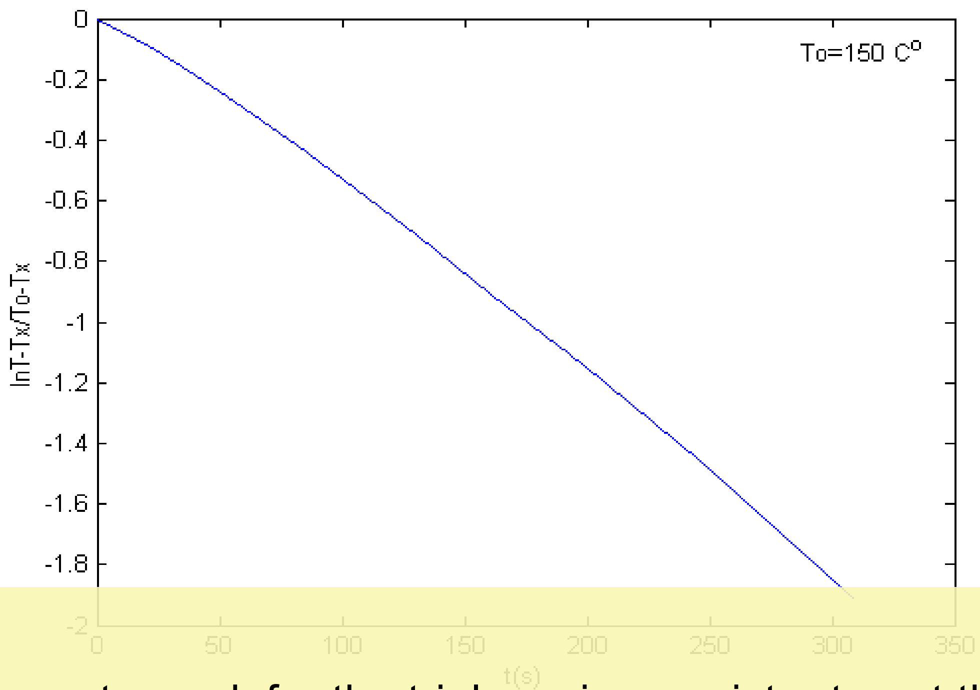

Figure (5.5) the variation of $(\ln \frac{\theta}{\theta_i})$ against time interval.

(Position of cylinder=[illegible] cm).

[illegible]

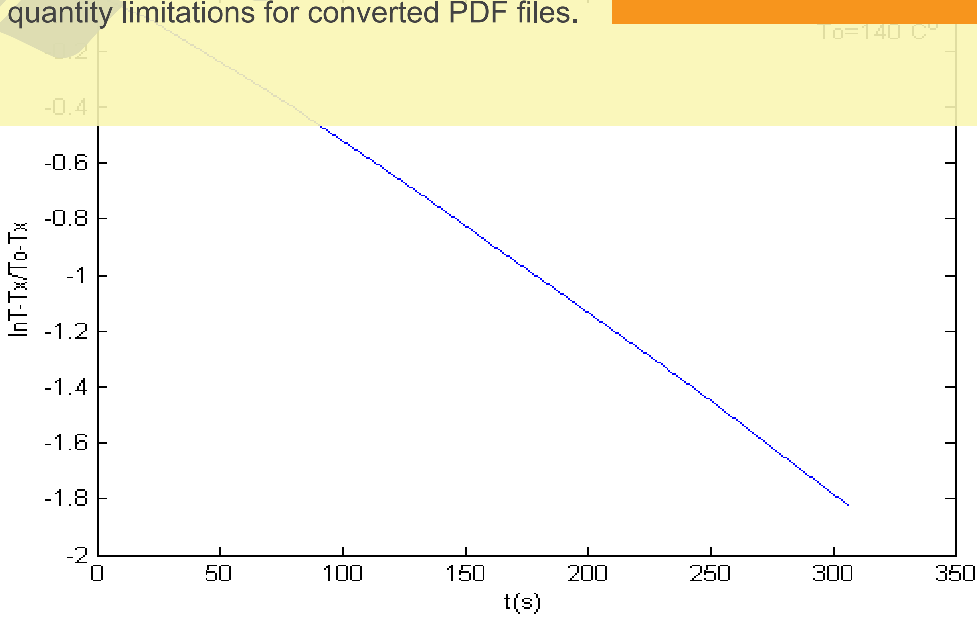

Figure (5.6) the variation of $(\ln \frac{\theta}{\theta_i})$ against time interval.

(Position of cylinder=3.7 cm)
(T=140,131,122,113,104,95,86,77,68,59,50)

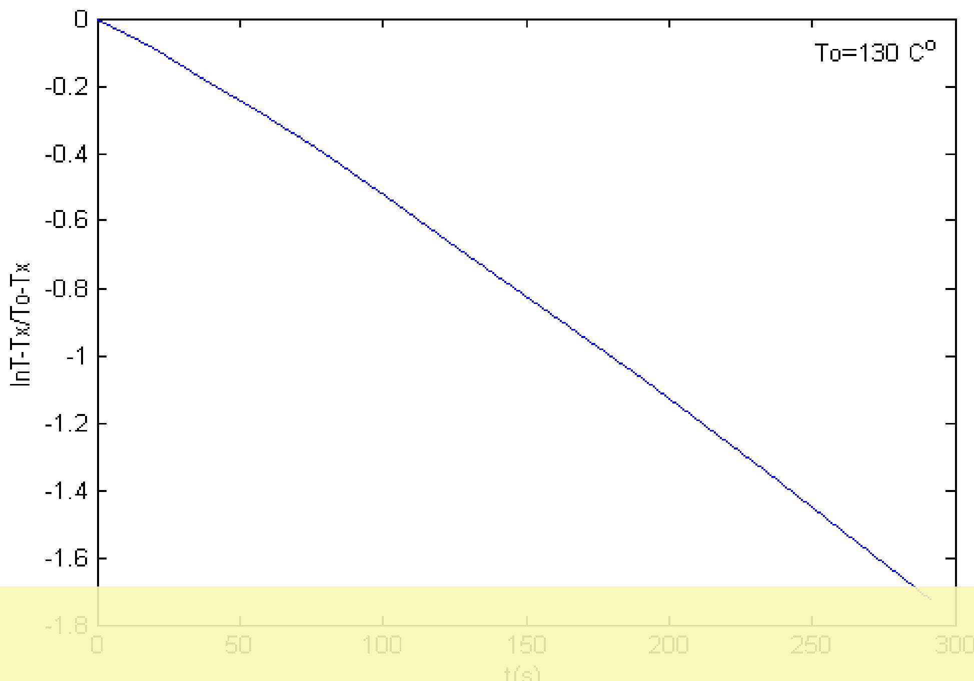

Figure (5.7) the variation of ($\ln\frac{\theta}{\theta_i}$) against time interval.

(Position of cylinder=3.7 cm) (T=130,122,114,106,98,90,82,74,66,58,50).

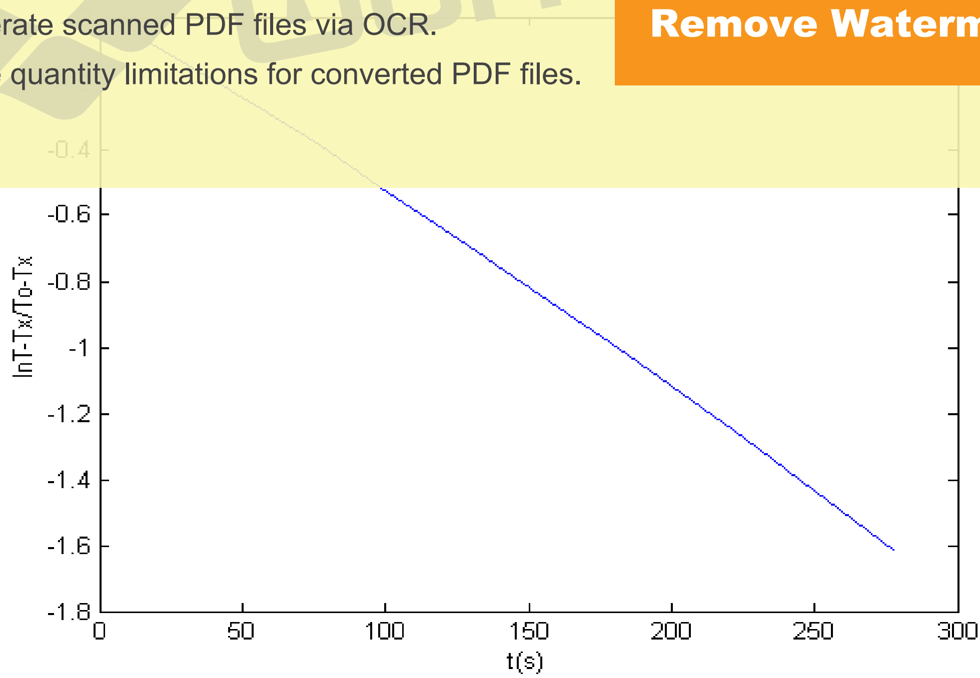

Figure (5.8) the variation of ($\ln\frac{\theta}{\theta_i}$) against time interval.

(Position of cylinder=3.7 cm)
(T=120,113,106,99,92,85,78,71,64,57,50).

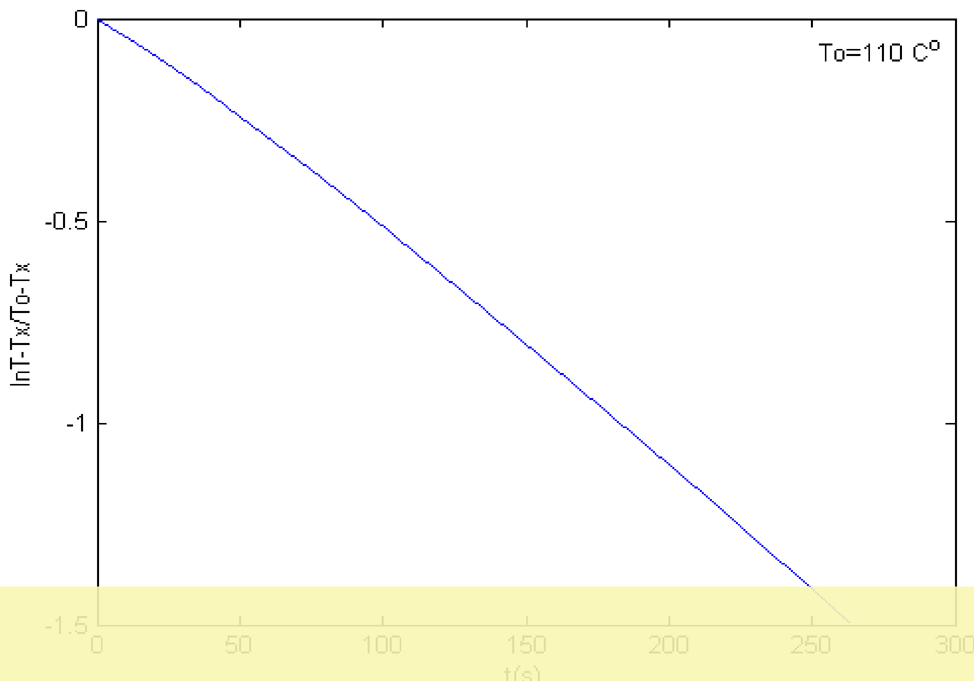

Figure (5.9) the variation of ($\ln\frac{\theta}{\theta_i}$) against time interval.

(Position of cylinder=3.7 cm). (T=110,104,98,92,86,80,74,68,62,56,50).

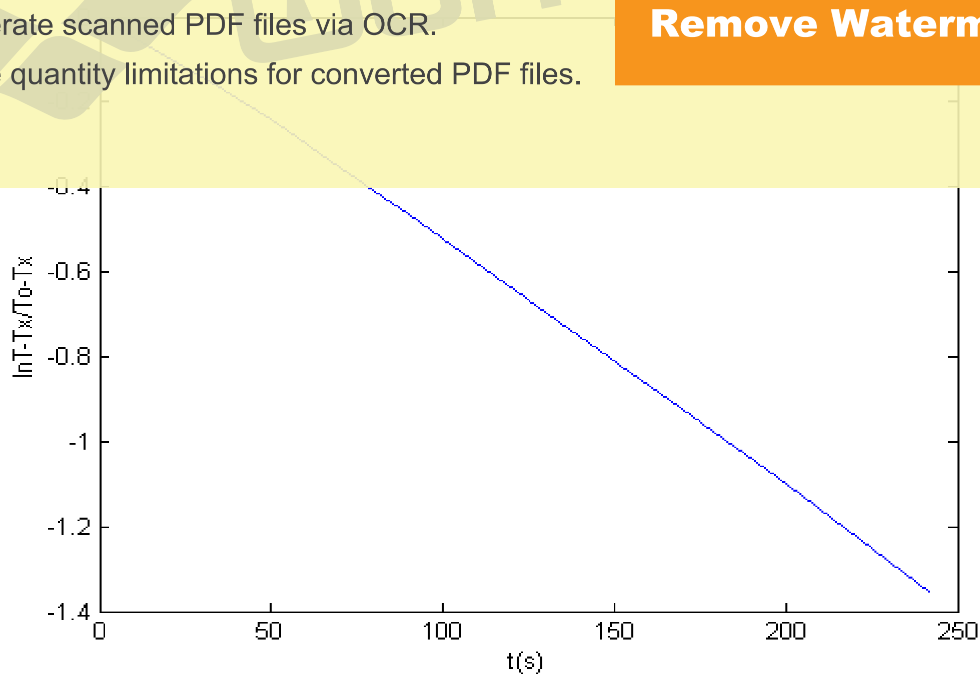

Figure (5.10) the variation of ($\ln\frac{\theta}{\theta_i}$) against time interval.

(Position of cylinder=3.7 cm).
(T=100,95,90,85,80,75,70,65,60,55,50).

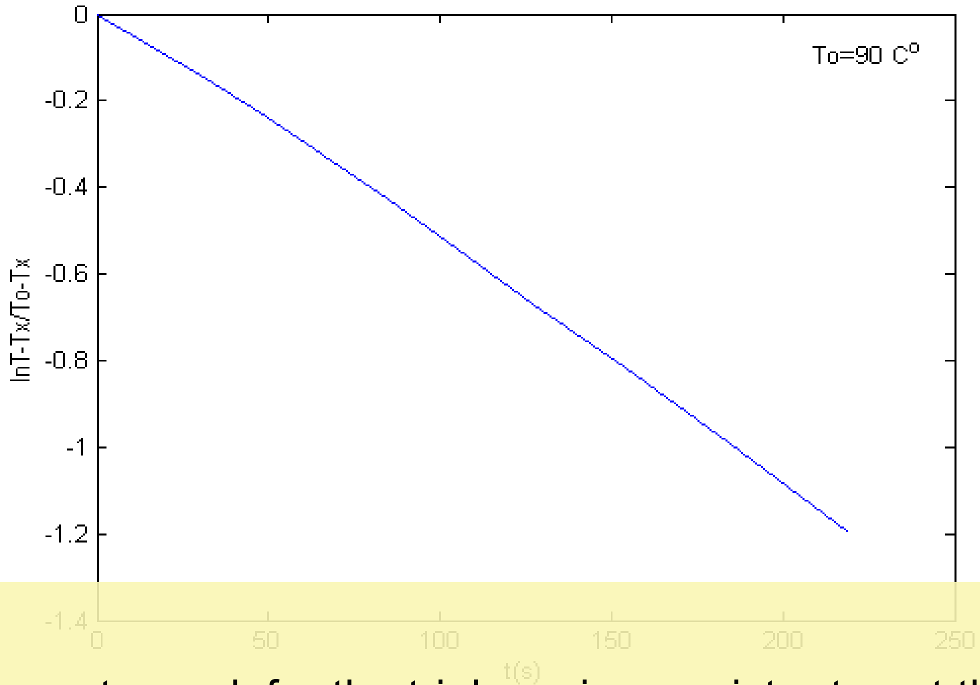

Figure (5.11) the variation of ($\ln\frac{\theta}{\theta_i}$) against time interval.

(Position of cylinder=3.7 cm). (T=90, 86, 82, 78, 74, 70, 66, 62, 58, 50).

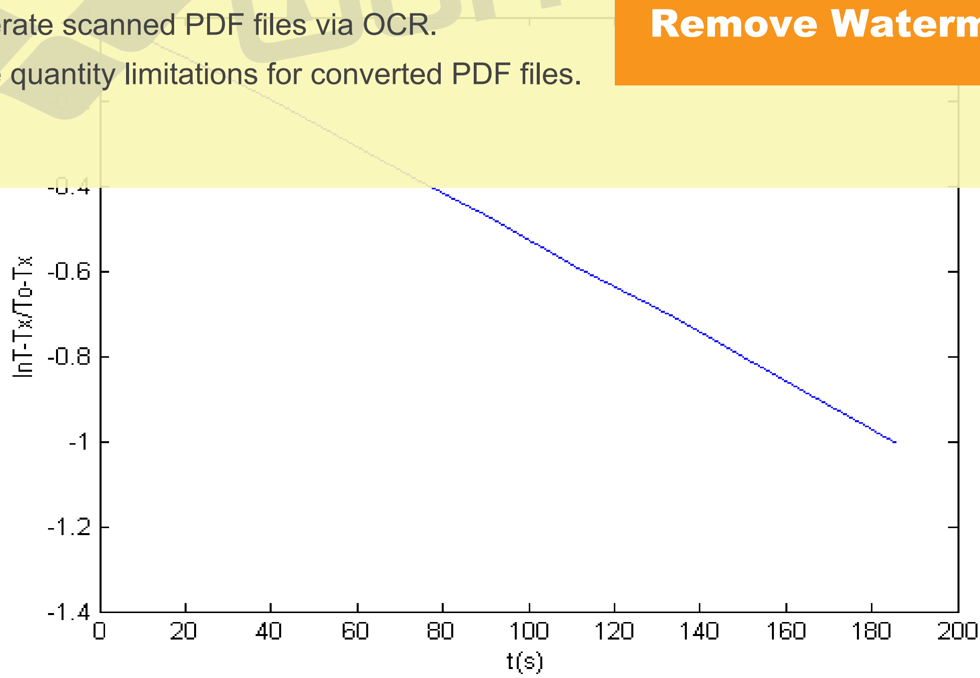

Figure (5.12) the variation of ($\ln\frac{\theta}{\theta_i}$) against time interval.

(Position of cylinder=3.7 cm).

(T=80,77,74,71,68,65,62,59,56,53,50).

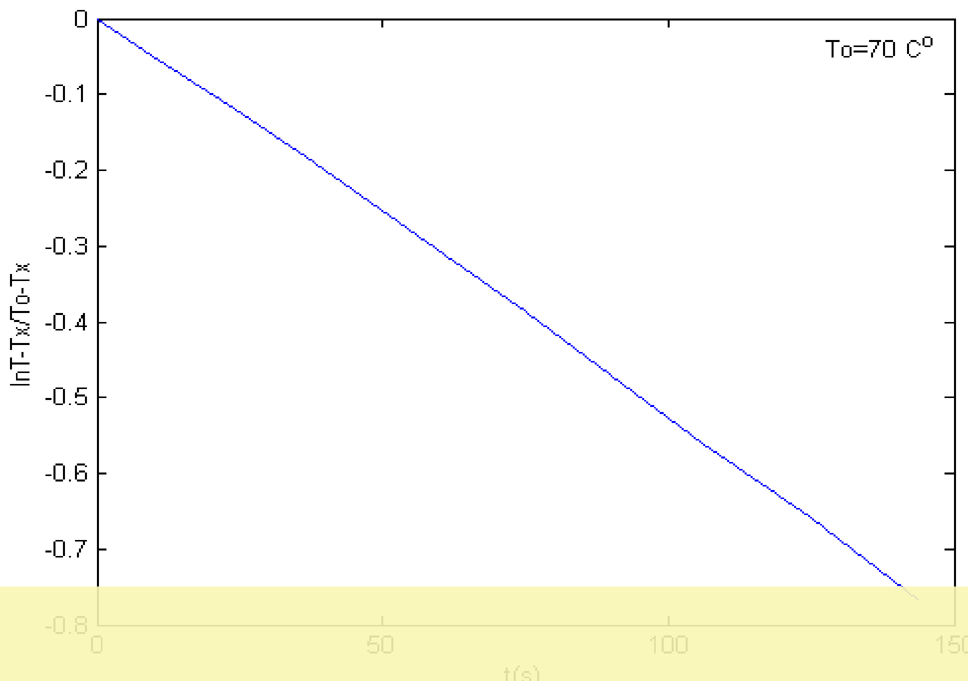

Figure (5.13) the variation of $(\ln\frac{\theta}{\theta_i})$ against time interval.

(Position of cylinder=3.7 cm). (T=70,68,66,64,62,60,58,56,54,52,50).

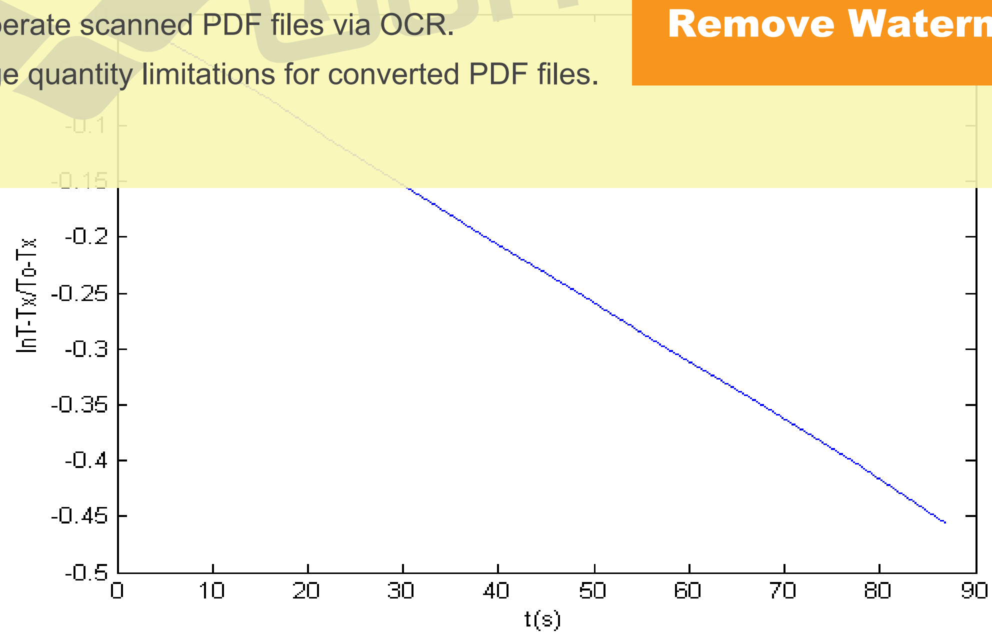

Figure (5.14) the variation of $(\ln\frac{\theta}{\theta_i})$ against time interval.

(Position of cylinder=3.7 cm). (T=60,59,58,57,56,55,54,53,52,51,50).

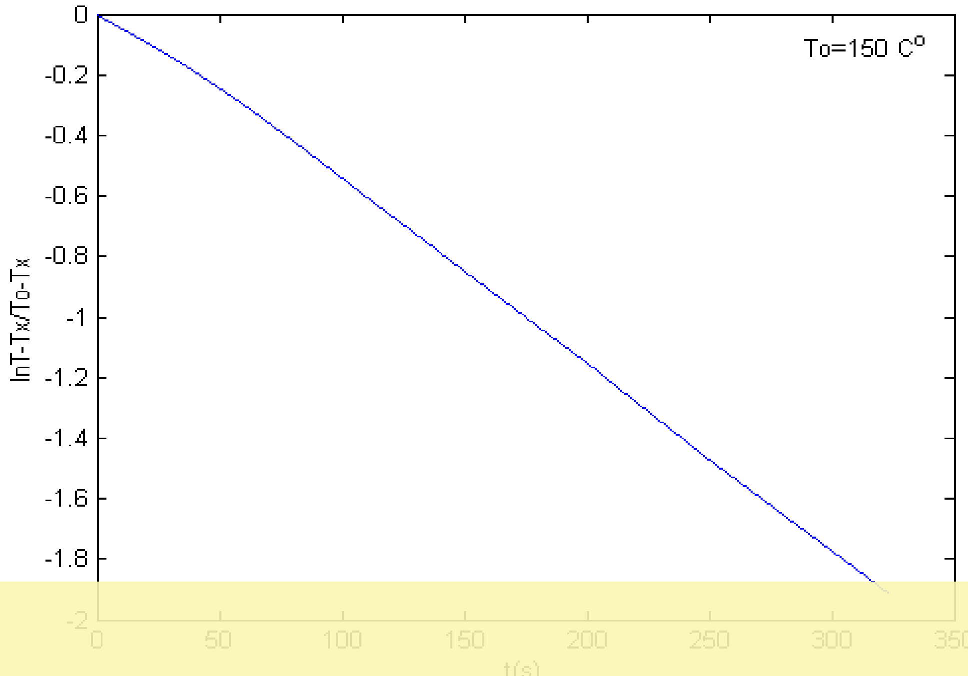

Figure (5.15) the variation of $(\ln\frac{\theta}{\theta_i})$ against time interval.

(Position of cylinder=7.75cm)(T=150,140,130,120,110,100,90,80,70,60,50).

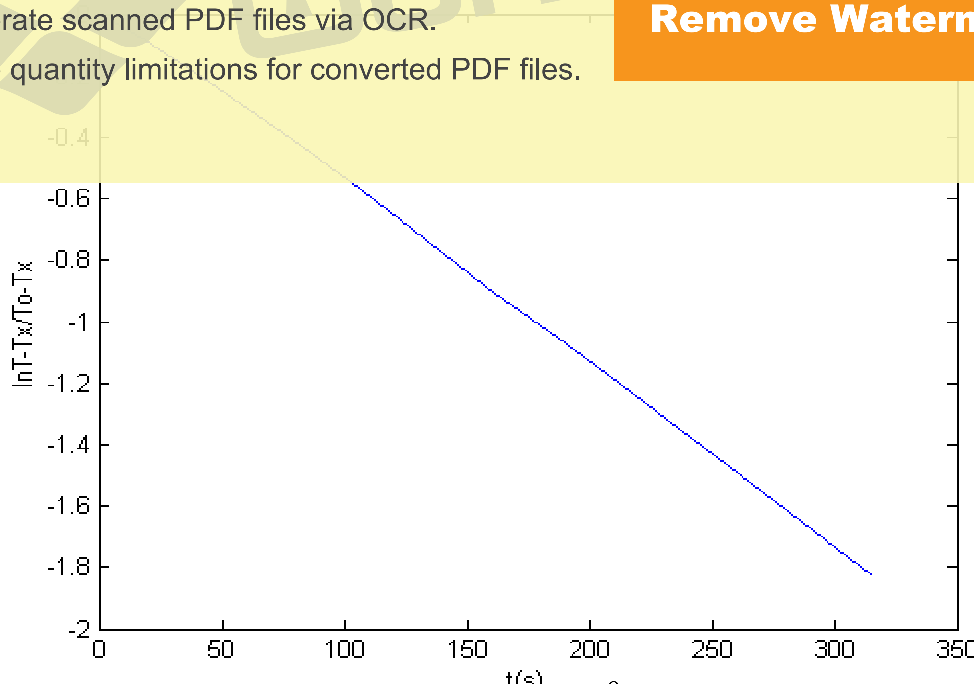

Figure (5.16) the variation of $(\ln\frac{\theta}{\theta_i})$ against time interval.

(Position of cylinder =7.75cm).

(T=140,131,122,113,104,95,86,77,68,59,50).

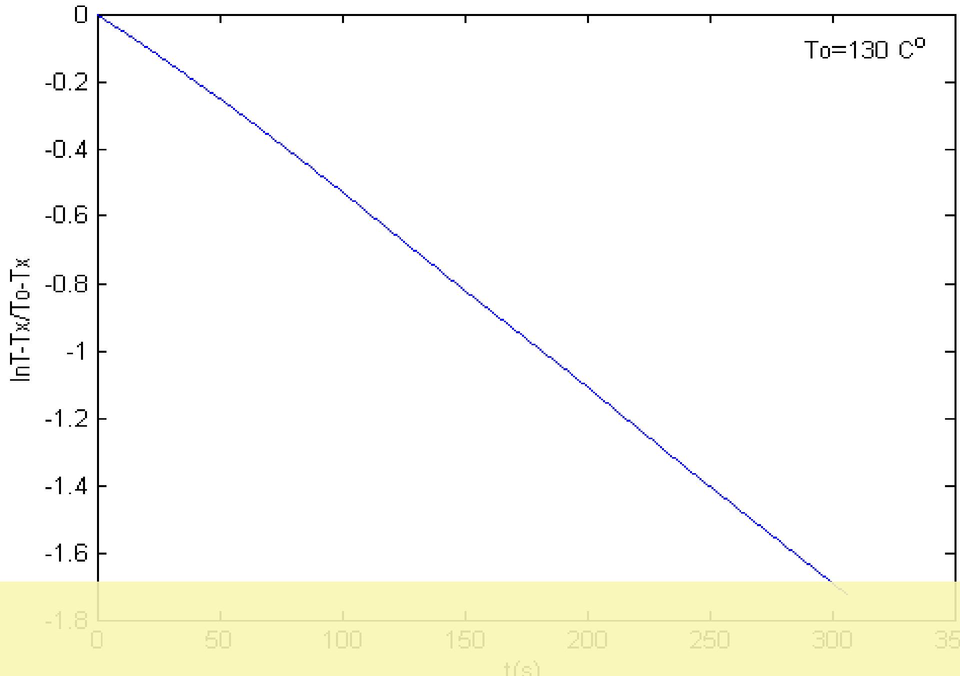

Figure (5.17) the variation of ($\ln\frac{\theta}{\theta_i}$) against time interval.

(Position of cylinder=7.75 cm). (T=130,122,114,106,98,90,82,74,66,58,50).

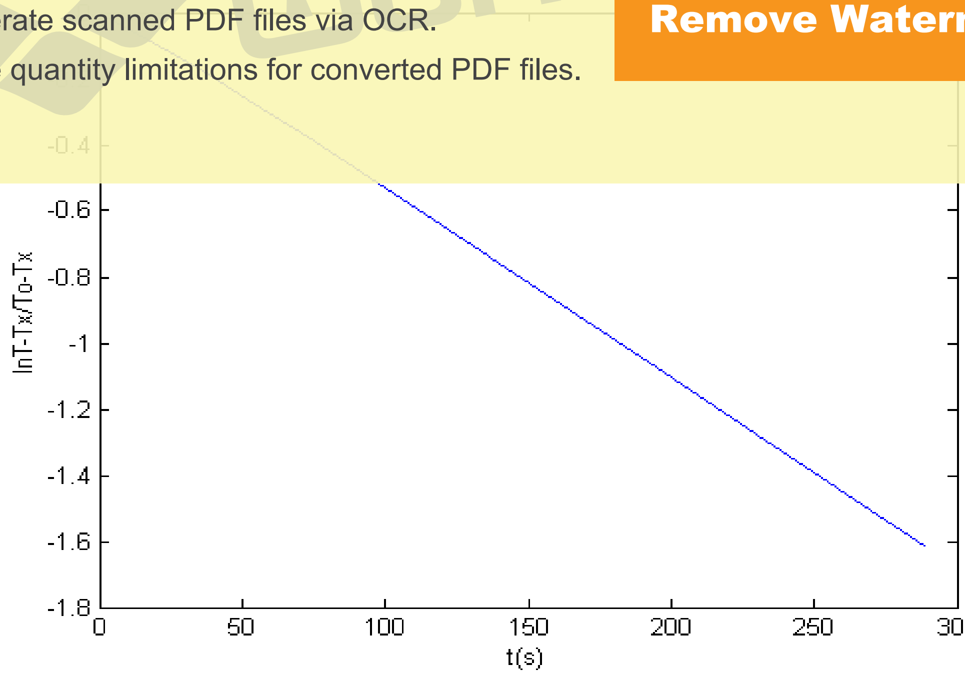

Figure (5.18) the variation of ($\ln\frac{\theta}{\theta_i}$) against time interval.

(Position of cylinder=7.75 cm).
(T=120,113,106,99,92,85,78,71,64,57,50).

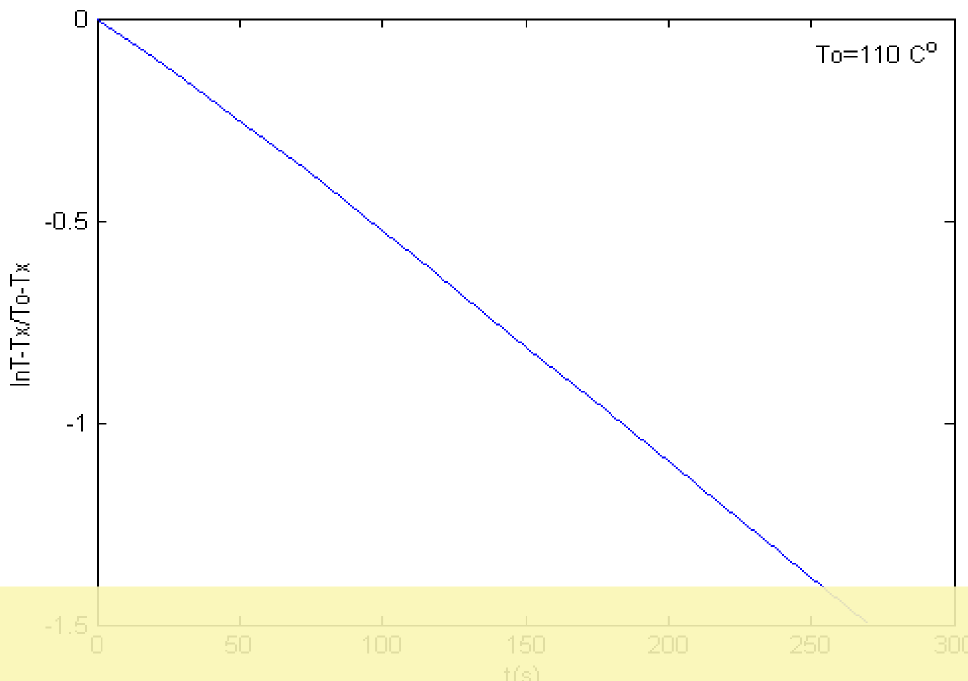

Figure (5.19) the variation of ($\ln\frac{\theta}{\theta_i}$) against time interval.

(Position of cylinder=7.75 cm). (T=110,104,98,92,86,80,74,68,62,56,50).

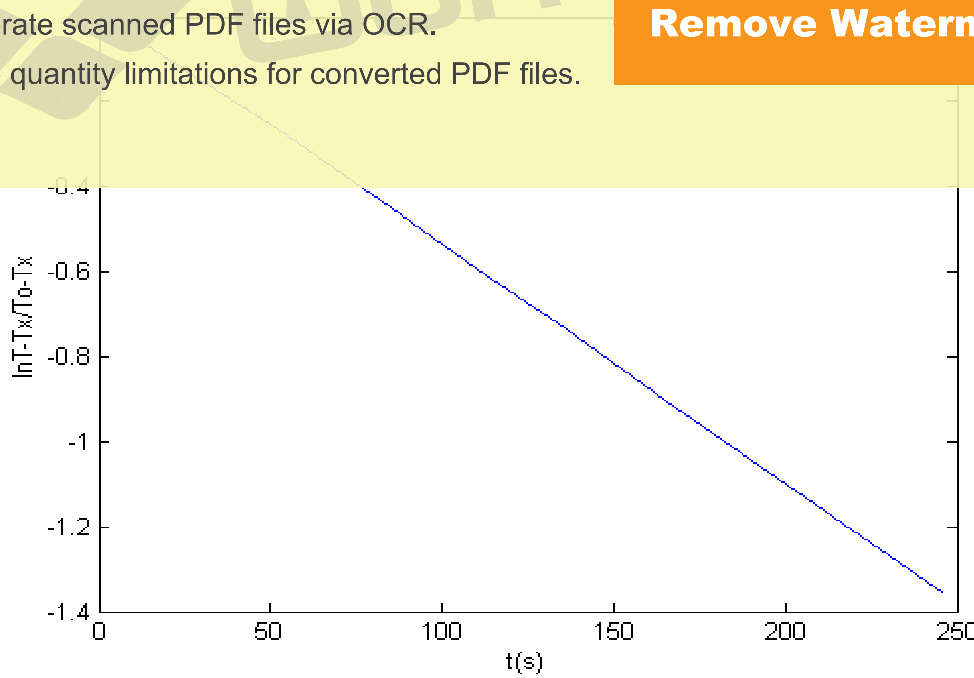

Figure (5.20) the variation of ($\ln\frac{\theta}{\theta_i}$) against time interval.

(Position of cylinder=7.75 cm).
(T=100,95,90,85,80,75,70,65,60,55,50).

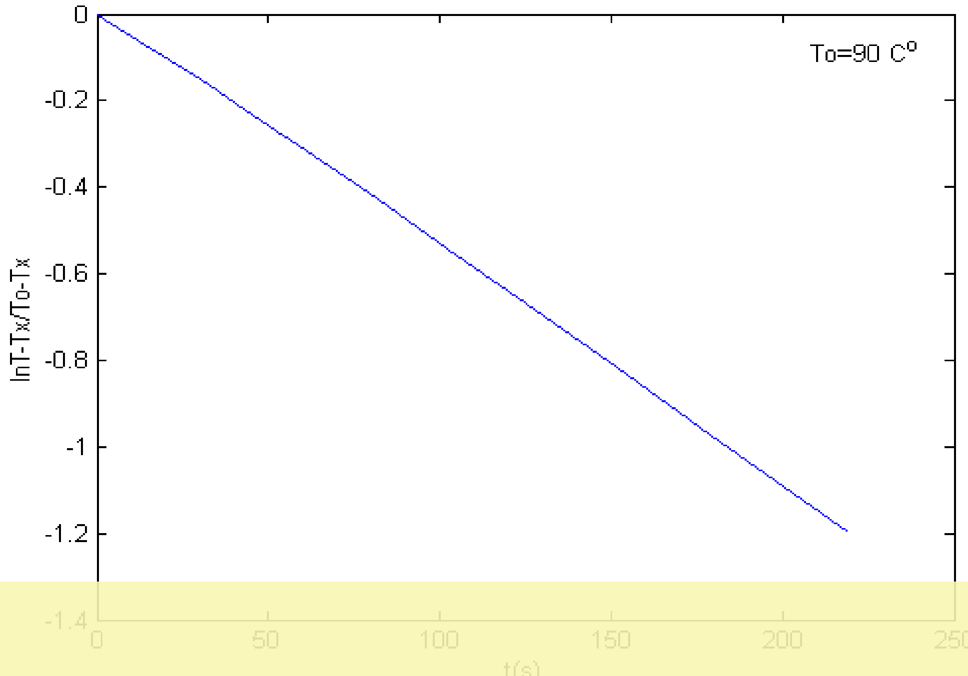

Figure (5.21) the variation of ($\ln\frac{\theta}{\theta_i}$) against time interval.

(Position of cylinder=7.75 cm). (T=90, 86, 82, 78, 74, 70, 66, 62, 58, 50).

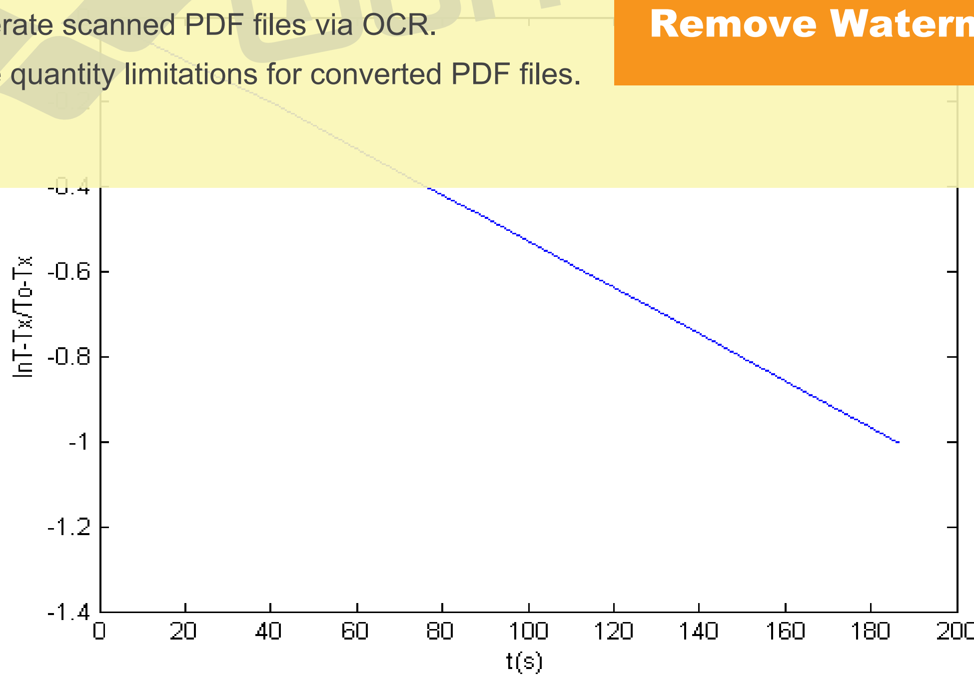

Figure (5.22) the variation of ($\ln\frac{\theta}{\theta_i}$) against time interval.

(Position of cylinder=7.75 cm).
(T=80,77,74,71,68,65,62,59,56,53,50).

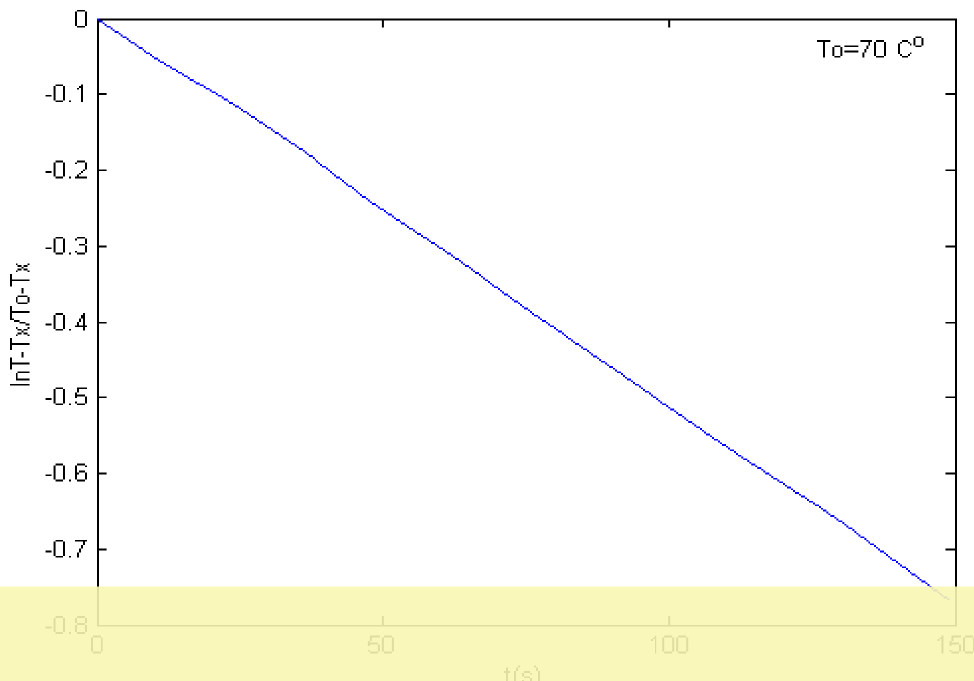

Figure (5.23) the variation of ($\ln\frac{\theta}{\theta_i}$) against time interval.

(Position of cylinder=7.75 cm). (T=70,68,66,64,62,60,58,56,54,52,50).

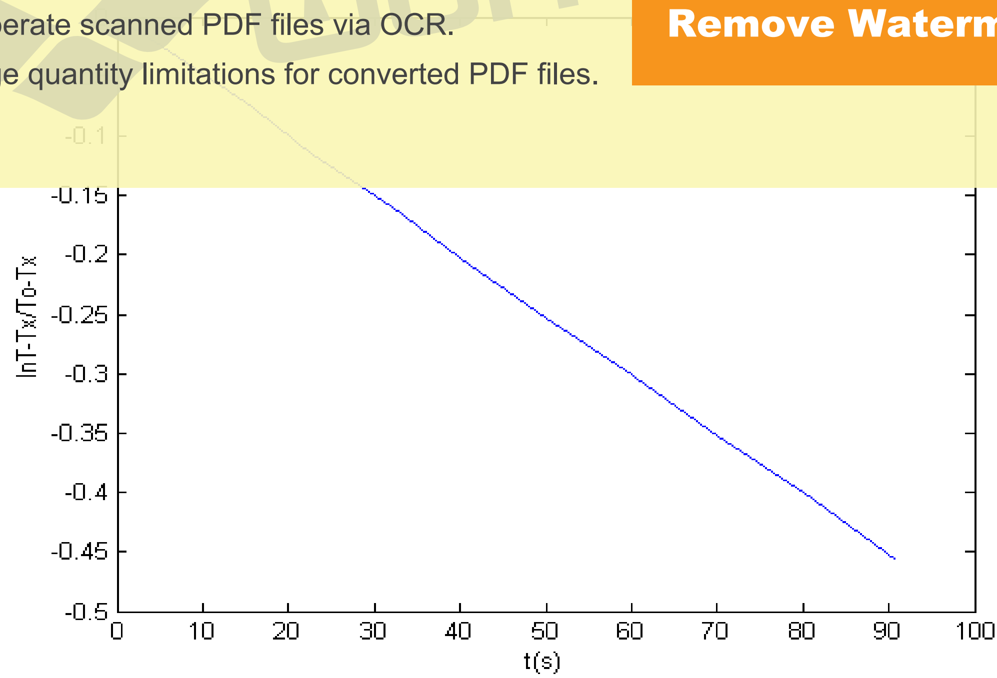

Figure (5.24) the variation of ($\ln\frac{\theta}{\theta_i}$) against time interval.

(Position of cylinder=7.75 cm).
(T=60,59,58,57,56,55,54,53,52,51,50).

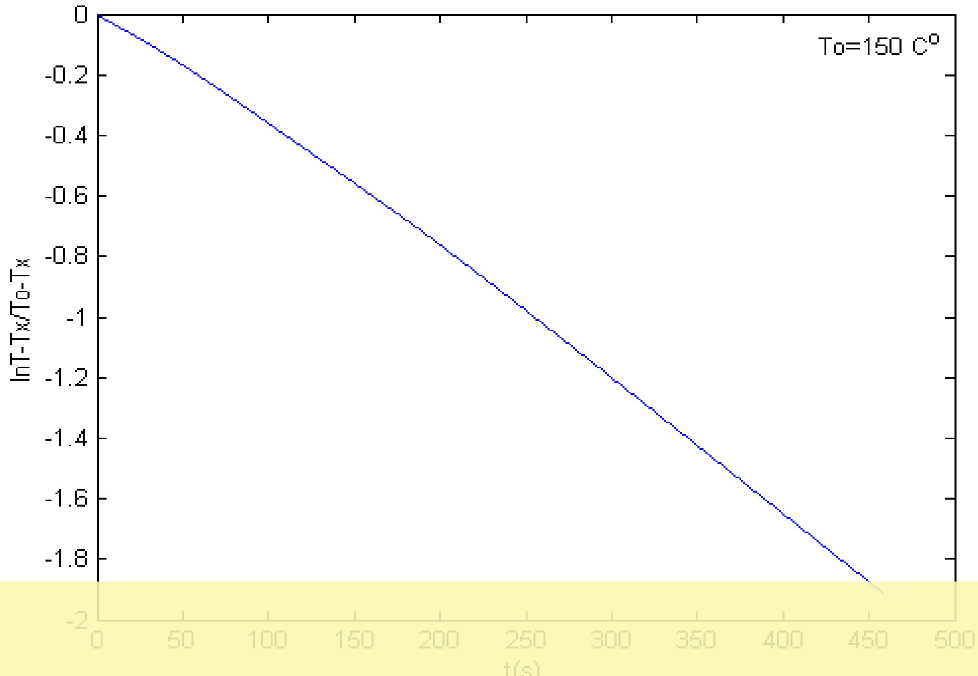

Figure (5.25) the variation of ($\ln\frac{\theta}{\theta_i}$) against time interval.

(Position of cylinder=15.[illegible]cm).

(T=150,14[illegible],130,[illegible],11[illegible] [illegible]

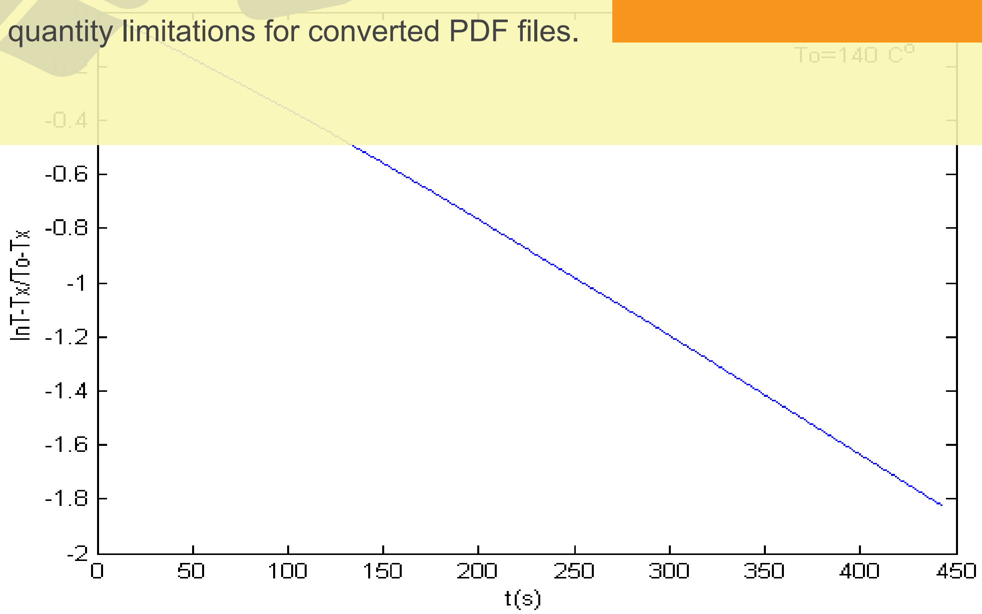

Figure (5.26) the variation of ($\ln\frac{\theta}{\theta_i}$) against time interval.

(Position of cylinder=15.25 cm).
(T=140,131,122,113,104,95,86,77,68,59,50).

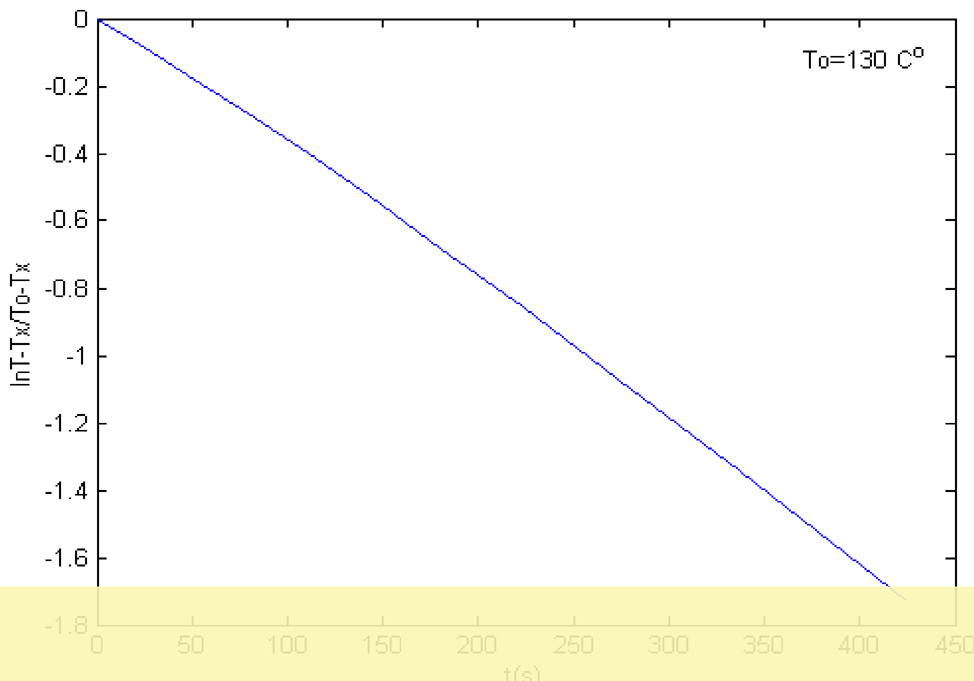

Figure (5.27) the variation of ($\ln\frac{\theta}{\theta_i}$) against time interval.

(Position of cylinder=1[illegible] cm).

(T=1[illegible]).

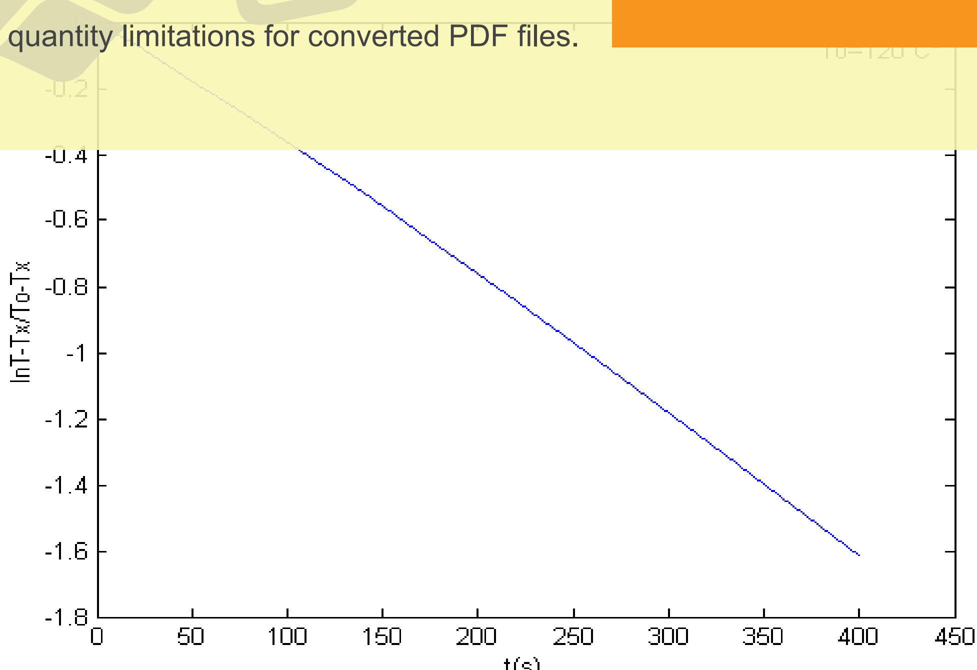

Figure (5.28) the variation of ($\ln\frac{\theta}{\theta_i}$) against time interval.

(Position of cylinder=15.25 cm).

(T=120,113,106,99,92,85,78,71,64,57,50).

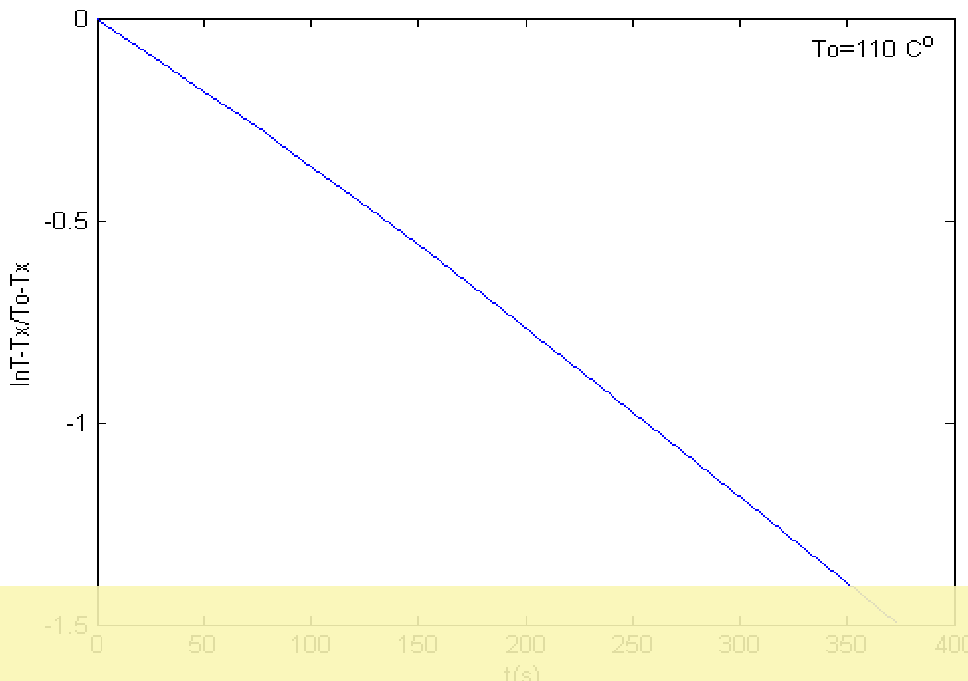

Figure (5.29) the variation of ($\ln\frac{\theta}{\theta_i}$) against time interval.

(Position of cylinder=15.25 cm). (T=110,104,98,92,86,80,74,68,62,56,50).

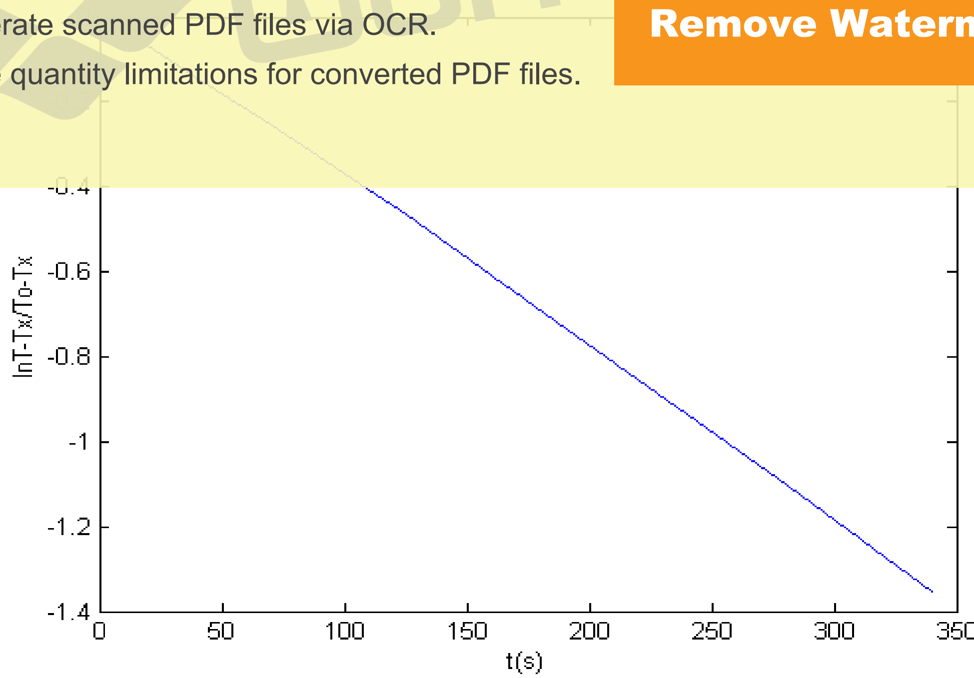

Figure (5.30) the variation of ($\ln\frac{\theta}{\theta_i}$) against time interval.

(Position of cylinder=15.25 cm).
(T=100,95,90,85,80,75,70,65,60,55,50).

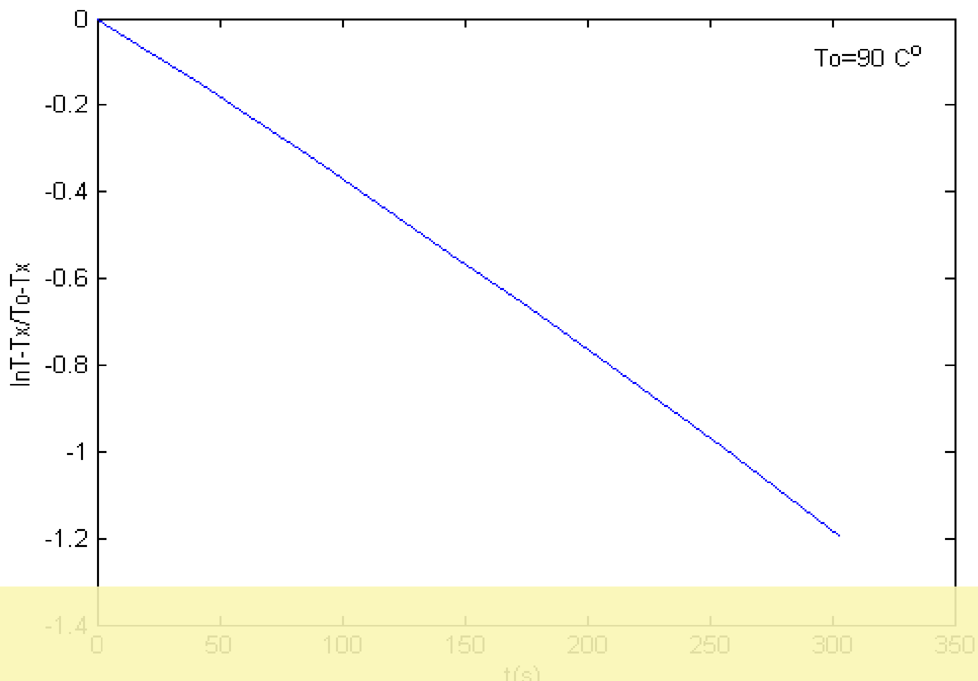

Figure (5.31) the variation of ($\ln\frac{\theta}{\theta_i}$) against time interval.

(Position of cylinder=15.25 cm). (T=90, 86, 82, 78, 74, 70, 66, 62, 58, 50).

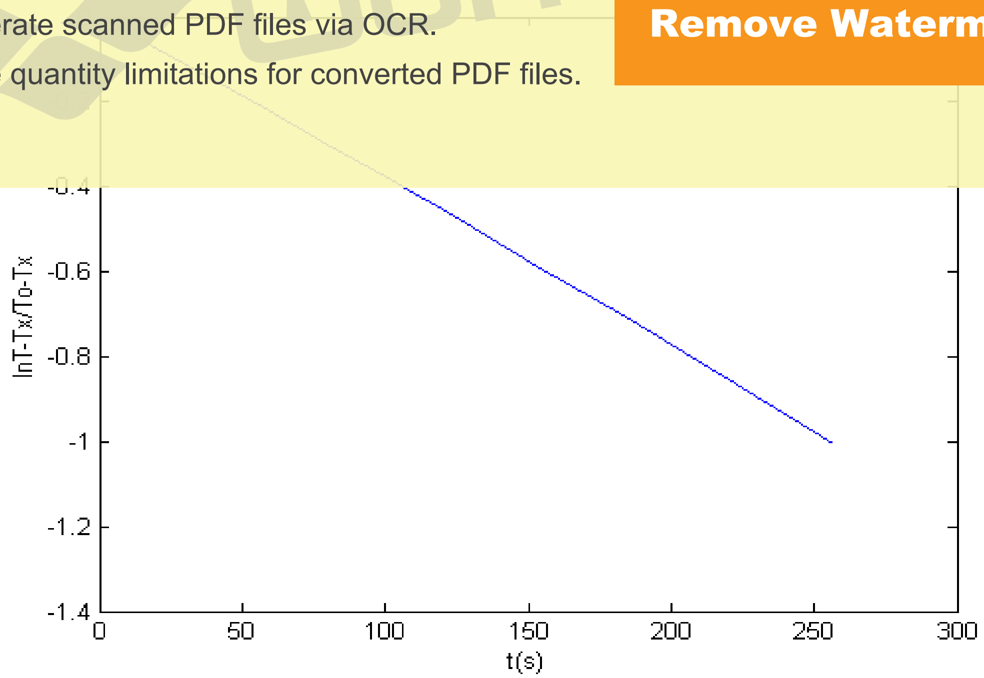

Figure (5.32) the variation of ($\ln\frac{\theta}{\theta_i}$) against time interval.

(Position of cylinder=15.25 cm).
(T=80,77,74,71,68,65,62,59,56,53,50).

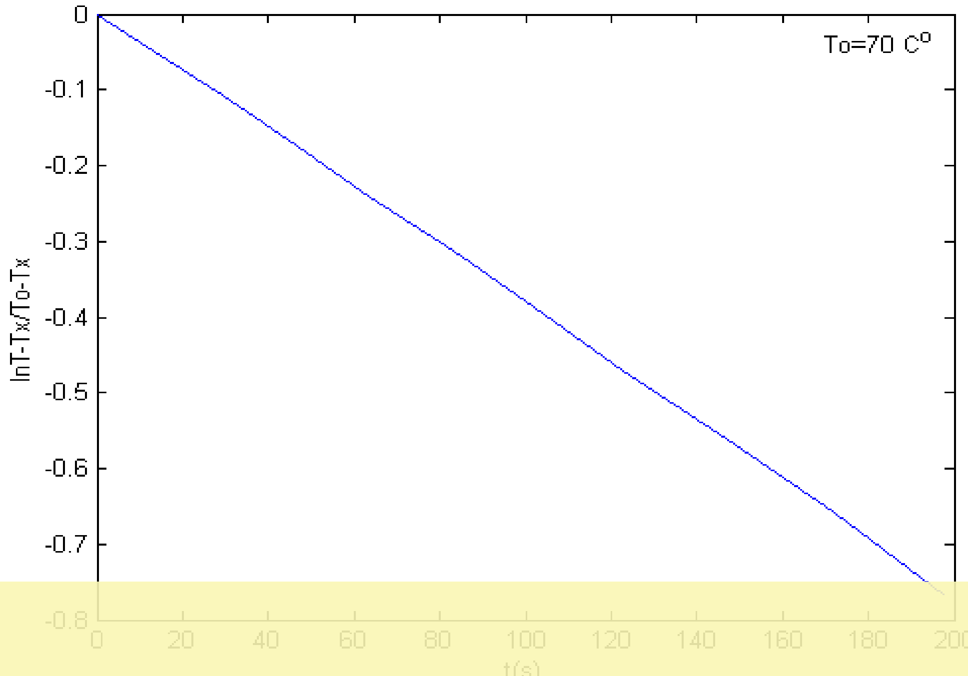

Figure (5.33) the variation of ($\ln\frac{\theta}{\theta_i}$) against time interval.

(Position of cylinder=15.25 cm). (T=70,68,66,64,62,60,58,56,54,52,50).

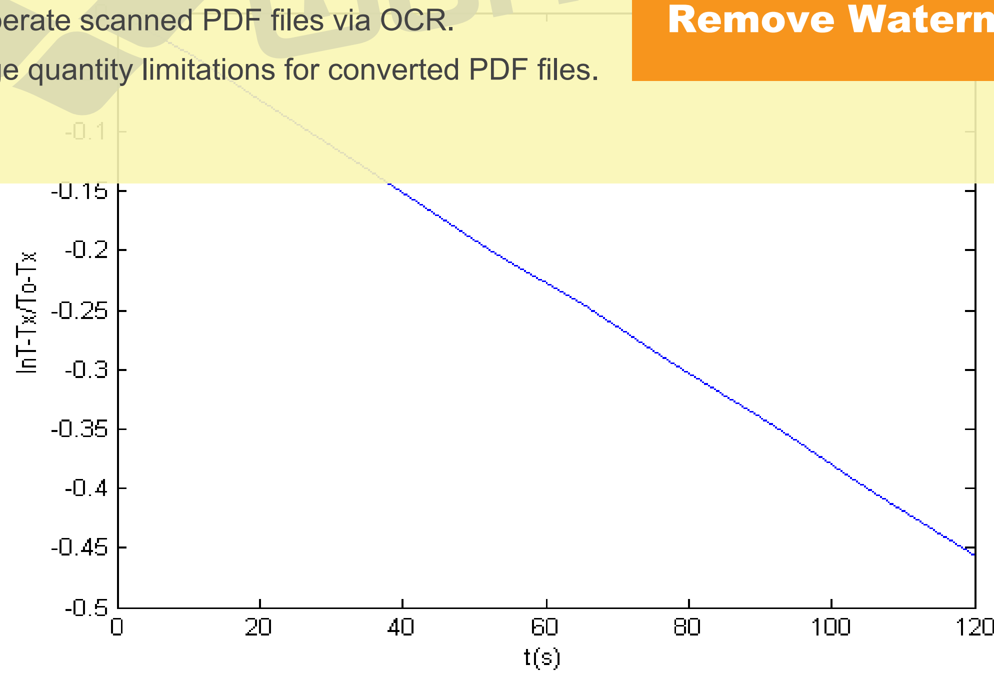

Figure (5.34) the variation of ($\ln\frac{\theta}{\theta_i}$) against time interval.

(Position of cylinder=15.25 cm).
(T=60,59,58,57,56,55,54,53,52,51,50).

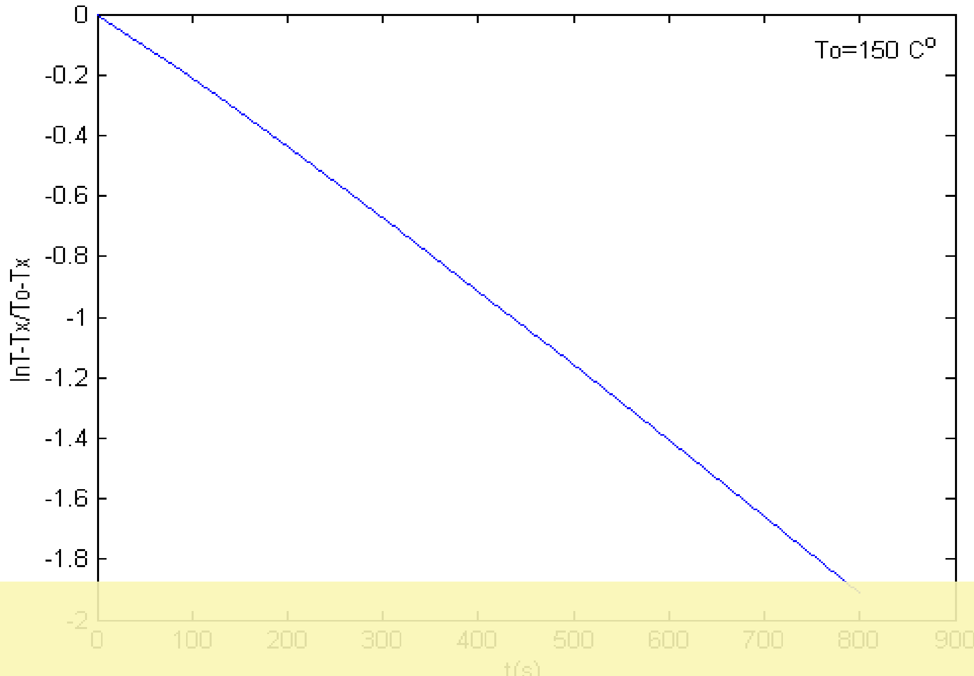

Figure (5.35) the variation of $(\ln\frac{\theta}{\theta_i})$ against time interval.

(Position of cylinder=19cm). (T=150,140,130,120,110,100,90,80,70,60,50).

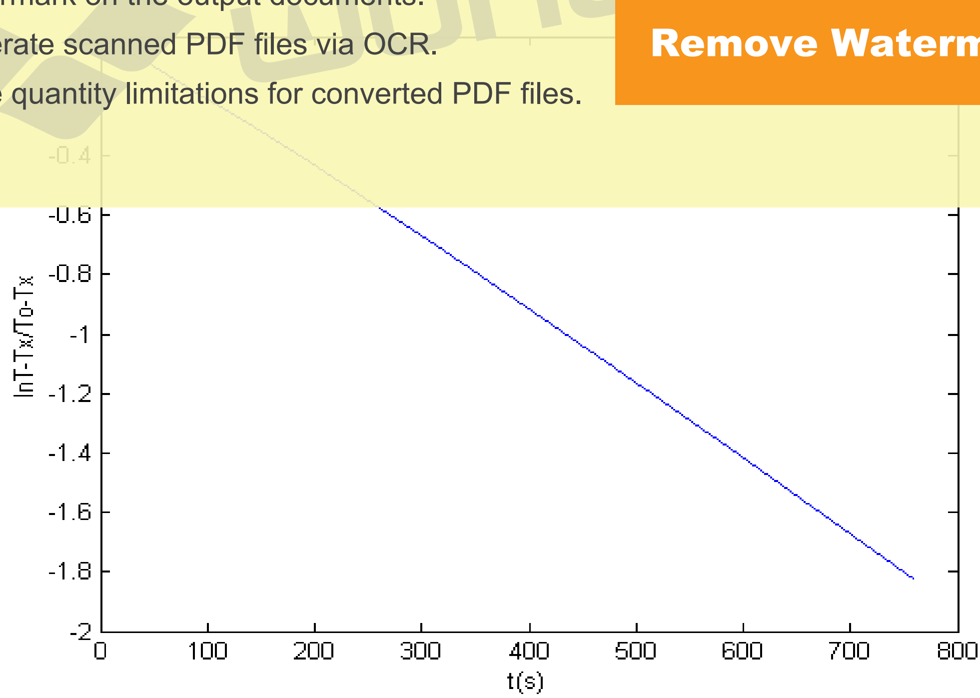

Figure (5.36) the variation of $(\ln\frac{\theta}{\theta_i})$ against time interval.

(Position of cylinder=19 cm).
(T=140,131,122,113,104,95,86,77,68,59,50).

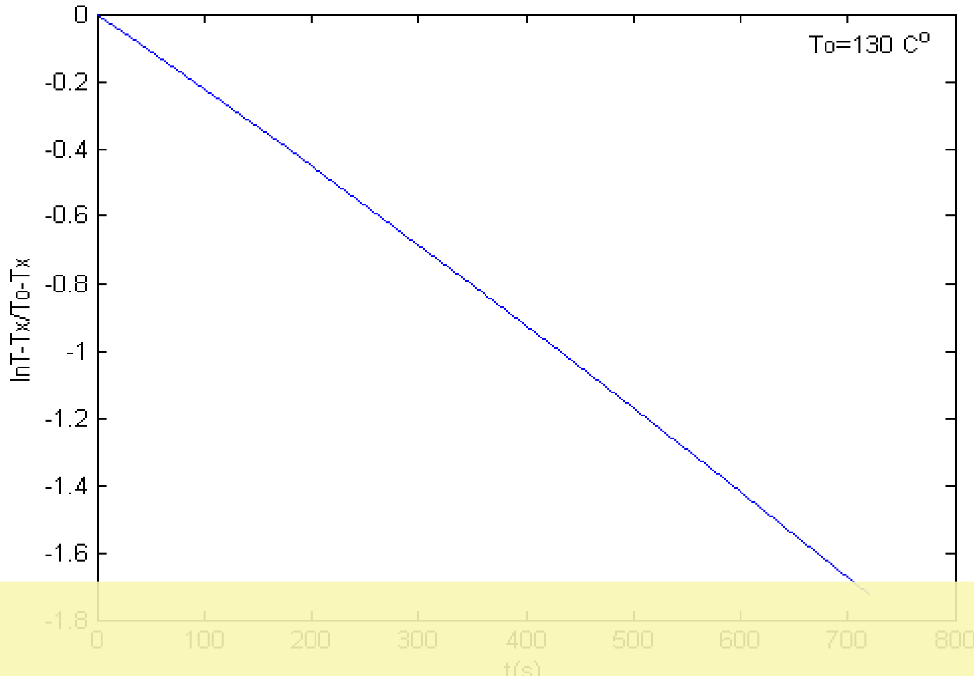

Figure (5.37) the variation of $(\ln\frac{\theta}{\theta_i})$ against time interval.

(Position of cylinder=19 cm). (T=130,122,114,106,98,90,82,74,66,58,50).

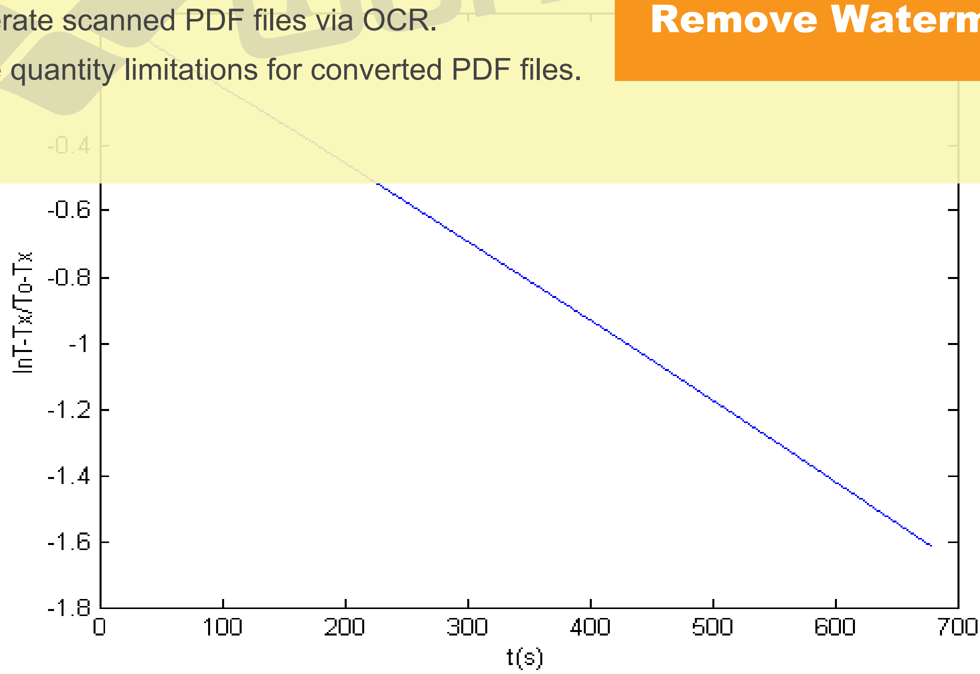

Figure (5.38) the variation of $(\ln\frac{\theta}{\theta_i})$ against time interval.

(Position of cylinder=19 cm).
(T=120,113,106,99,92,85,78,71,64,57,50).

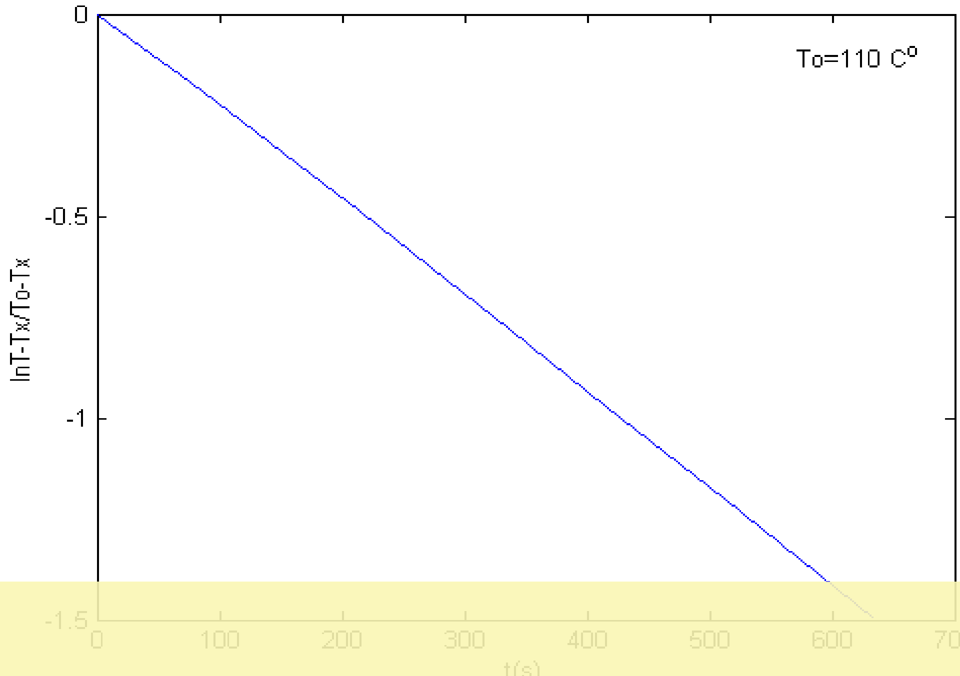

Figure (5.39) the variation of ($\ln\frac{\theta}{\theta_i}$) against time interval.

(Position of cylinder=19 cm). (T=110,104,98,92,86,80,74,68,62,56,50).

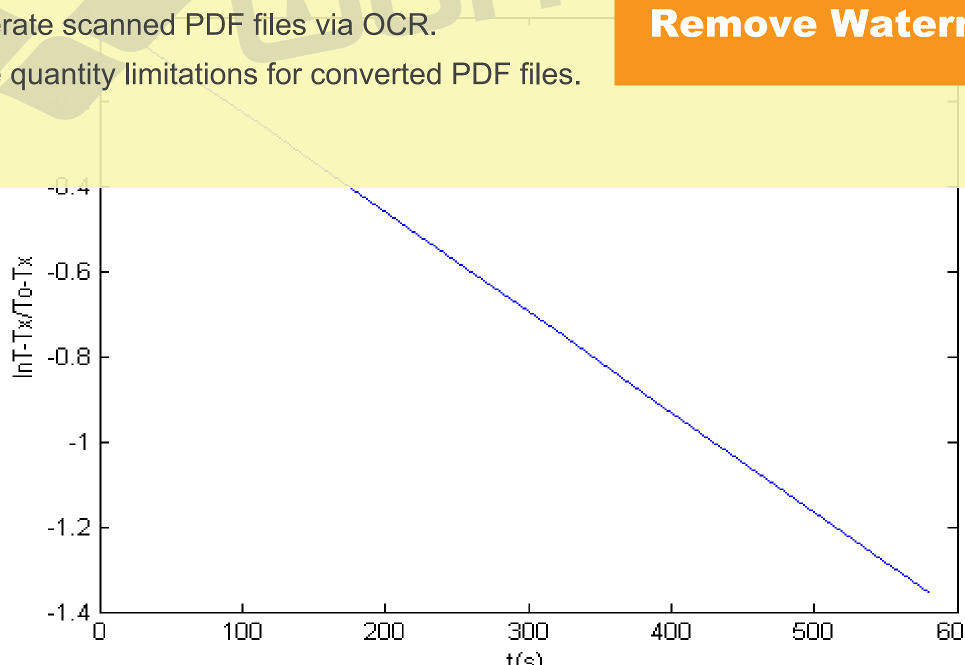

Figure (5.40) the variation of ($\ln\frac{\theta}{\theta_i}$) against time interval.

(Position of cylinder=19 cm).
(T=100,95,90,85,80,75,70,65,60,55,50).

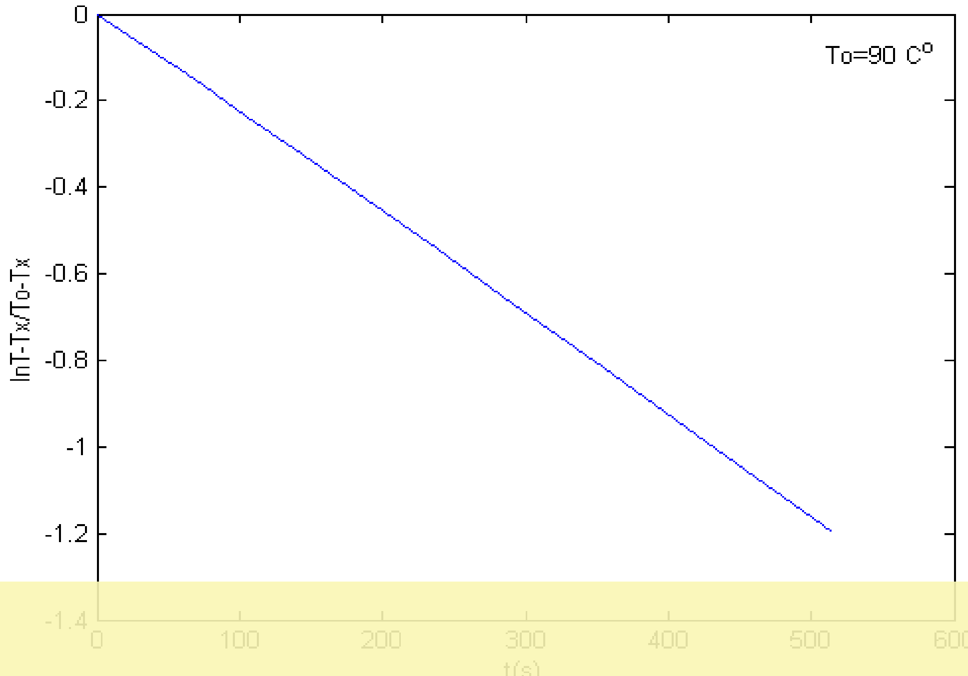

Figure (5.41) the variation of ($\ln\frac{\theta}{\theta_i}$) against time interval.

(Position of cylinder=19 cm). (T=90, 86, 82, 78, 74, 70, 66, 62, 58, 50).

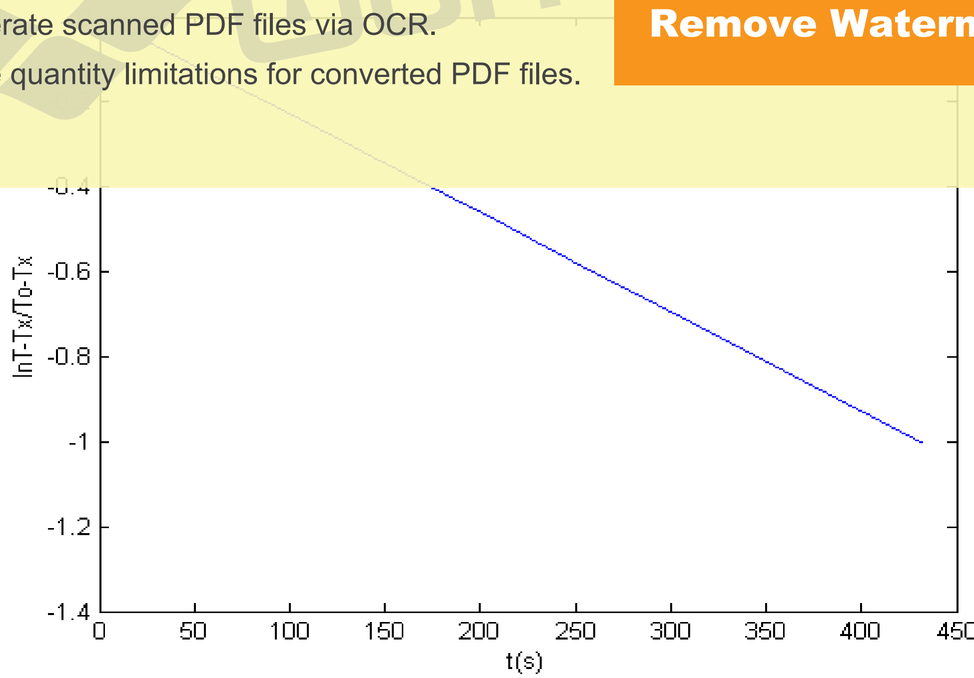

Figure (5.42) the variation of ($\ln\frac{\theta}{\theta_i}$) against time interval.

(Position of cylinder=19 cm).
(T=80,77,74,71,68,65,62,59,56,53,50).

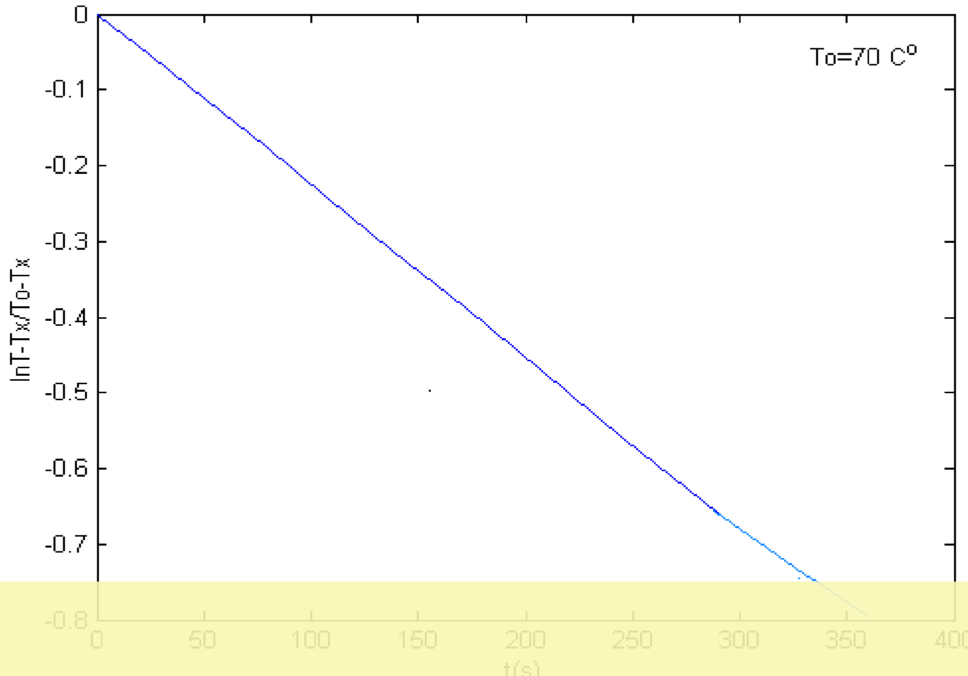

Figure (5.43) the variation of $(\ln\frac{\theta}{\theta_i})$ against time interval.

(Position of cylinder=19 cm). (T=70,68,66,64,62,60,58,56,54,52,50).

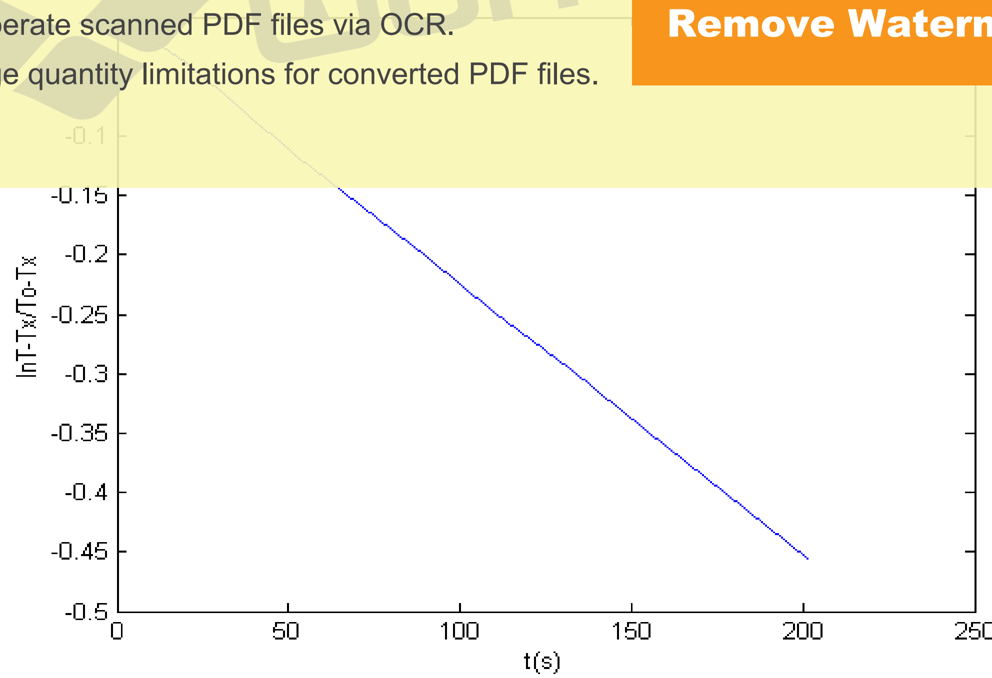

Figure (5.44) the variation of $(\ln\frac{\theta}{\theta_i})$ against time interval.

(Position of cylinder=19 cm).
(T=60,59,58,57,56,55,54,53,52,51,50).

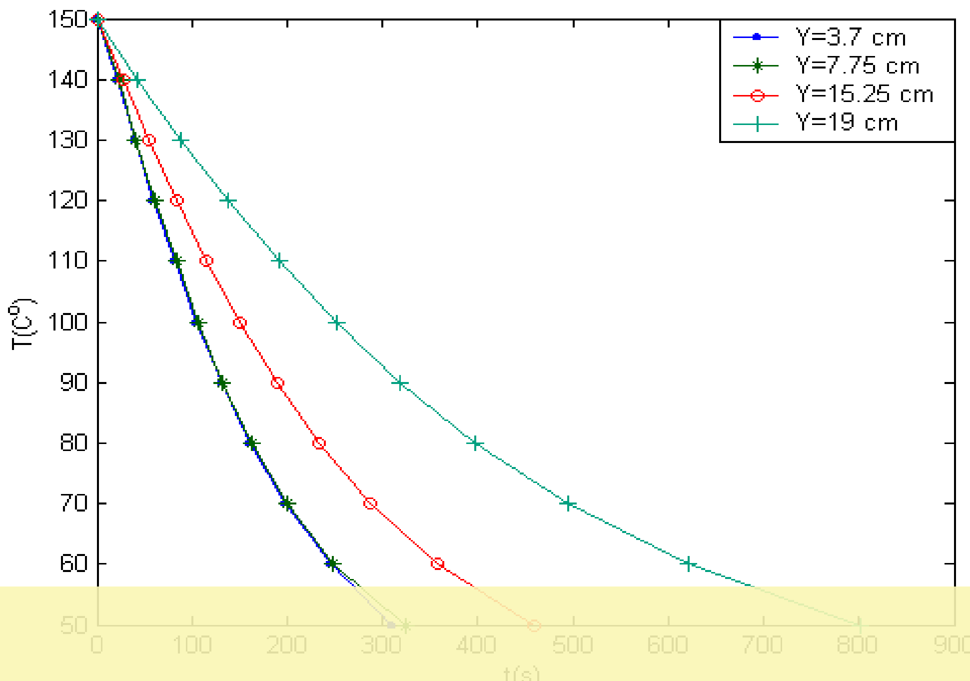

Figure (5.45) variation of temperature against time interval for different cylinder position at some reference temperature (T_o).

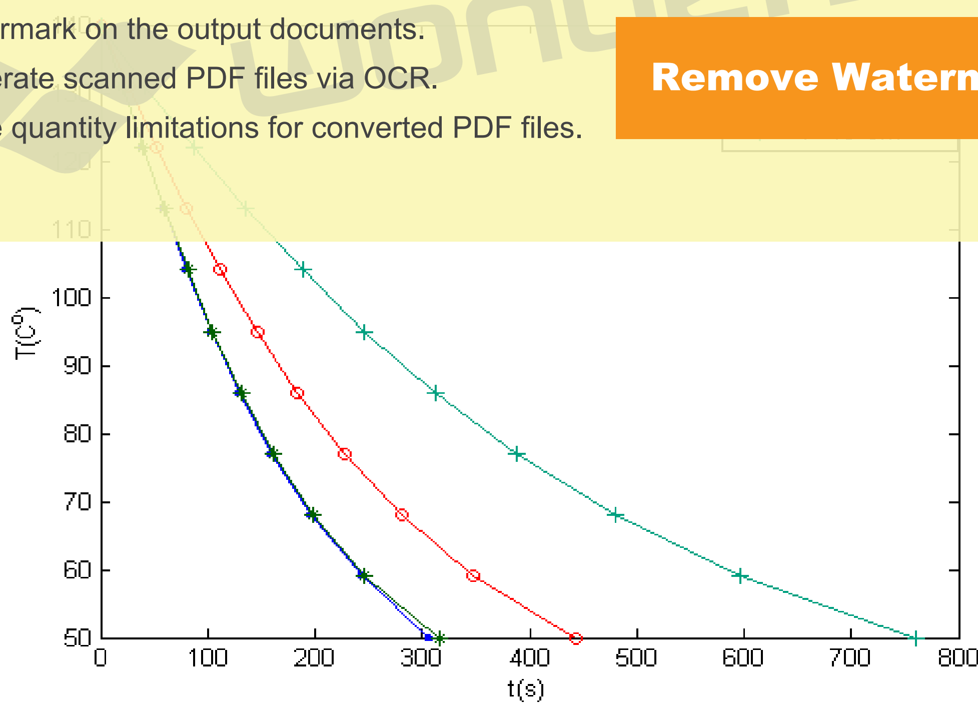

Figure (5.46) variation of temperature against time interval for different cylinder position at some reference temperature (T_o).

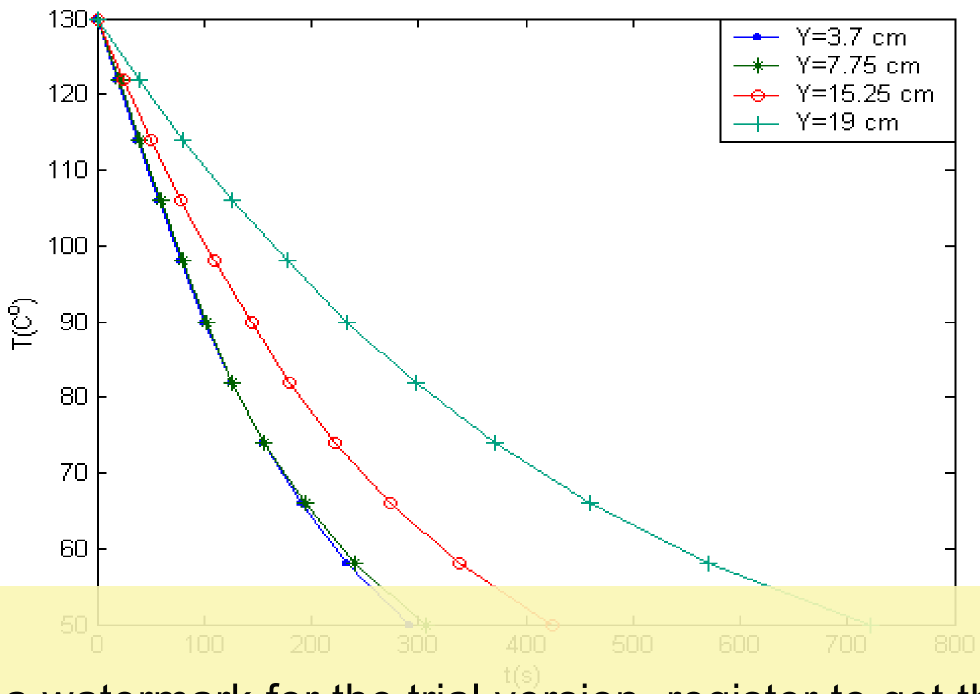

Figure (5.47) variation of temperature against time interval for different cylinder position at some reference temperature (T_o).

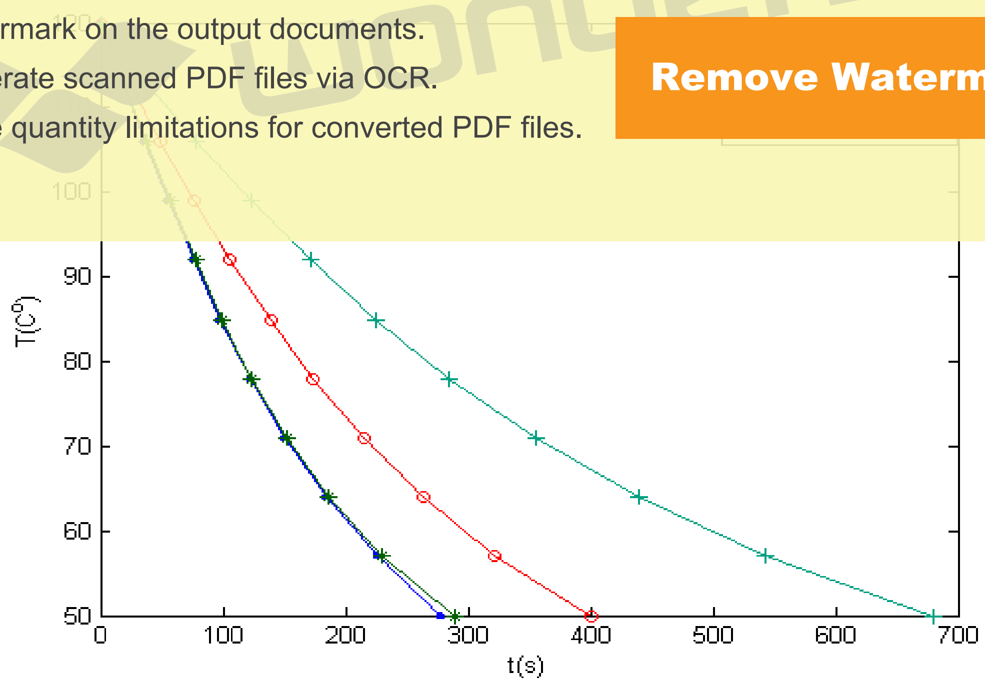

Figure (5.48) variation of temperature against time interval for different cylinder position at some reference temperature (T_o).

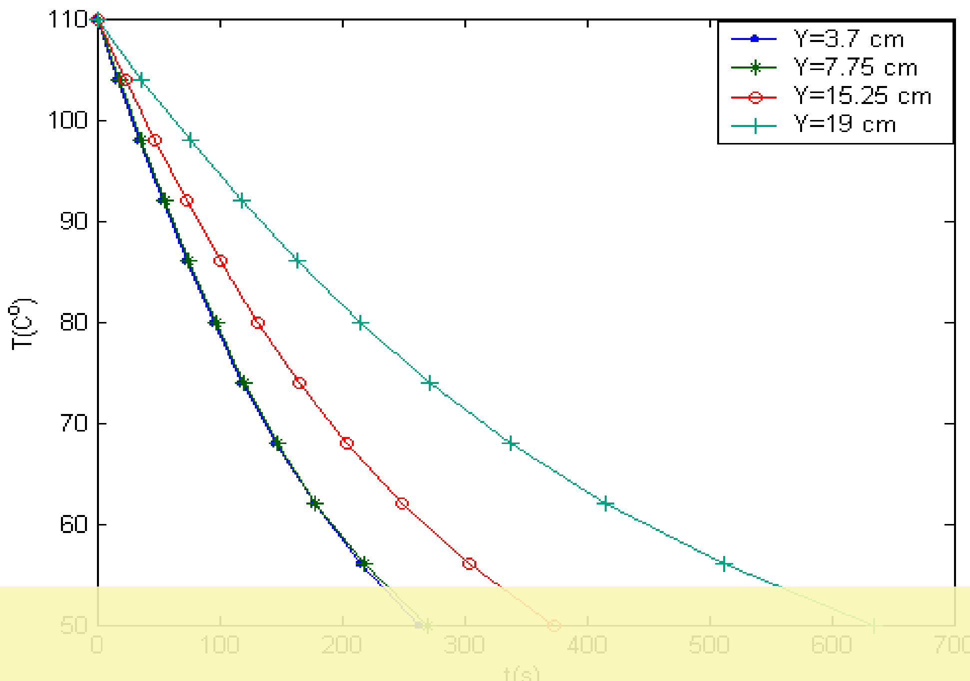

Figure (5.49) variation of temperature against time interval for different cylinder position at some reference temperature (T_o).

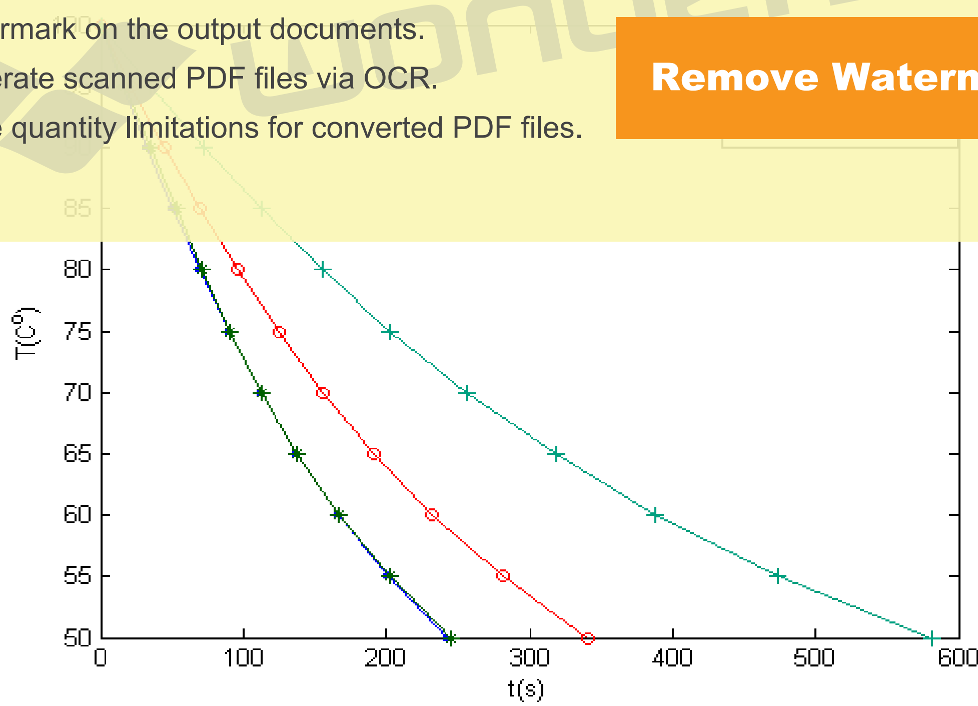

Figure (5.50) variation of temperature against time interval for different cylinder position at some reference temperature (T_o).

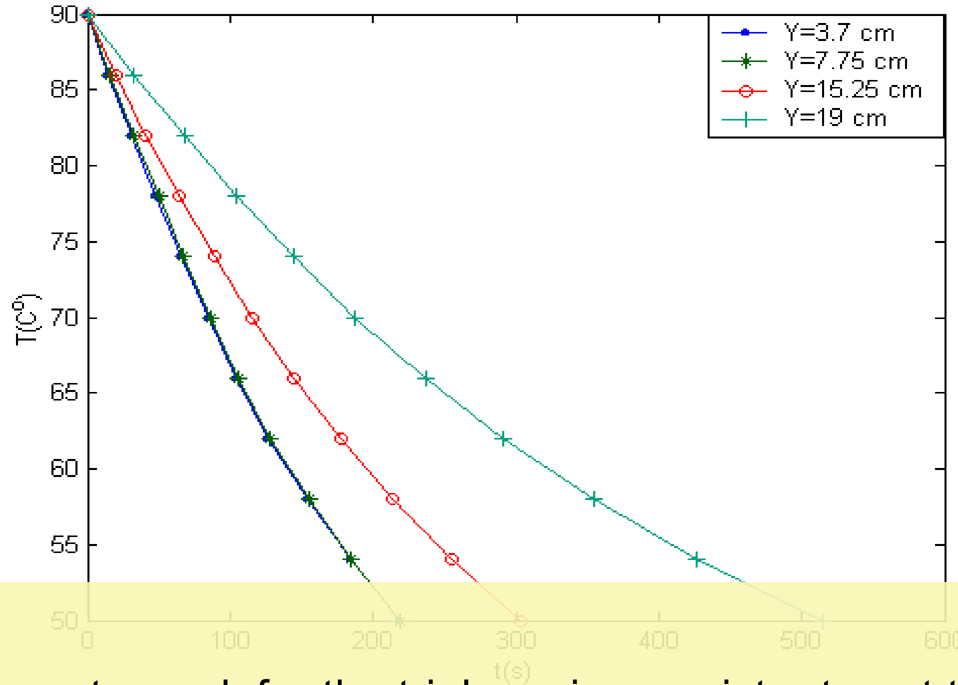

Figure (5.51) variation of temperature against time interval for different cylinder position at some reference temperature (T_o).

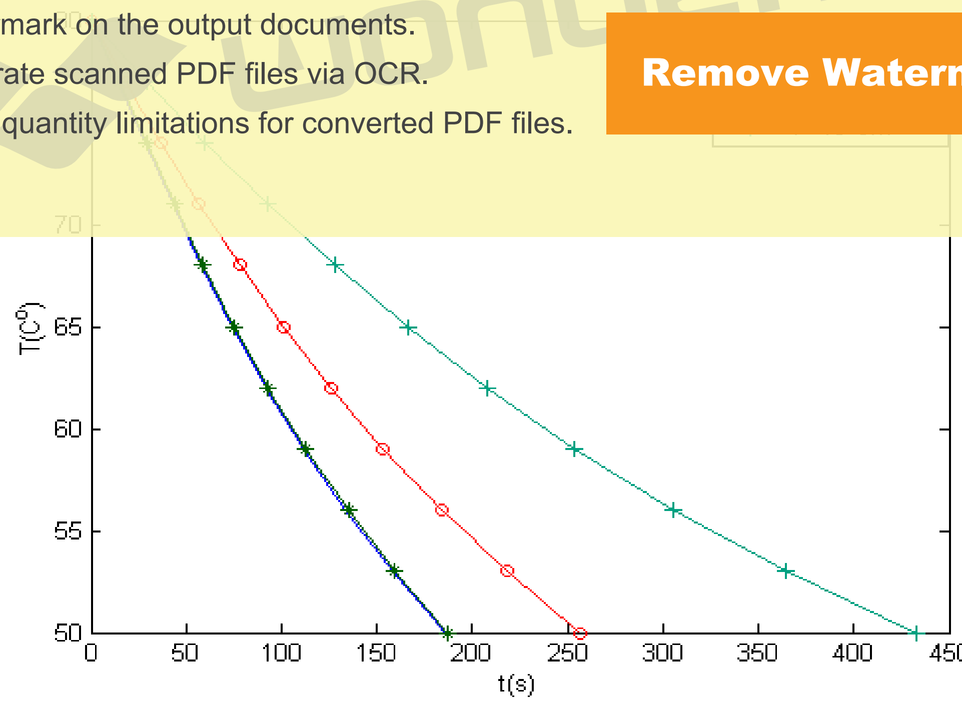

Figure (5.52) variation of temperature against time interval for different cylinder position at some reference temperature (T_o).

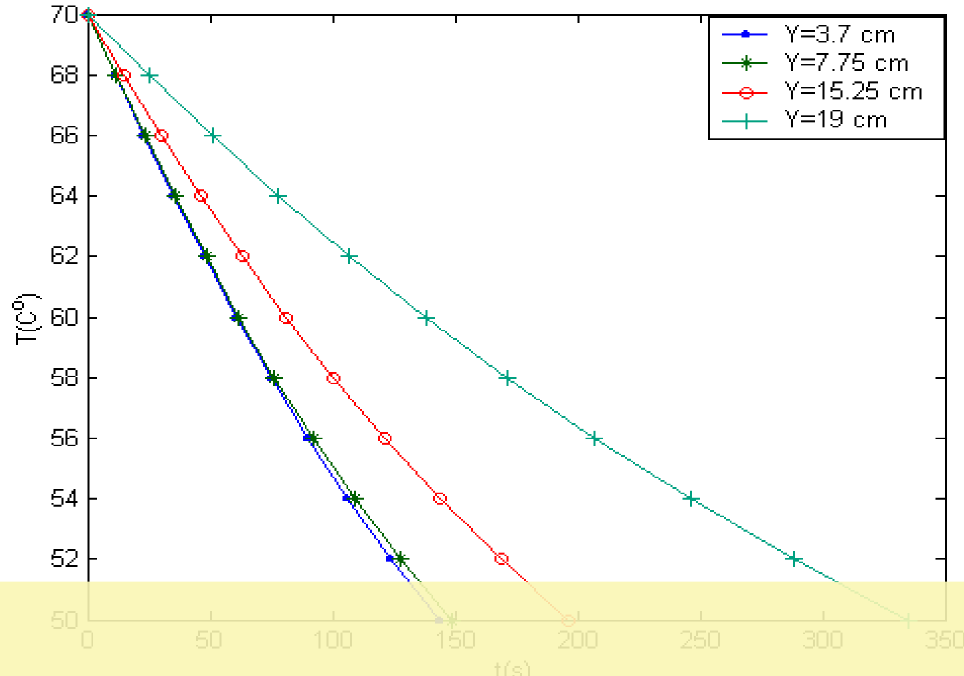

Figure (5.53) variation of temperature against time interval for different cylinder position at some reference temperature (T_o).

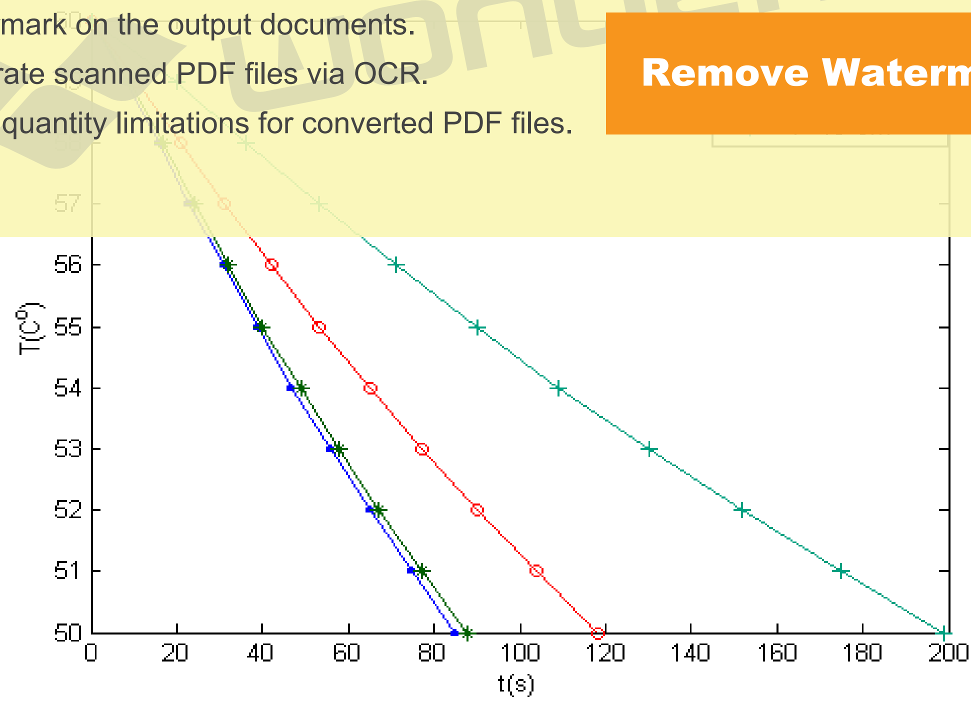

Figure (5.54) variation of temperature against time interval for different cylinder position at some reference temperature (T_o).

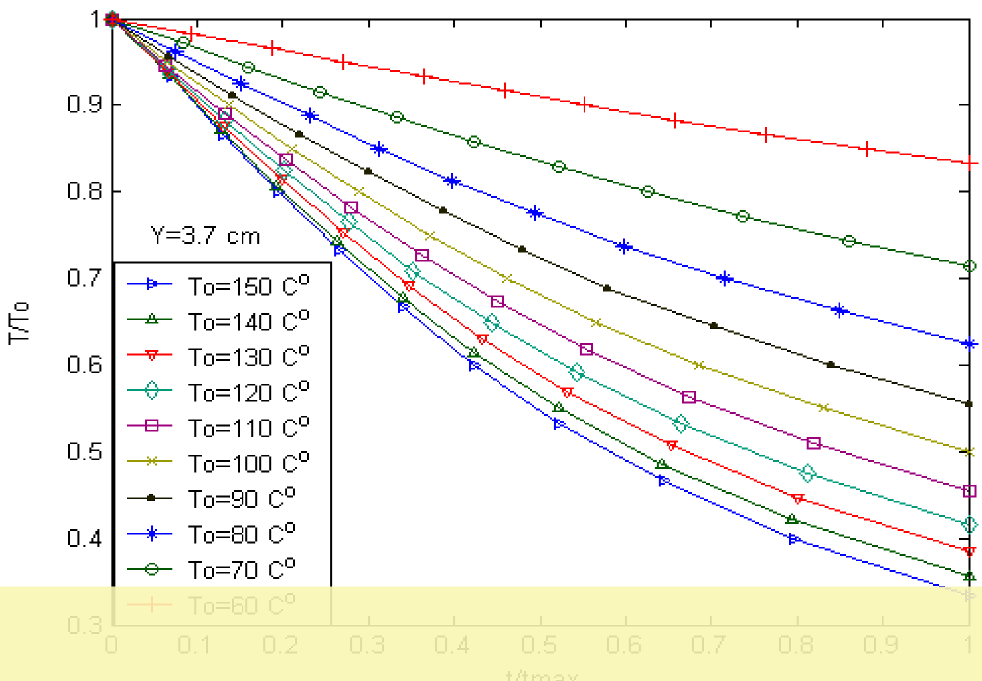

Figure (5.55) variation of temperature ratio (T/T_o) against time ratio (t/t

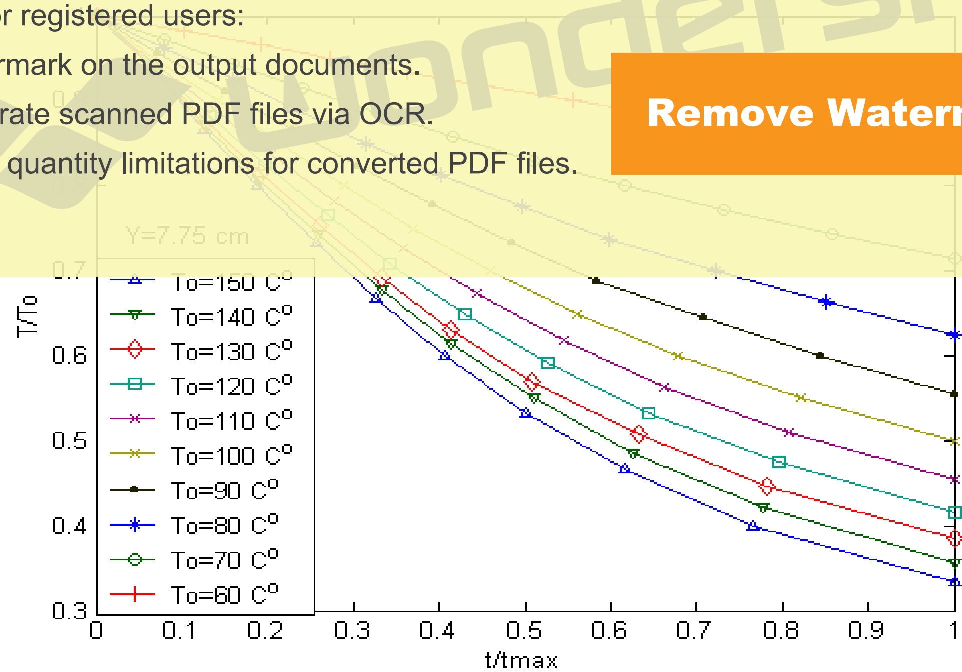

Figure (5.56) variation of temperature ratio (T/T_o) against time ratio (t/t_{max}).

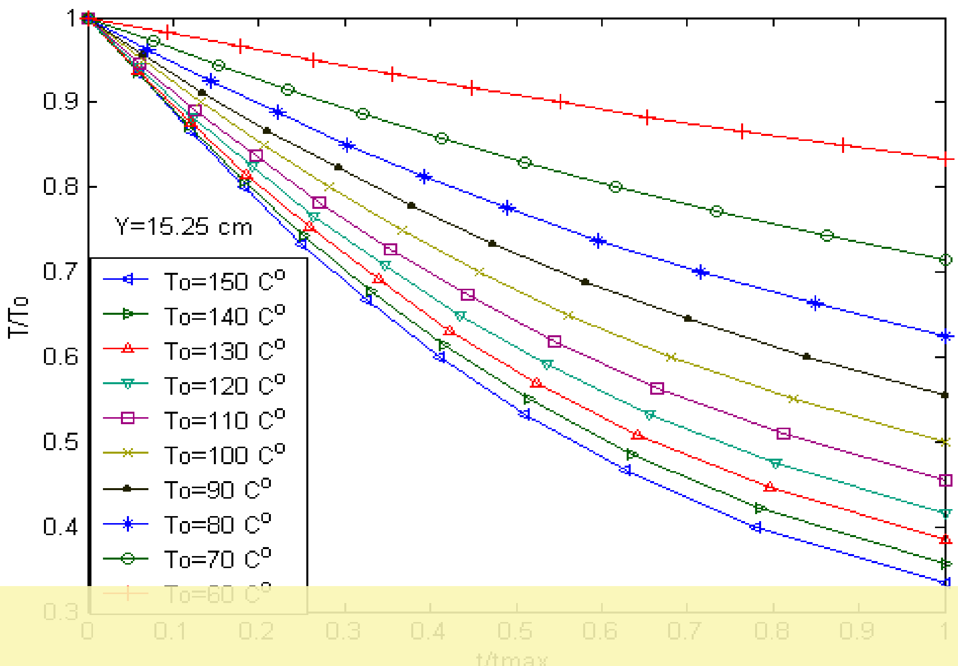

Figure (5.57) variation of temperature ratio (T/T_o) against time ratio (t/t_{max}).

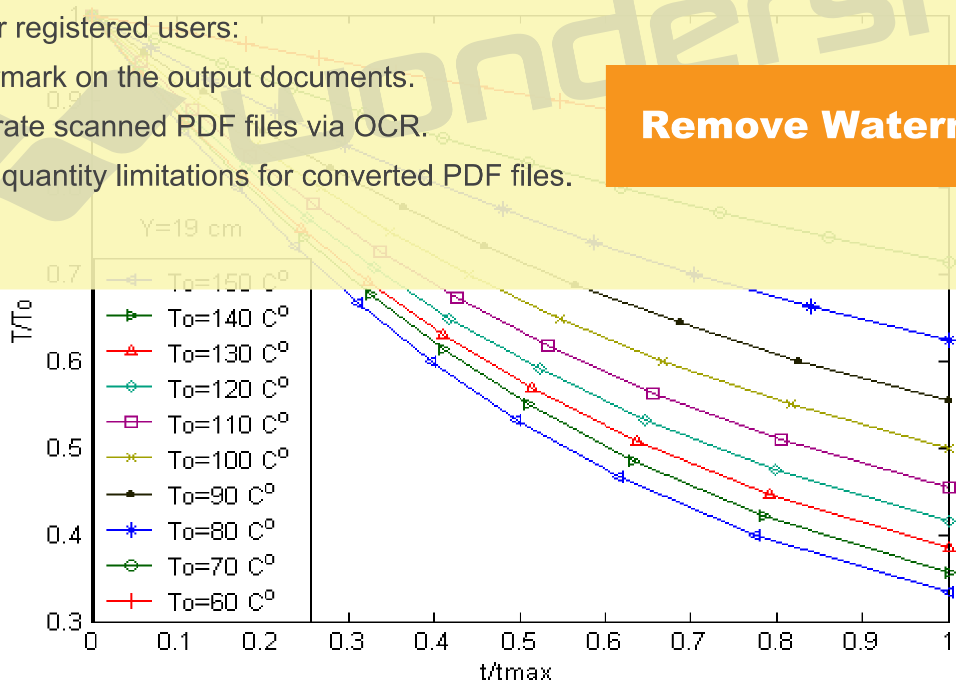

Figure (5.58) variation of temperature ratio (T/T_o) against time ratio (t/t_{max}).

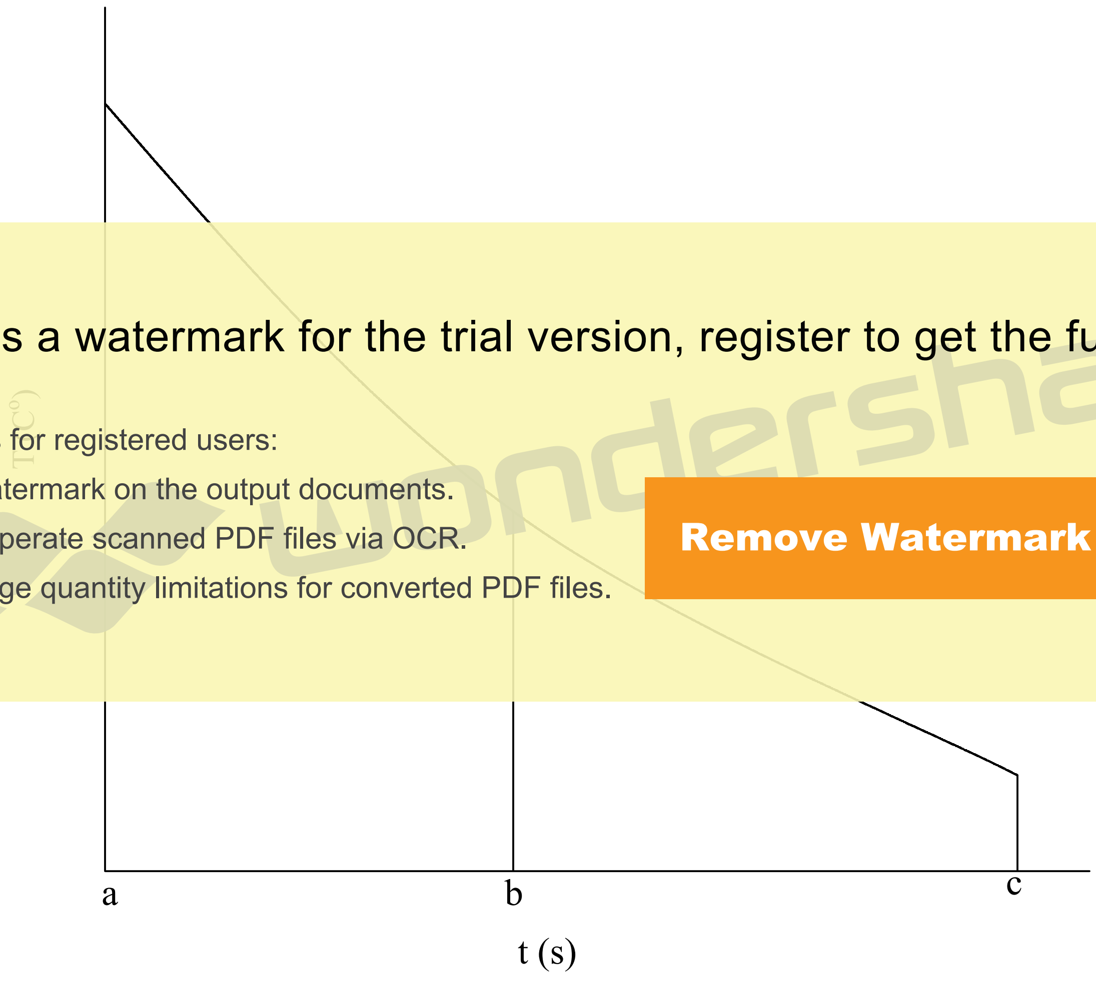

Figure (5.59): General Shape of Temperature Variation

5.3 computational Results

From the experimental results, theoretical results proposed in this chapter are obtained by using MATLAP 6.1 computer program. For each reference temperature (T_o), two parameters were carried out for the purpose of the discussion. These parameters were summarized as the heat transfer coefficient and Nusselt number. These results are divided into four groups:-

a. Determination for the variation of local heat transfer coefficient and Nusselt number with time interval.
b. Determination for the variation of mean heat transfer coefficient and Nusselt number with time or cylinder position.
c. Determination for the variation of heat transfer coefficient and Nusselt number with temperature ratio of (T/T_{max}).
d. Determination for the variation of average heat transfer coefficient and Nusselt number with cylinder po[illegible]

5.3.1 Variation of (h_{local}) and (Nu_{local}) with time interval.

From figure (5.1-5.4) and by using MATLAB 6.1 program, the local heat transfer coefficient5 and Nusselt number with time at that moment will be obtained as shown in figures (5.64-5.83). At same reference temperature (T_o) with different cylinder position, the local heat transfer coefficient and Nusselt will be increased because of temperature deference is decreased depending on transient conduction equation. The rate of increasing in local heat transfer coefficient and Nusselt number with time at that moment will be increased as cylinder position associated with air flow that means, the cylinder position (Y=19 cm) is placed in dead zone that is means with out air then the rate of heat transfer coefficient will be very slow, the cylinder position (Y=15.25 cm) is placed in front of discontinues wall then the rate of heat transfer is larger then at cylinder position (Y=19 cm) but is less than cylinder position (Y=3.7,7.75 cm) that is placed in front of air flow in a duct then the rate of heat transfer is larger then them that means, the rate of heat transfer will be decreased as cylinder position is increased.

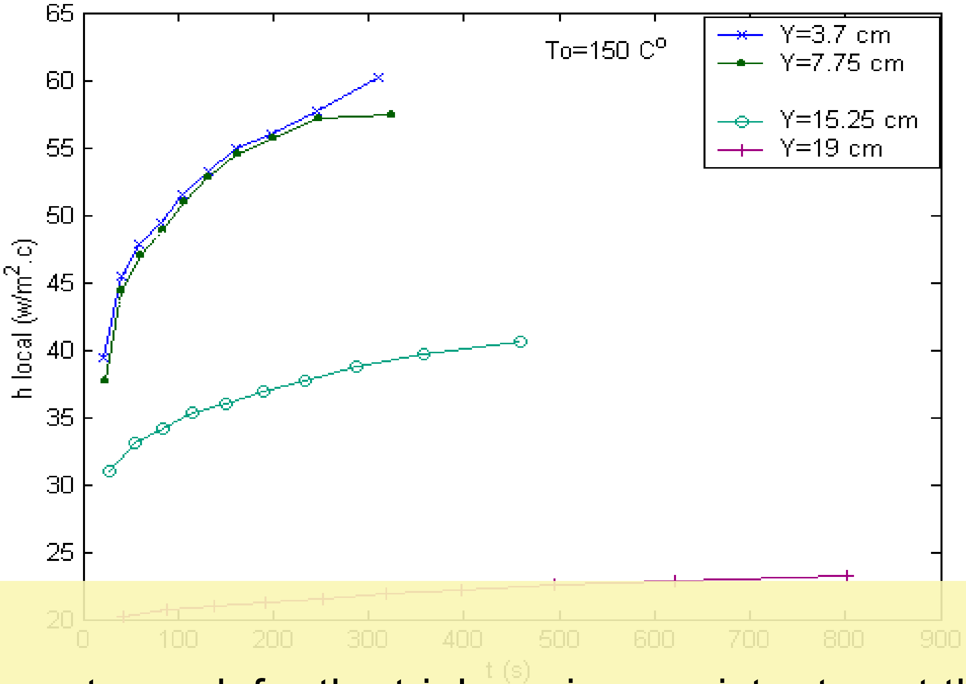

Figure (5.64) the variation of local heat transfer coefficient against time interval.(T=150,140,130,120,110,100,90,80,70,60,50).

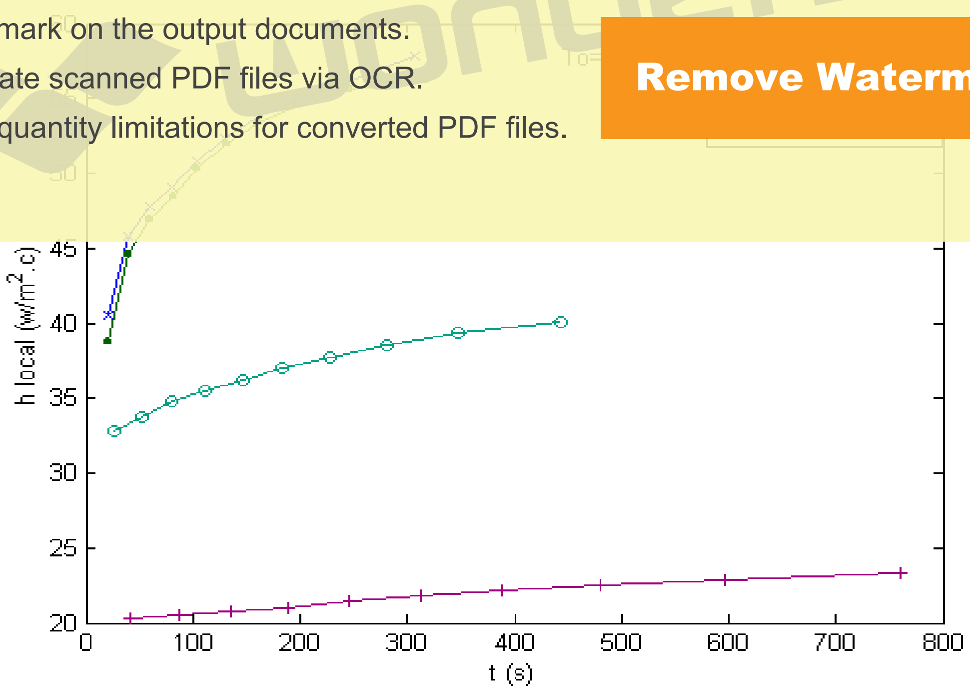

Figure (5.65) the variation of local heat transfer coefficient against time interval.(T=140,131,122,113,104,95,86,77,68,59,50).

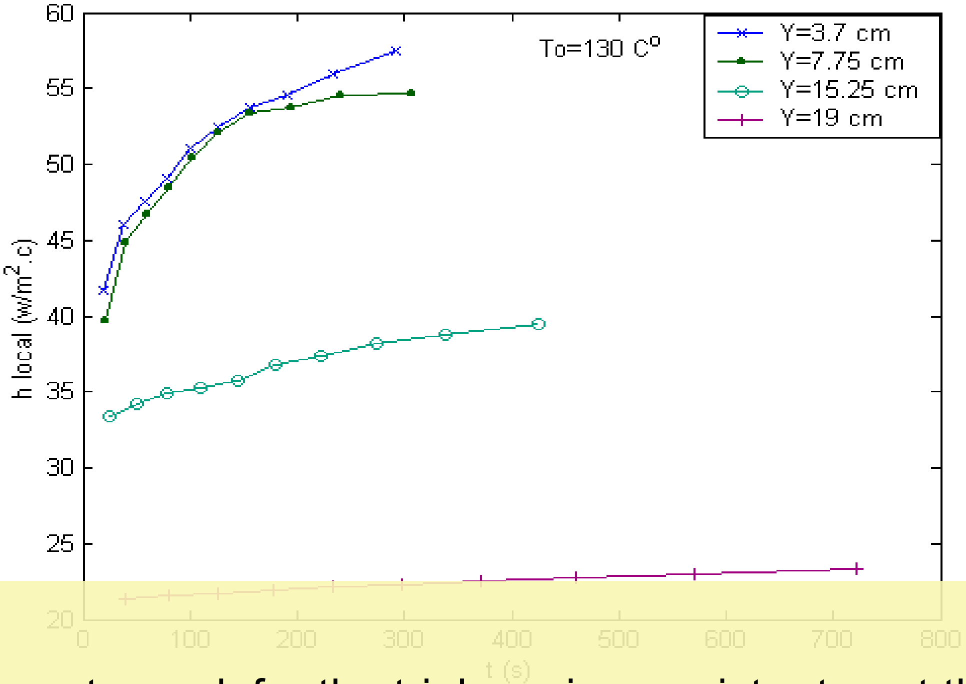

Figure (5.66) the variation of local heat transfer coefficient against time interval.(T=130,122,114,106,98,90,82,74,66,58,50).

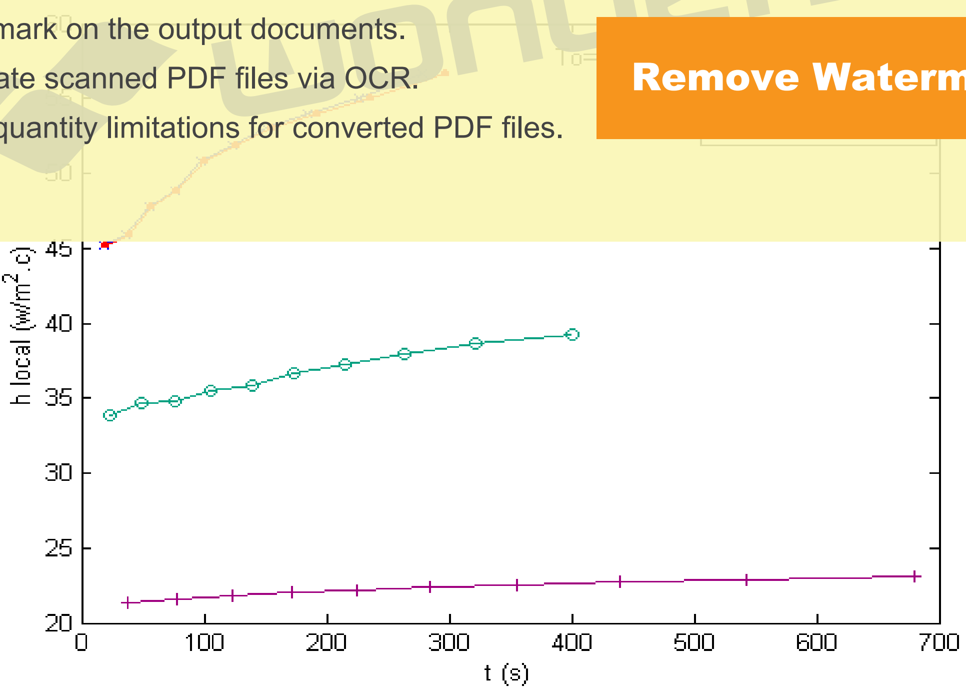

Figure (5.67) the variation of local heat transfer coefficient against time interval.(T=120,113,106,99,92,85,78,71,64,57,50).

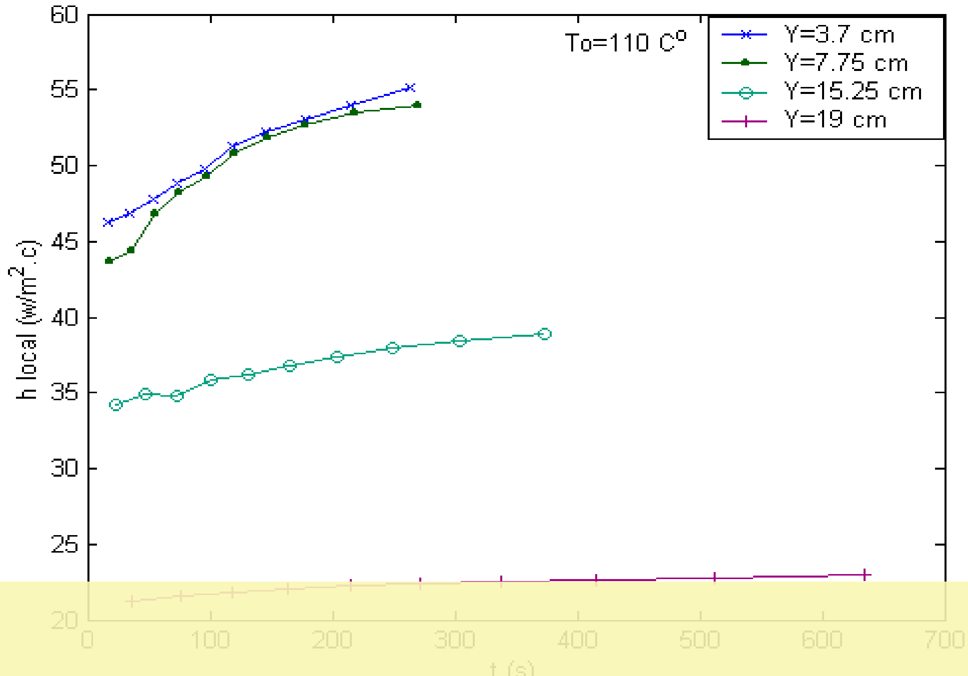

Figure (5.68) the variation of local heat transfer coefficient against time interval.(T=110,104,98,92,86,80,74,68,62,56,50).

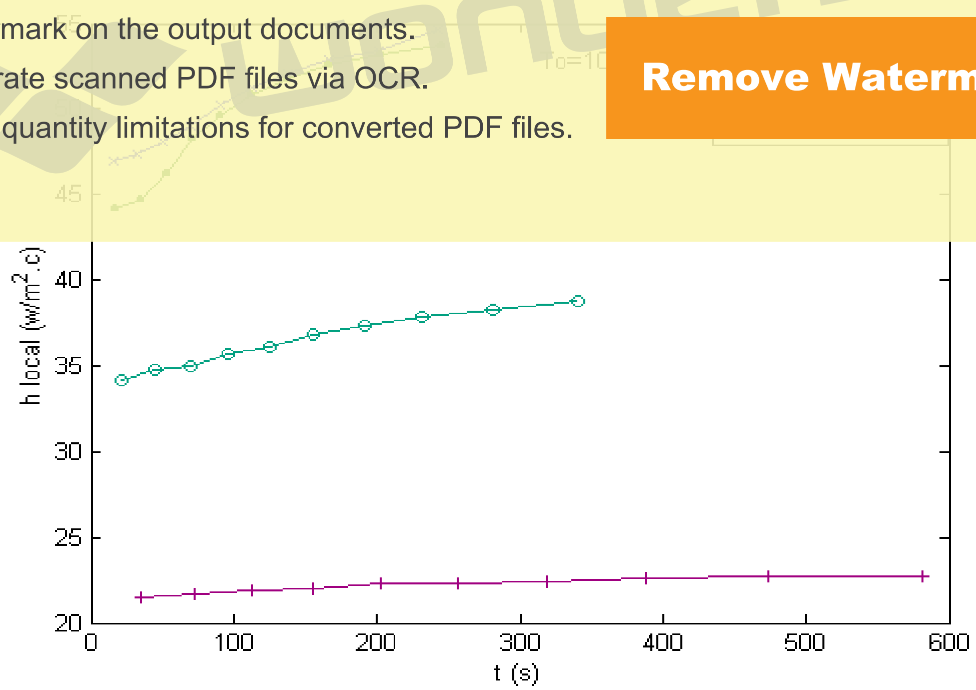

Figure (5.69) the variation of local heat transfer coefficient against time interval.(T=100,95,90,85,80,75,70,65,60,55,50).

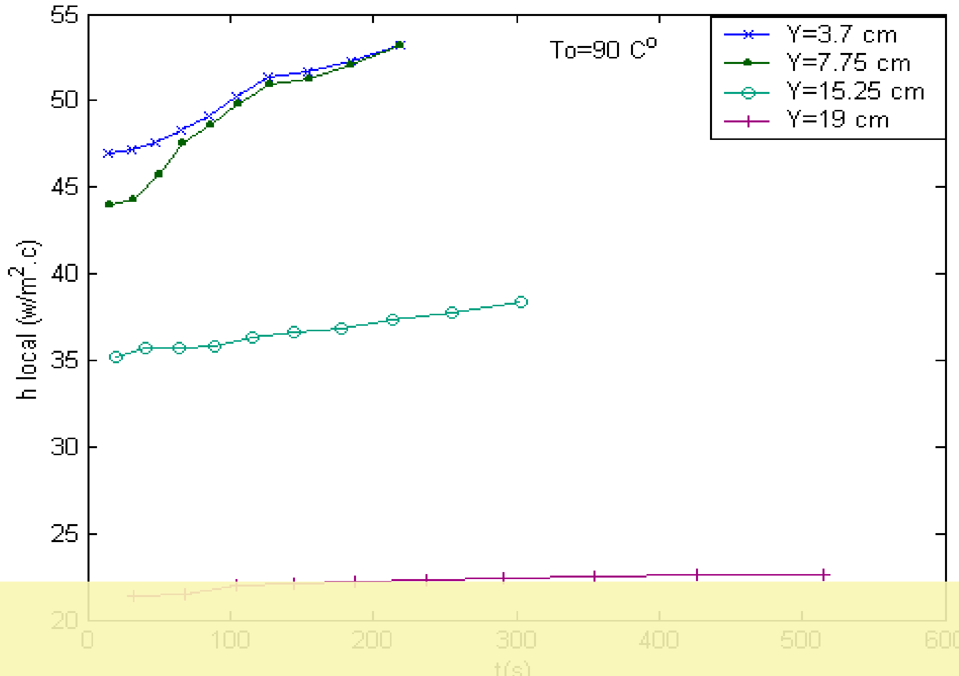

Figure (5.70) the variation of local heat transfer coefficient against time interval.(T=90,86,82,78,74,70,66,62,58,54,50)

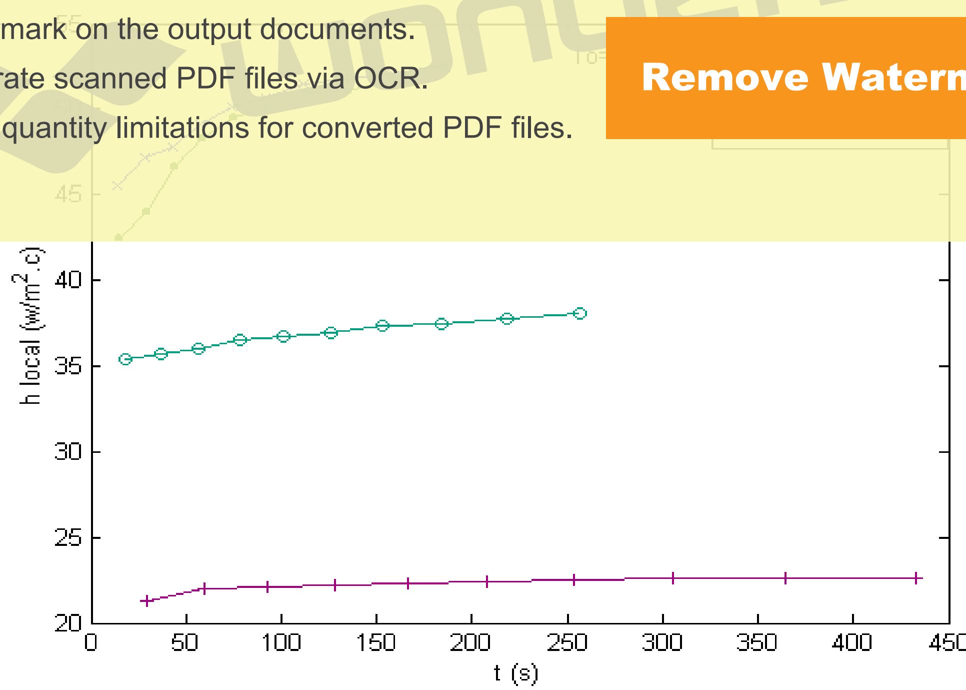

Figure (5.71) the variation of local heat transfer coefficient against time interval.(T=80,77,74,71,68,65,62,59,56,53,50).

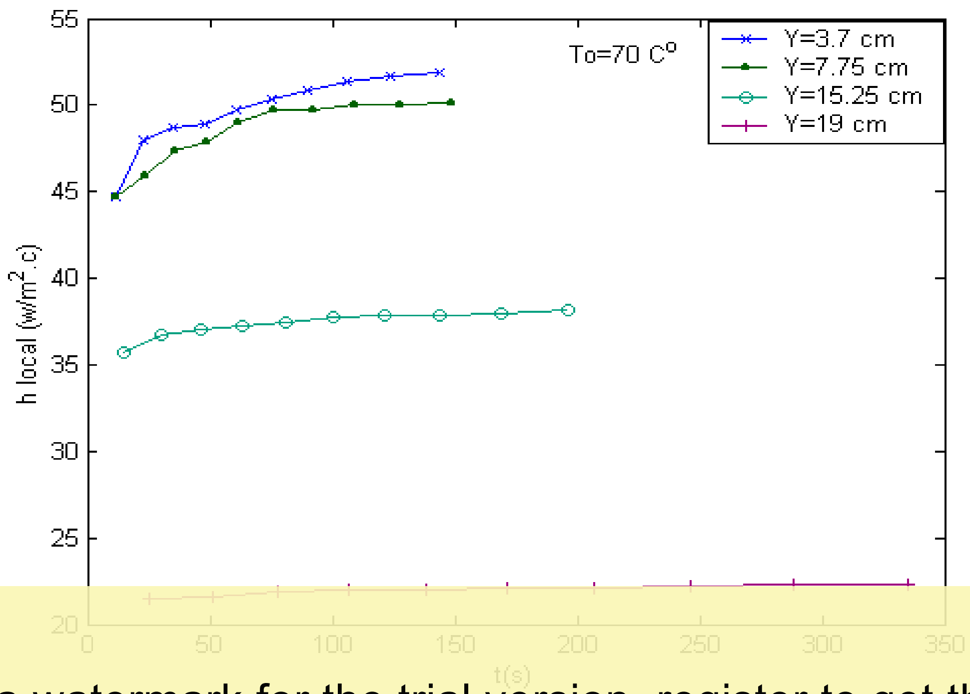

Figure (5.72) the variation of local heat transfer coefficient against time interval.(T=70,68,66,64,62,60,58,56,54,52,50).

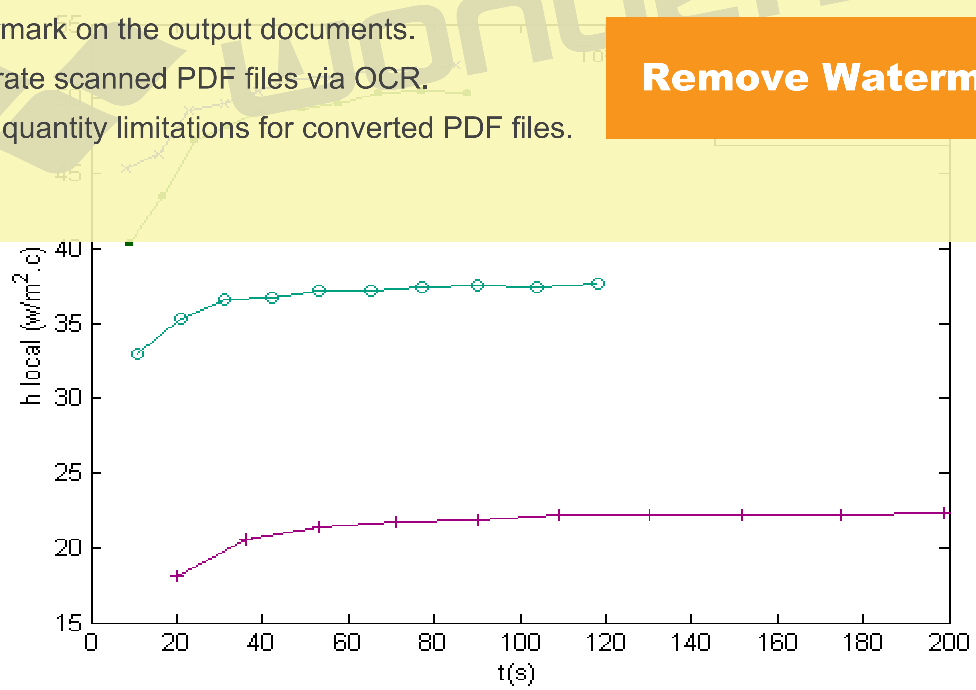

Figure (5.73) the variation of local heat transfer coefficient against time interval.(T=60,59,58,57,56,55,54,53,52,51,50).

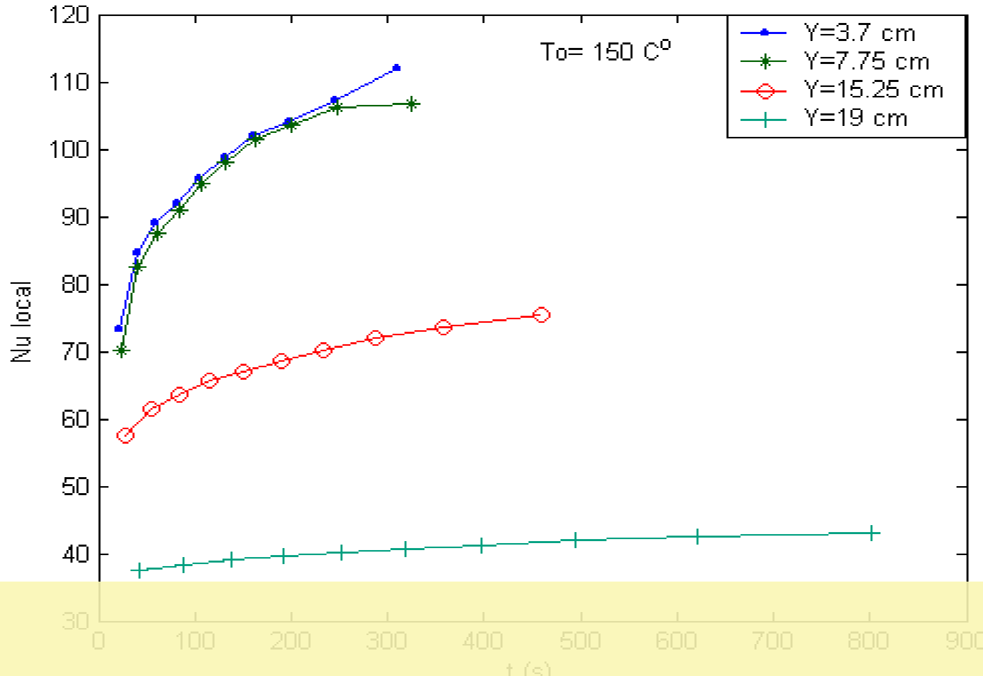

Figure (5.74) the variation of local Nusselt number against time interval.
(T=150,140,130,120,110,100,90,80,70,60,50).

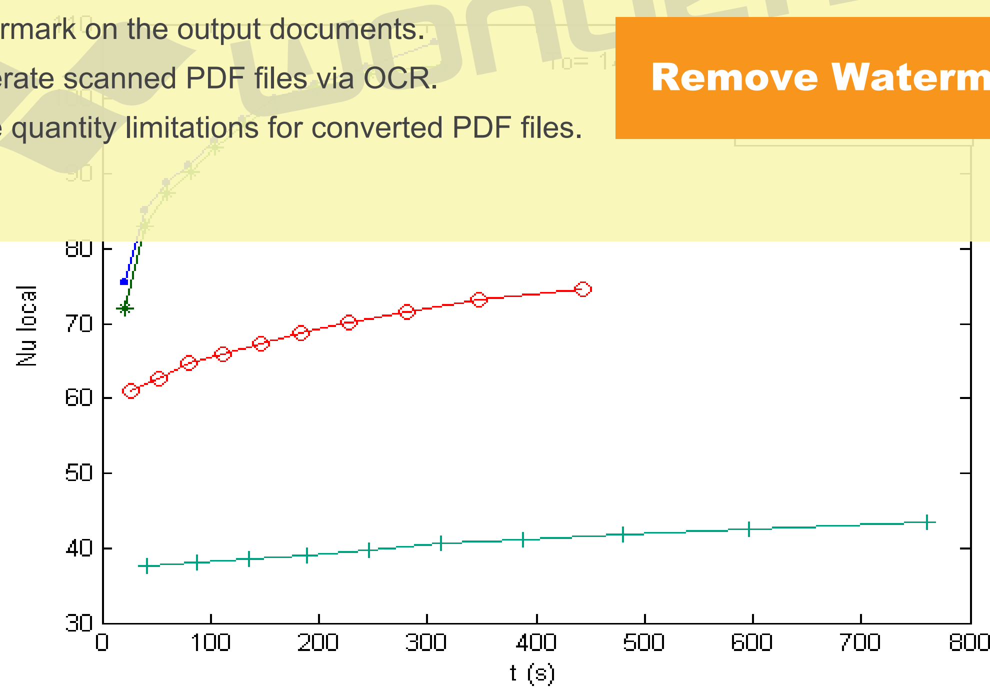

Figure (5.75) the variation of local Nusselt number against time interval.
(T=140,131,122,113,104,95,86,77,68,59,50).

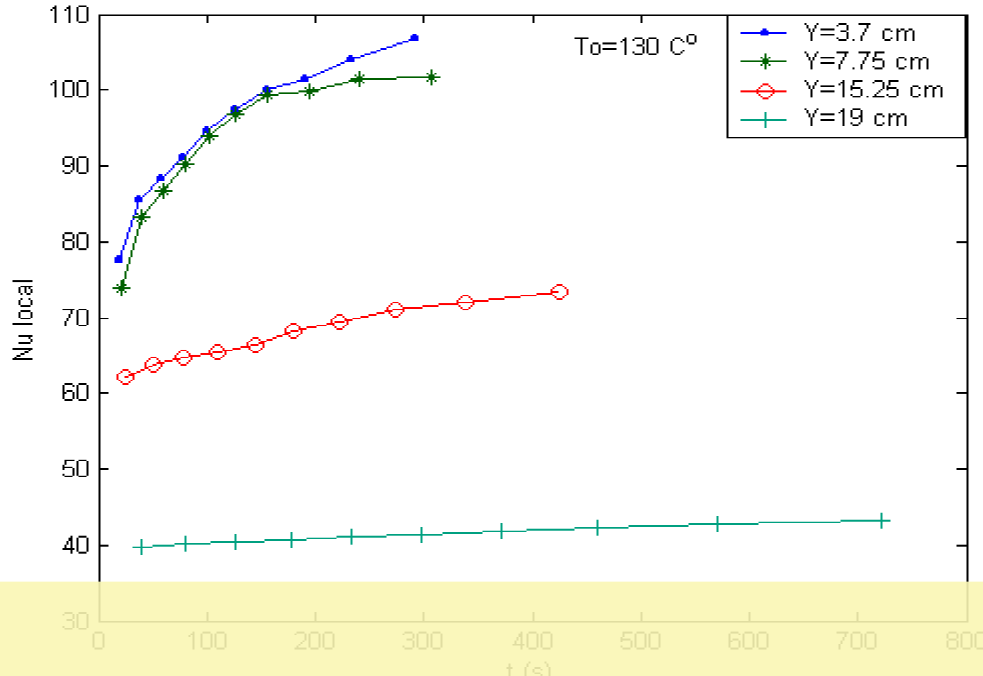

Figure (5.76) the variation of local Nusselt number against time interval.
(T=130,122,114,106,98,90,82,74,66,58,50).

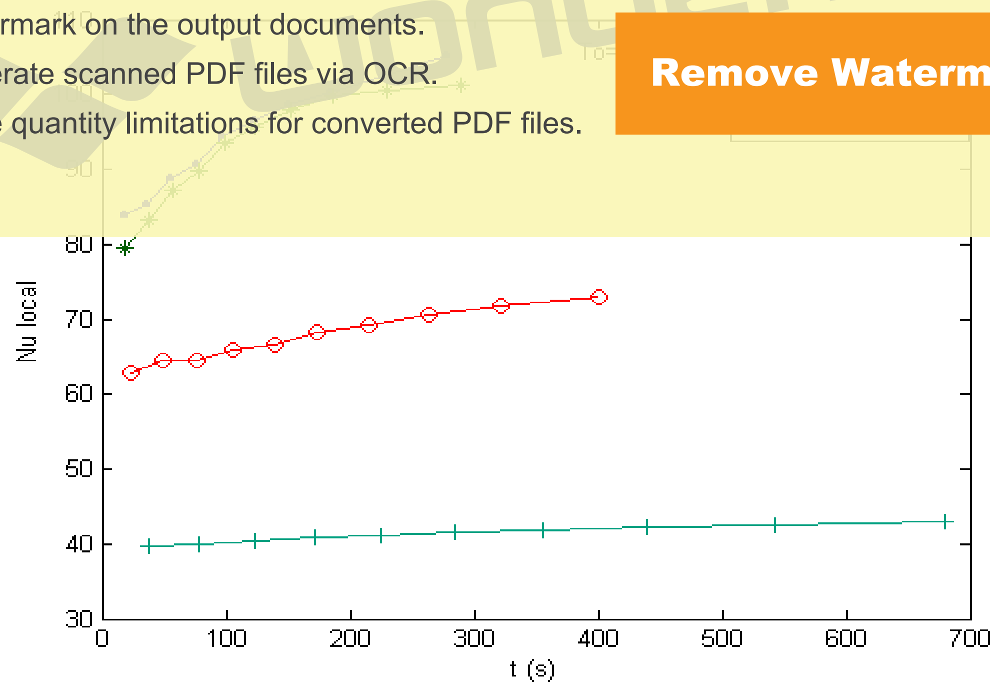

Figure (5.77) the variation of local Nusselt number against time interval.
(T=120,113,106,99,92,85,78,71,64,57,50).

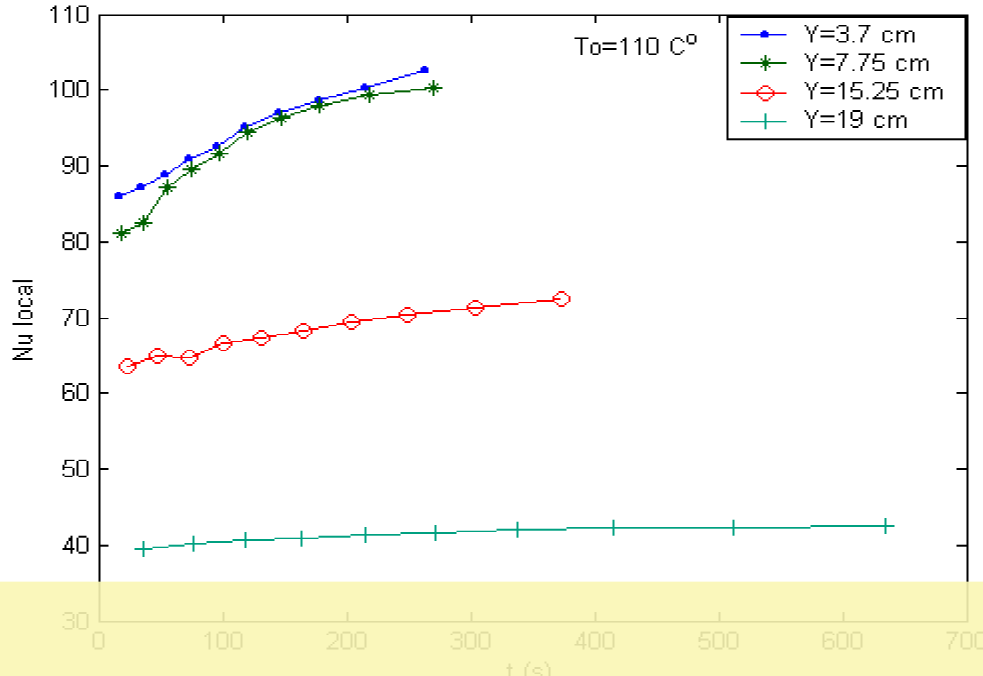

Figure (5.78) the variation of local Nusselt number against time interval.
(T=110,104,98,92,86,80,74,68,62,56,50).

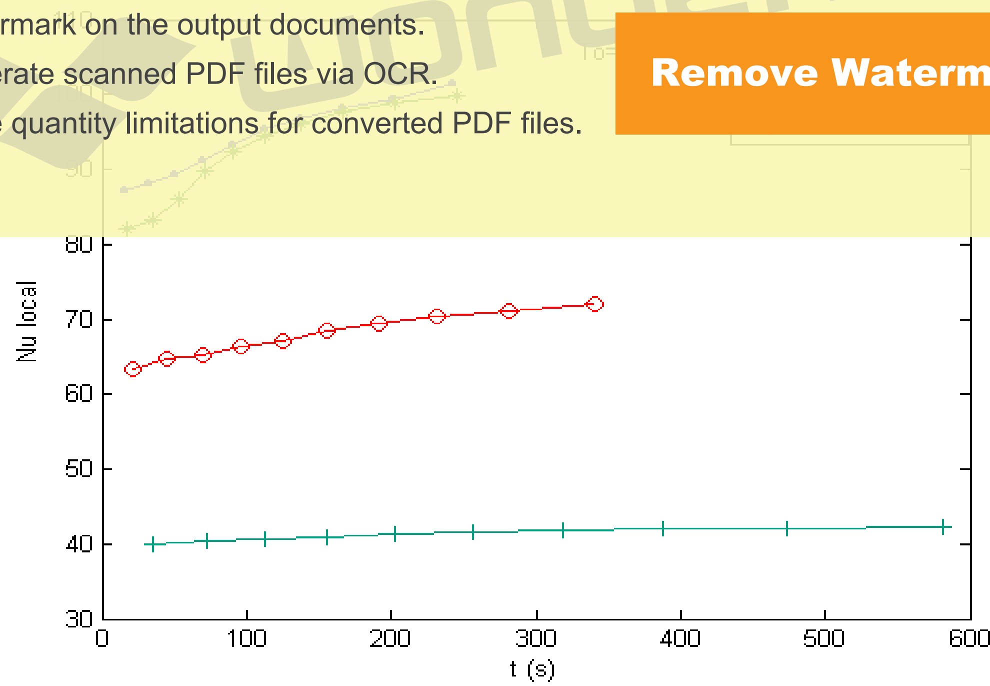

Figure (5.79) the variation of local Nusselt number against time interval.
(T=100,95,90,85,80,75,70,65,60,55,50).

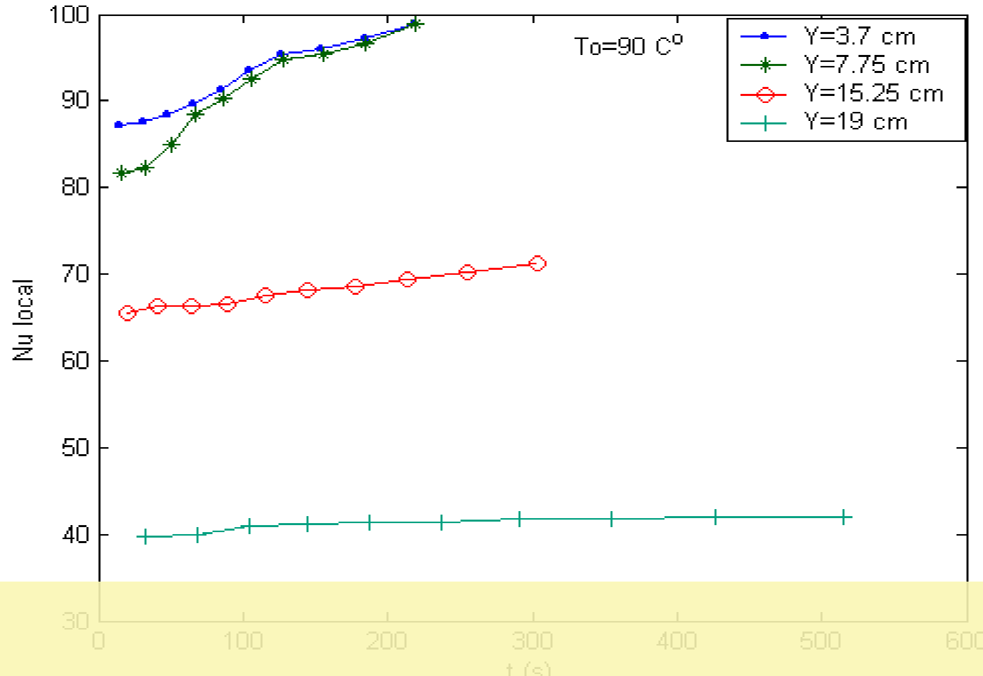

Figure (5.80) the variation of local Nusselt number against time interval.
(T=90,86,82,78,74,70,66,62,58,54,50).

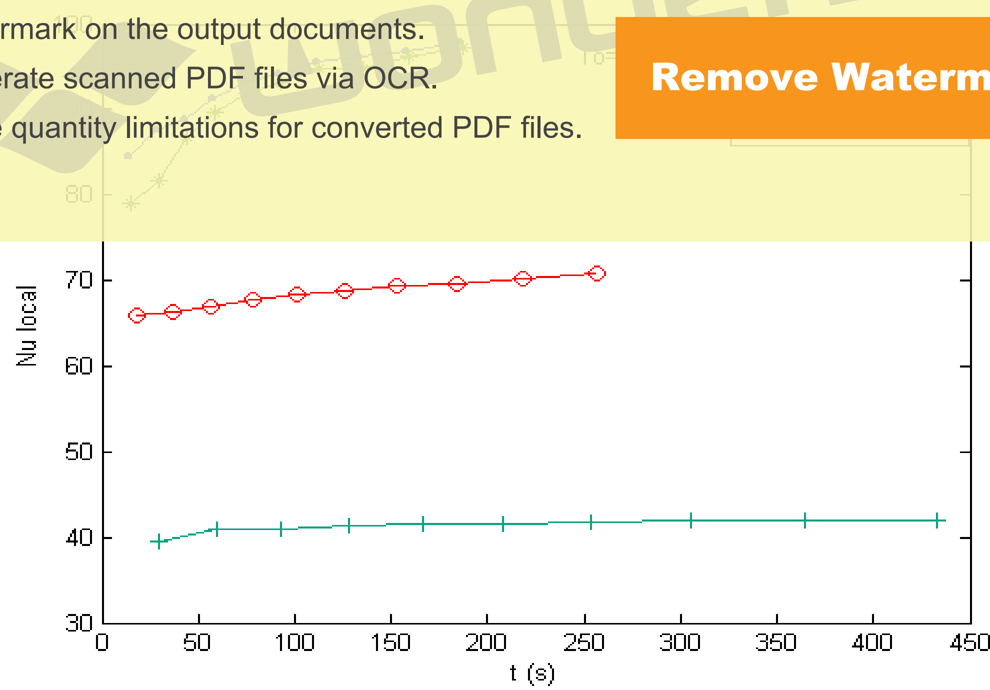

Figure (5.81) the variation of local Nusselt number against time interval.
(T=80,77,74,71,68,65,62,59,56,53,50).

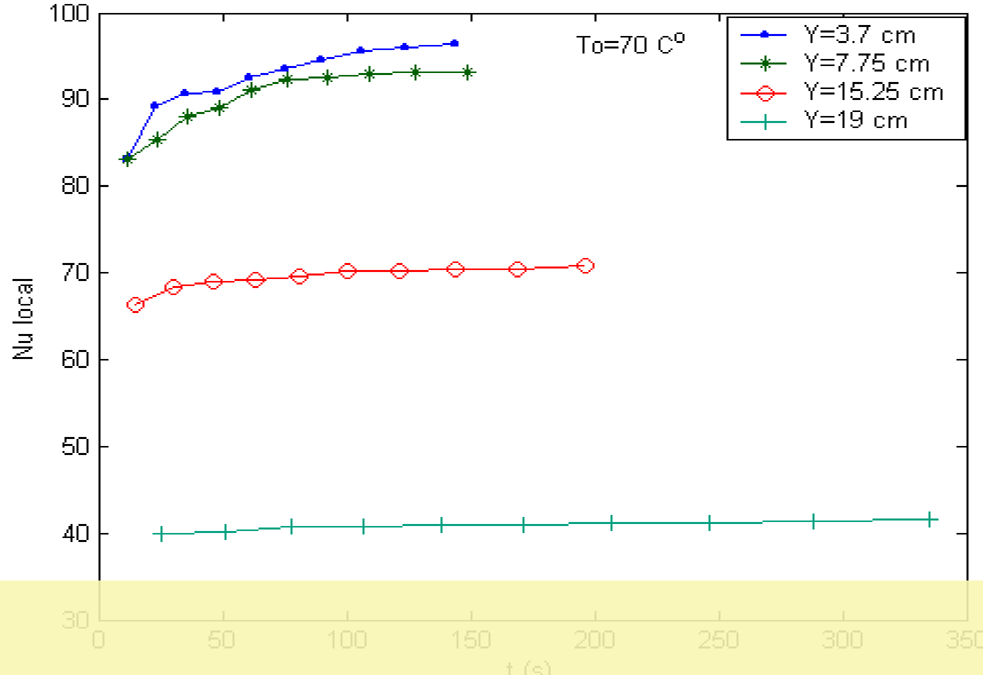

Figure (5.82) the variation of local Nusselt number against time interval.
(T=70,68,66,64,62,60,58,56,54,52,50).

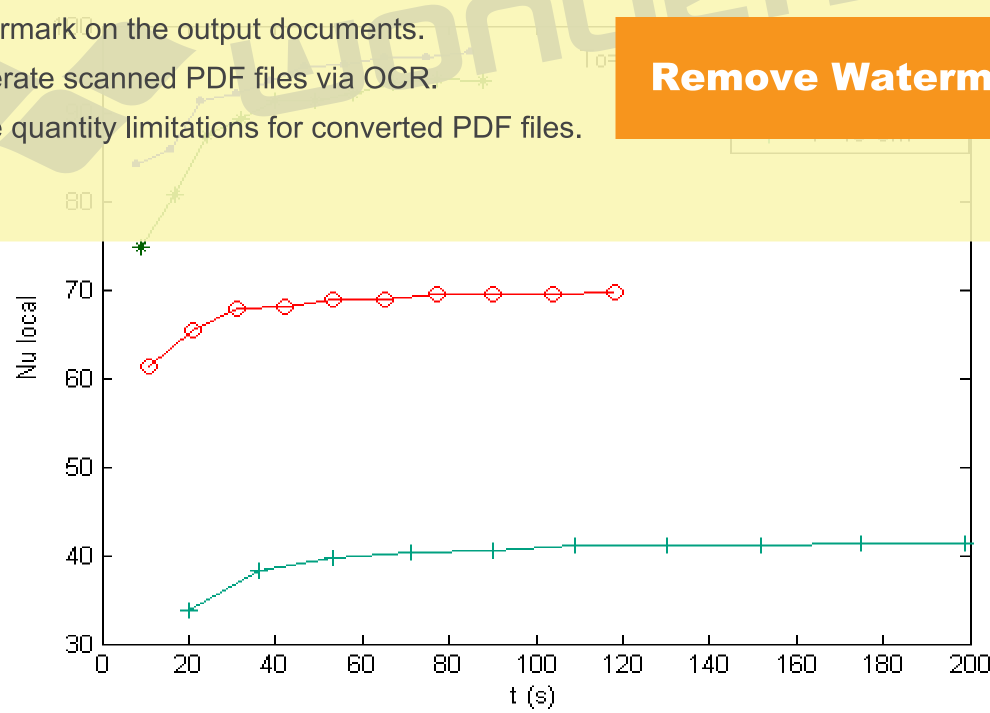

Figure (5.83) the variation of local Nusselt number against time interval.
(T=60,59,58,57,56,55,54,53,52,51,50).

5.3.2 Variation of (h_m) with (Nu_m) with time with cylinder position.

From each curve in figure (5.64-5.83), the mean heat transfer coefficient and Nusselt number will be obtained by using MATLAB 6.1 and plotted against time that the temperature (T=50) will be obtained at some reference temperature (T_o) as shown in figures (5.105-5.124) or a against cylinder position at time that (T=50) will be obtained as shown in figures (5.84-5.103). As mentioned before that the rate of heat transfer will be decreased as cylinder position is increased because of the pattern flow on each cylinder shown in figure (5.60-5.63). So, because all of these, the mean heat transfer coefficient and mean Nusselt number will be decreased as cylinder position or time is increased. As can be seen they ha[illegible] the ge[illegible] shape shown in figure (5.104-5.125). Be[illegible]een point [illegible] and [illegible] the temperature decreases rapidl[illegible] along [illegible] curve. After point (b) the rate of [illegible] temperature [illegible] time or cylind[illegible] approximately a straight line beyond point (c) and until the end of the cylinder position or time the temperature drops gradually with the increases of time or cylindrical position. To explain the shape of the curve in figures (5.104-5.125) the case of the pattern flow on each cylinder position shown in figures (5.60-5.63) will first be examined, that means the cylinder position (Y=3.7, 7.75 cm) in (a b) region is placed in from of air flow then the rate of heat transfer is large than other cylinder position, cylinder position (y=15.25 cm) that it is place In front of discontinues wall that means the rate of heat transfer less than them but it is larger than cylinder position (Y=19 cm) that it is placed in a dead zone with out air that means the rate of heat transfer is less than them and also, the slope of curve in figures (5.105-5.124)will be deceased as reach to dead zone until become zero at dead zone ((i.e. no change in mean heat transfer coefficient and Nusselt number with time at dead zone because of low effected of flow)).

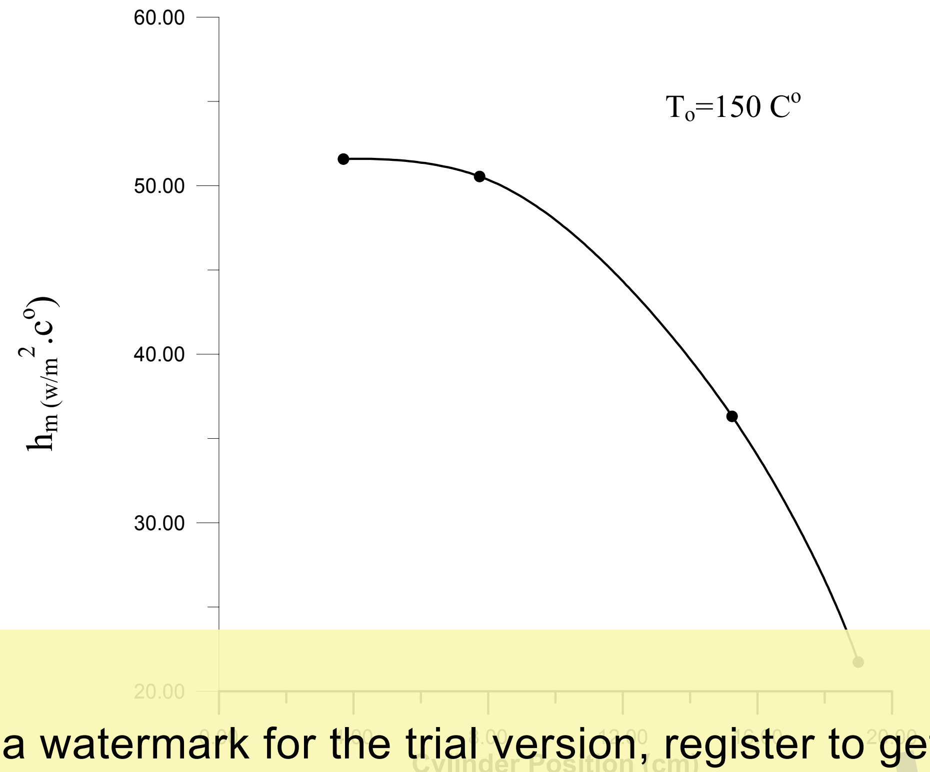

Figure (5.84): the variation of mean heat transfer coefficient to attain temperature of 50 C^o against position of cylinder.

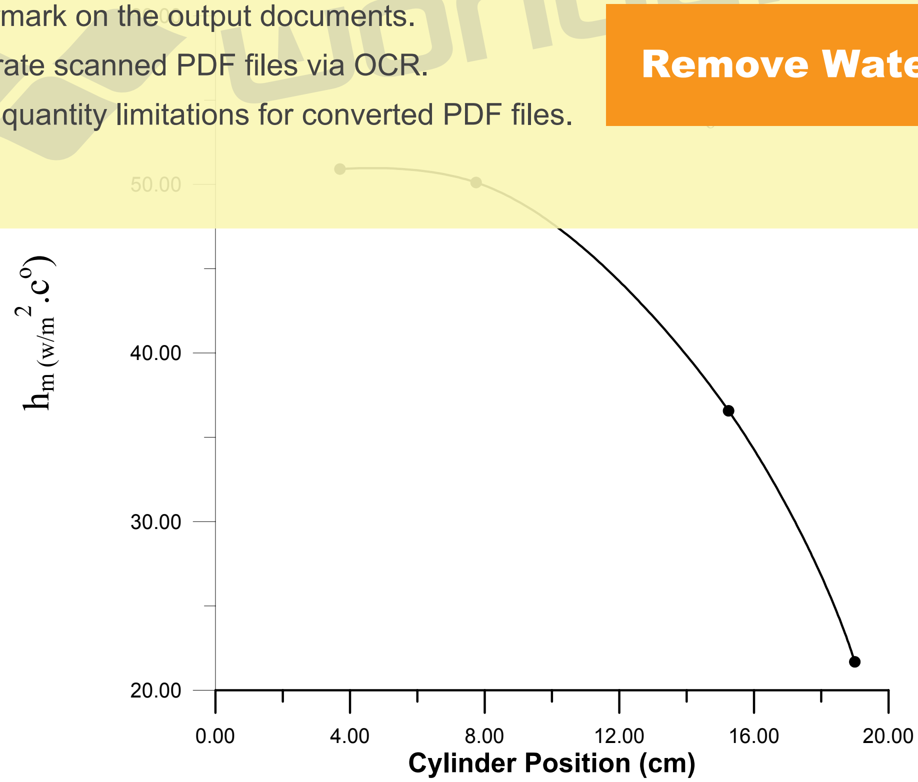

Figure (5.85): the variation of mean heat transfer coefficient to attain temperature of 50 C^o against position of cylinder.

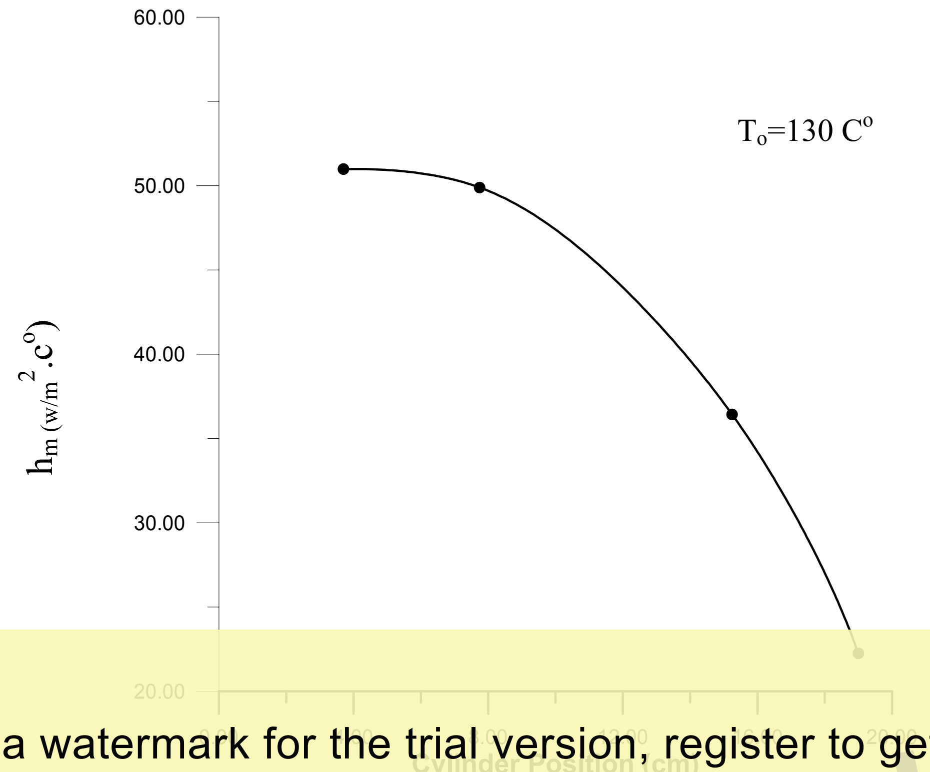

Figure (5.86): the variation of mean heat transfer coefficient to attain temperature of 50 C^o against position of cylinder.

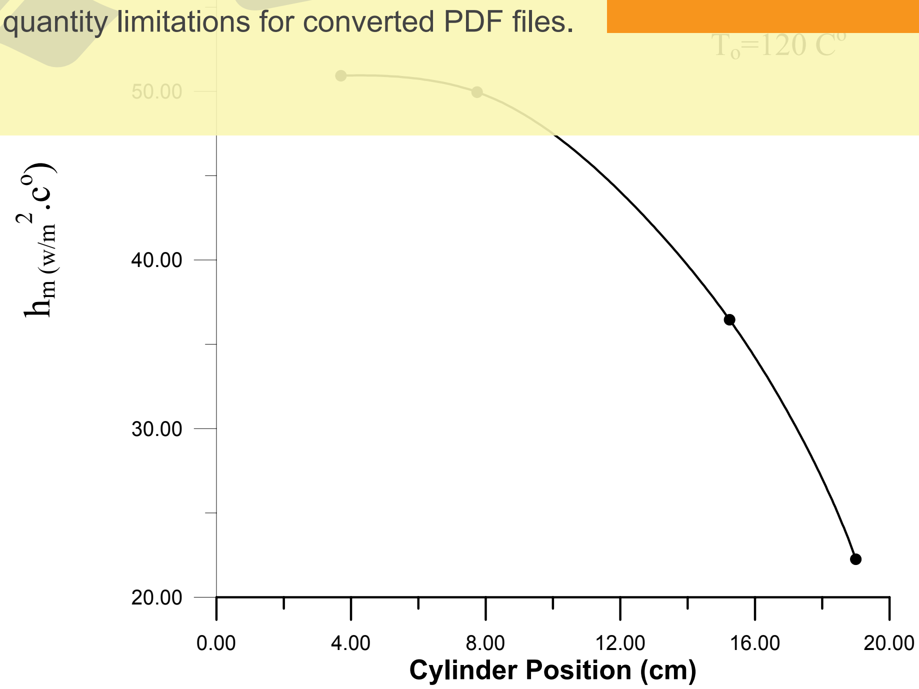

Figure (5.87): the variation of mean heat transfer coefficient to attain temperature of 50 C^o against position of cylinder.

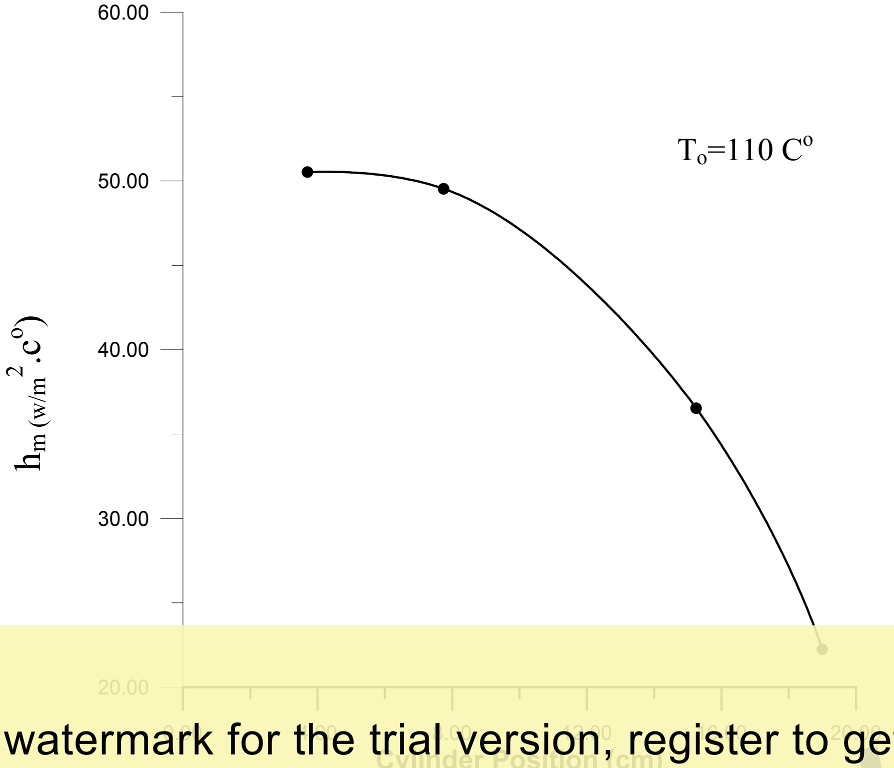

Figure (5.88): the variation of mean heat transfer coefficient to attain temperature of 50 C^o against position of cylinder.

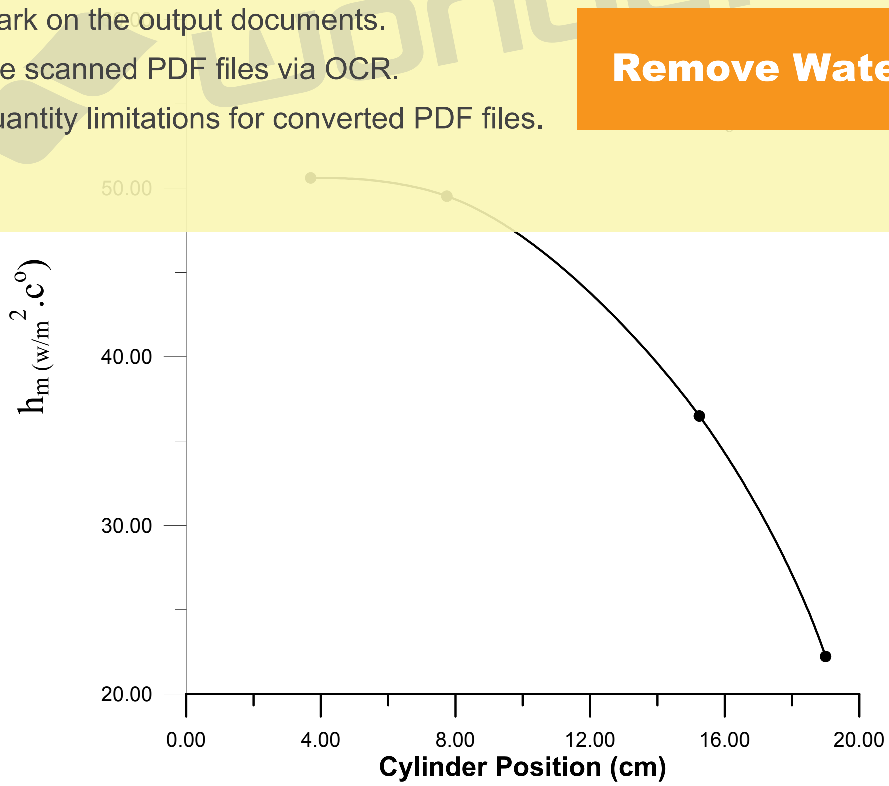

Figure (5.89): the variation of mean heat transfer coefficient to attain temperature of 50 C^o against position of cylinder.

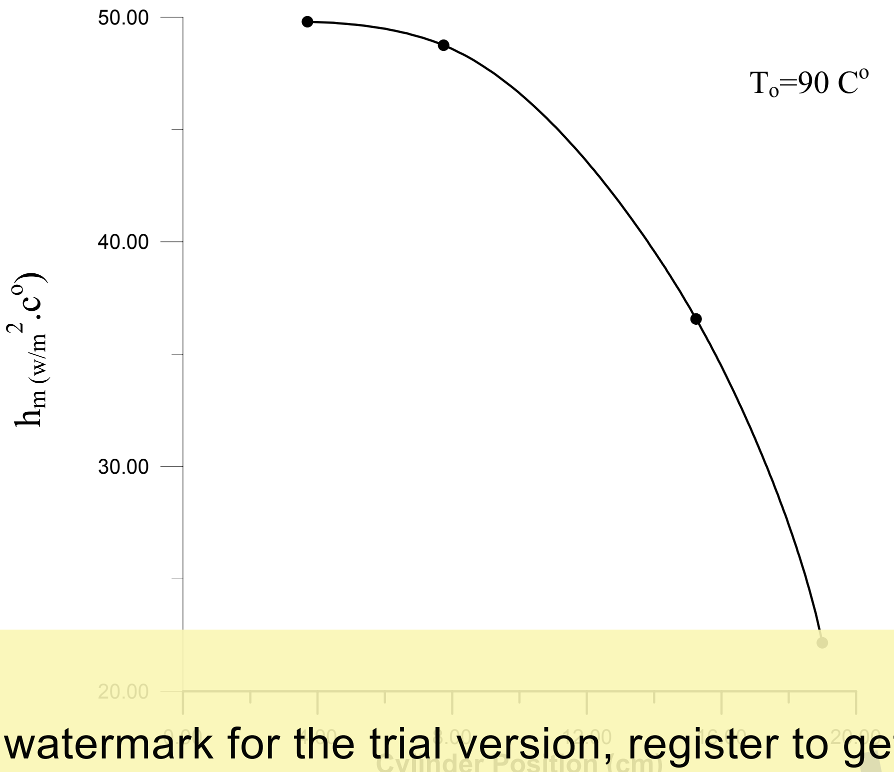

Figure (5.90): the variation of mean heat transfer coefficient to attain temperature of 50 C^o against position of cylinder

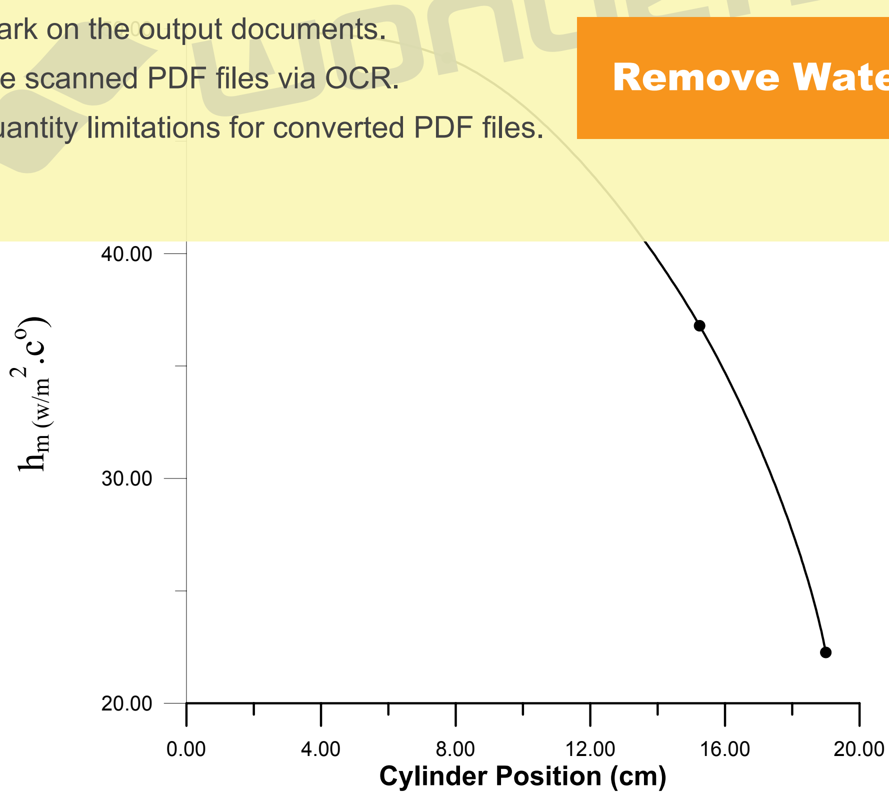

Figure (5.91): the variation of mean heat transfer coefficient to attain temperature of 50 C^o against position of cylinder

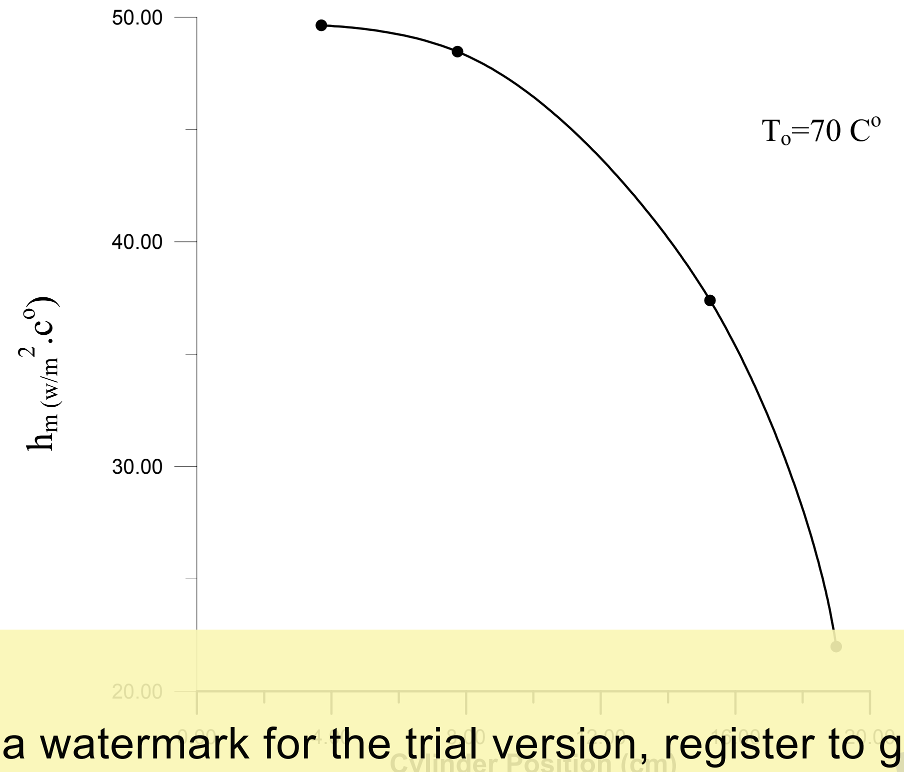

Figure (5.92): the variation of mean heat transfer coefficient to attain temperature of 50 C° against position of cylinder.

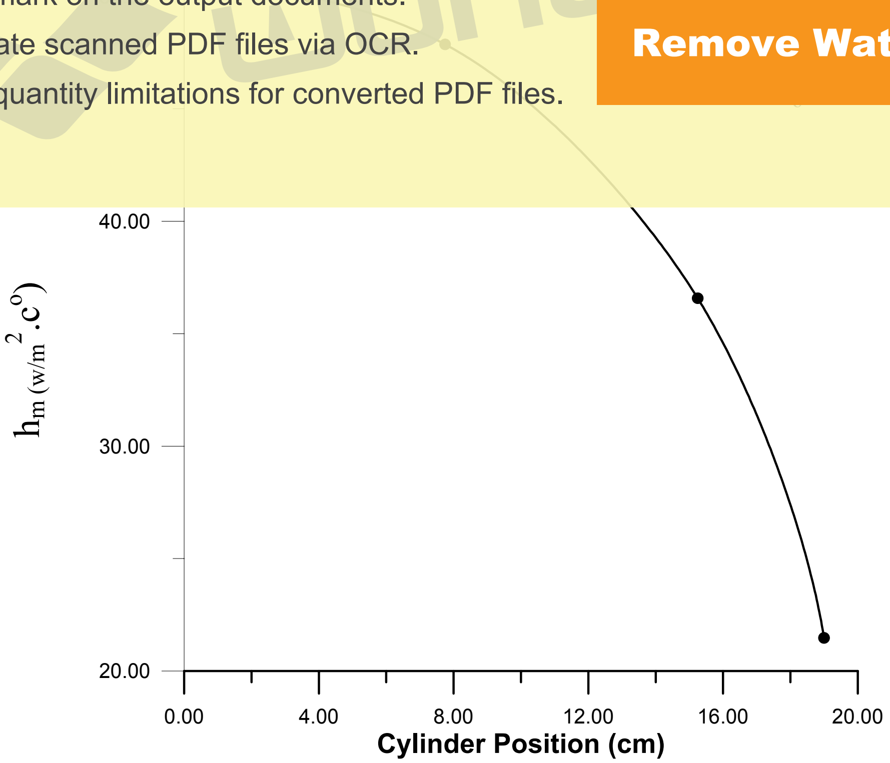

Figure (5.93): the variation of mean heat transfer coefficient to attain temperature of 50 C° against position of cylinder.

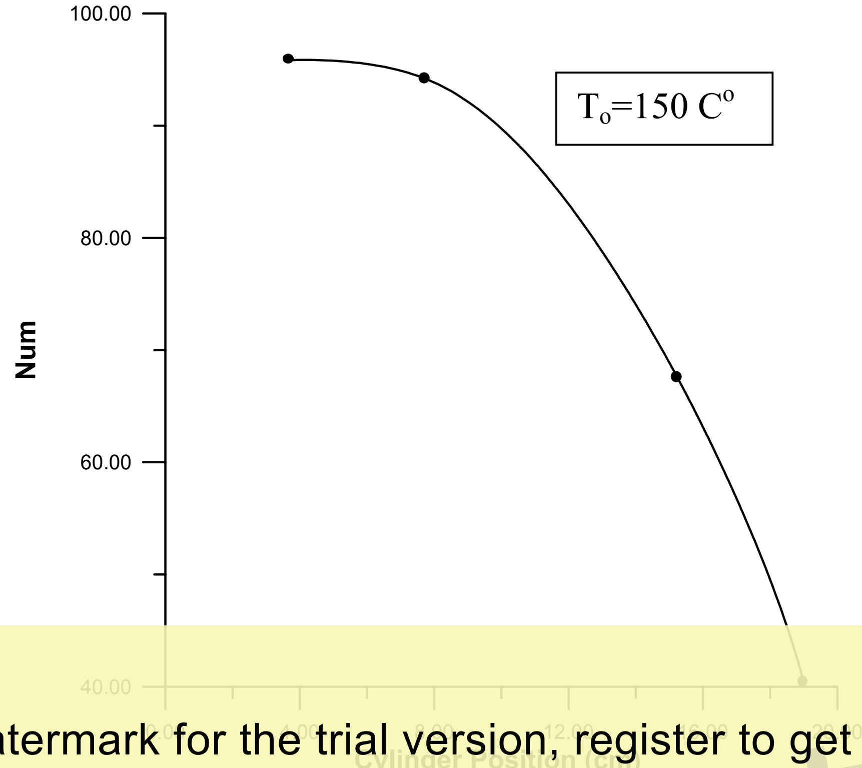

Figure (5.94): The variation of mean Nusselt number to attain temperature of 50 C^o against position of cylinder.

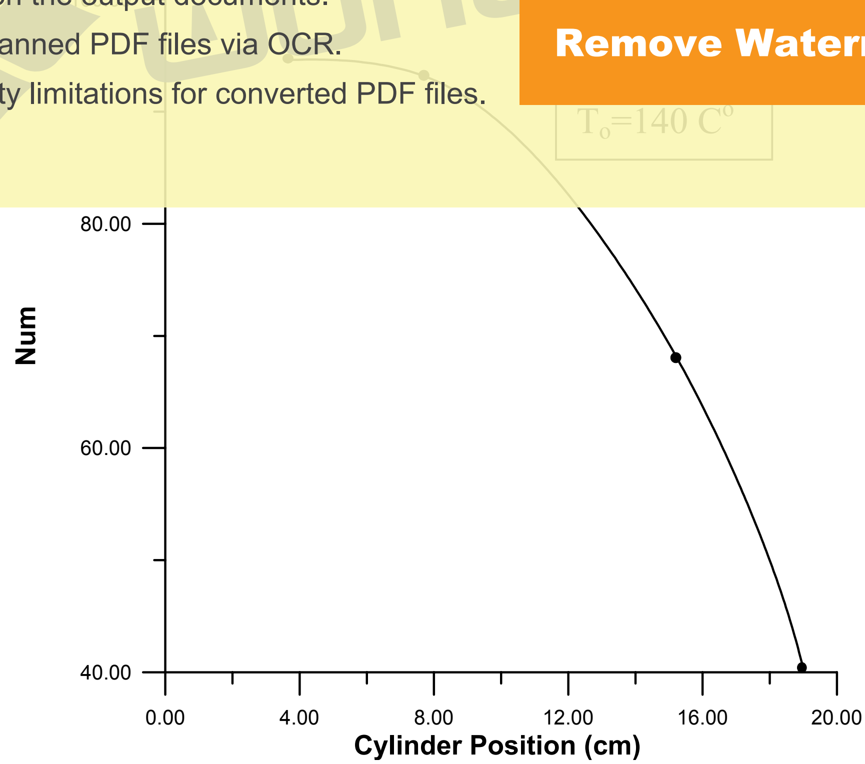

Figure (5.95): The variation of mean Nusselt number to attain temperature of 50 C^o against position of cylinder.

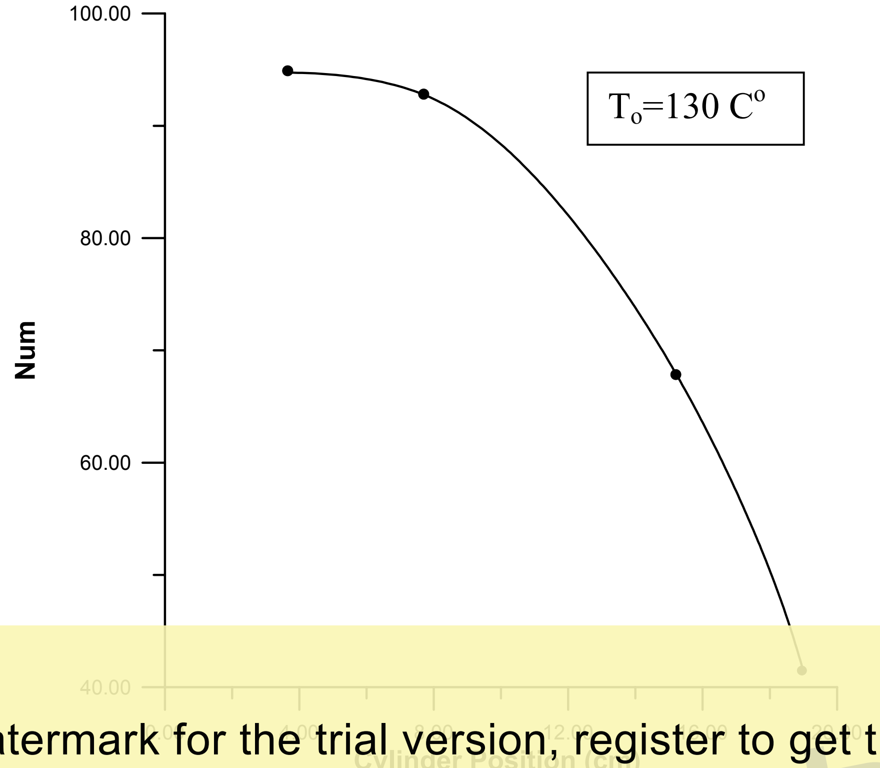

Figure (5.96): The variation of mean Nusselt number to attain temperature of 50 C° against position of cylinder.

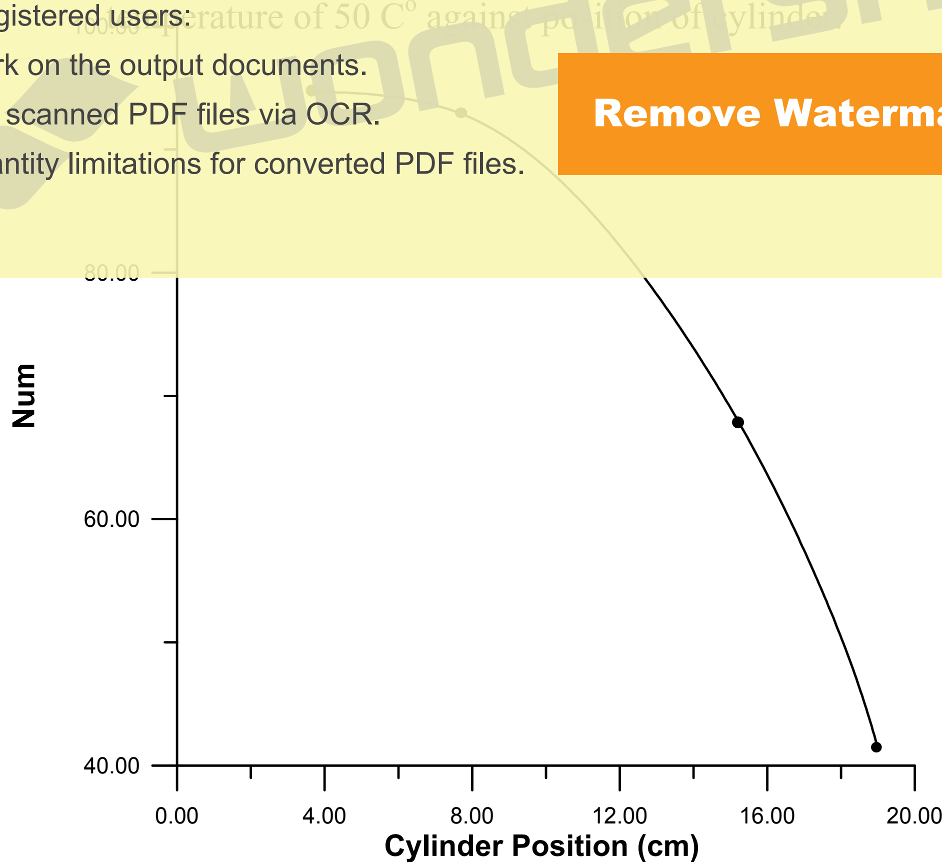

Figure (5.97): The variation of mean Nusselt number to attain temperature of 50 C° against position of cylinder.

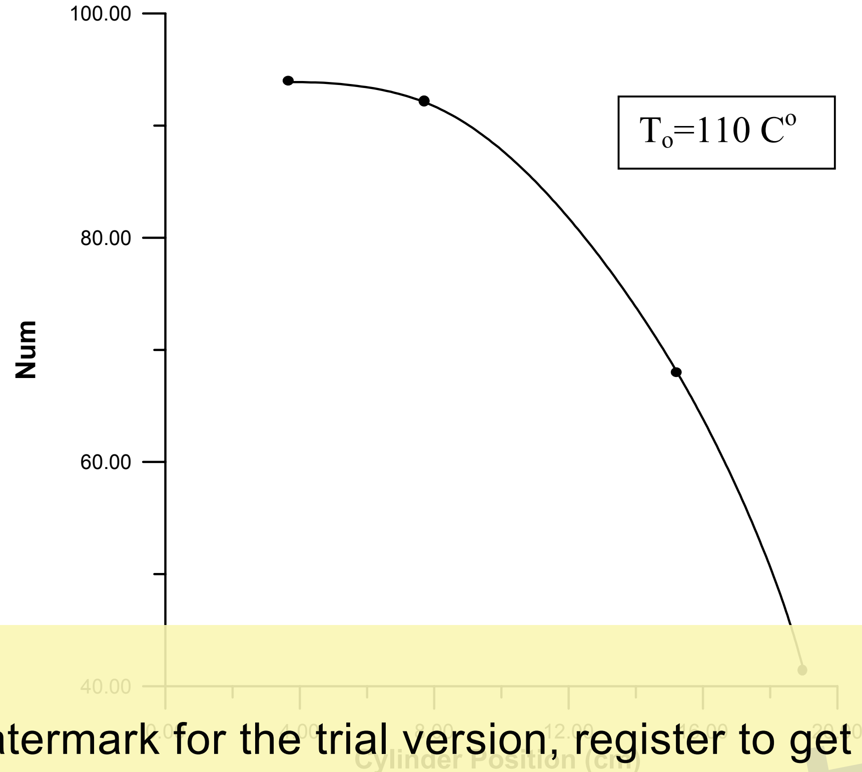

Figure (5.98): The variation of mean Nusselt number to attain temperature of 50 C° against position of cylinder.

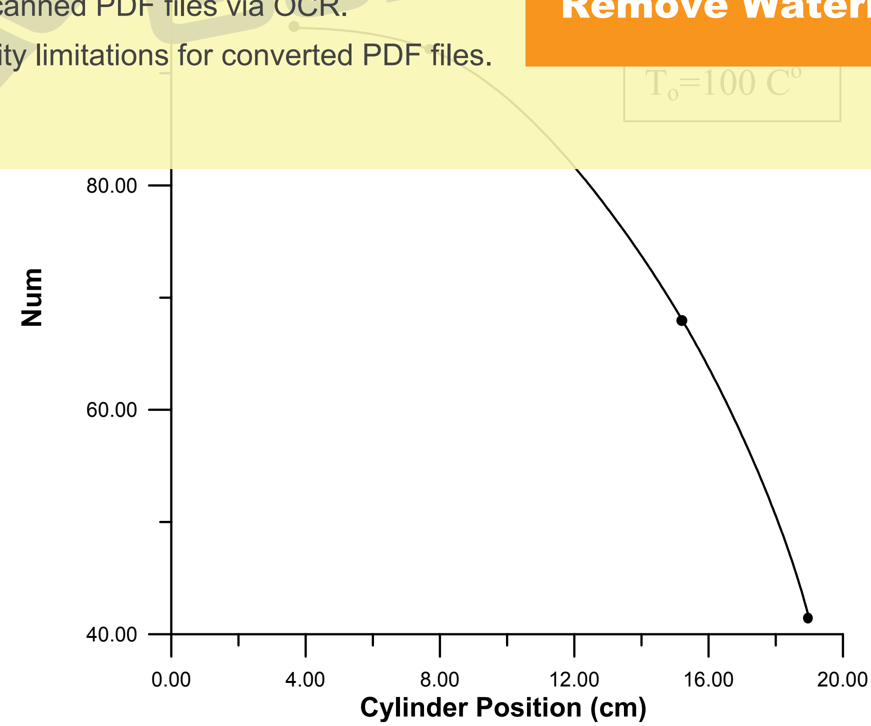

Figure (5.99): The variation of mean Nusselt number to attain temperature of 50 C° against position of cylinder.

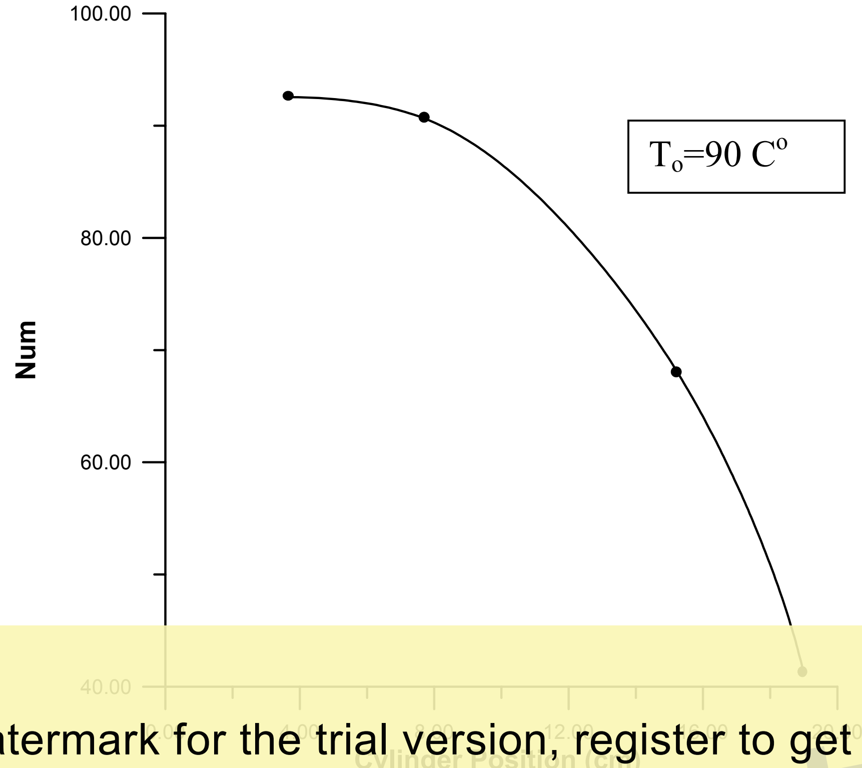

Figure (5.100): The variation of mean Nusselt number to attain temperature of 50 C^o against position of cylinder.

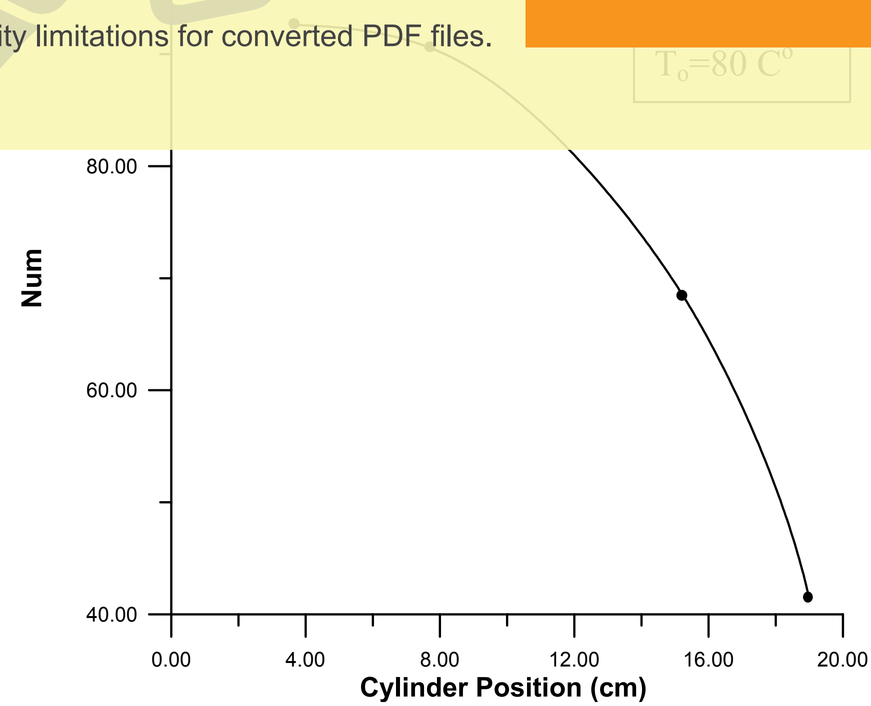

Figure (5.101): The variation of mean Nusselt number to attain temperature of 50 C^o against position of cylinder.

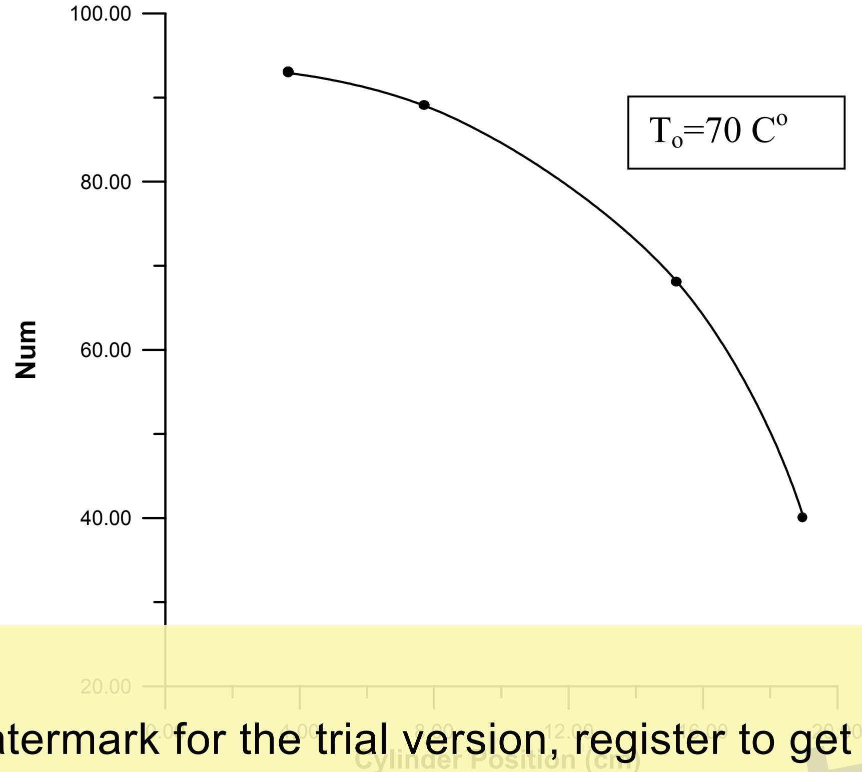

Figure (5.102): The variation of mean Nusselt number to attain temperature of 50 C^o against position of cylinder.

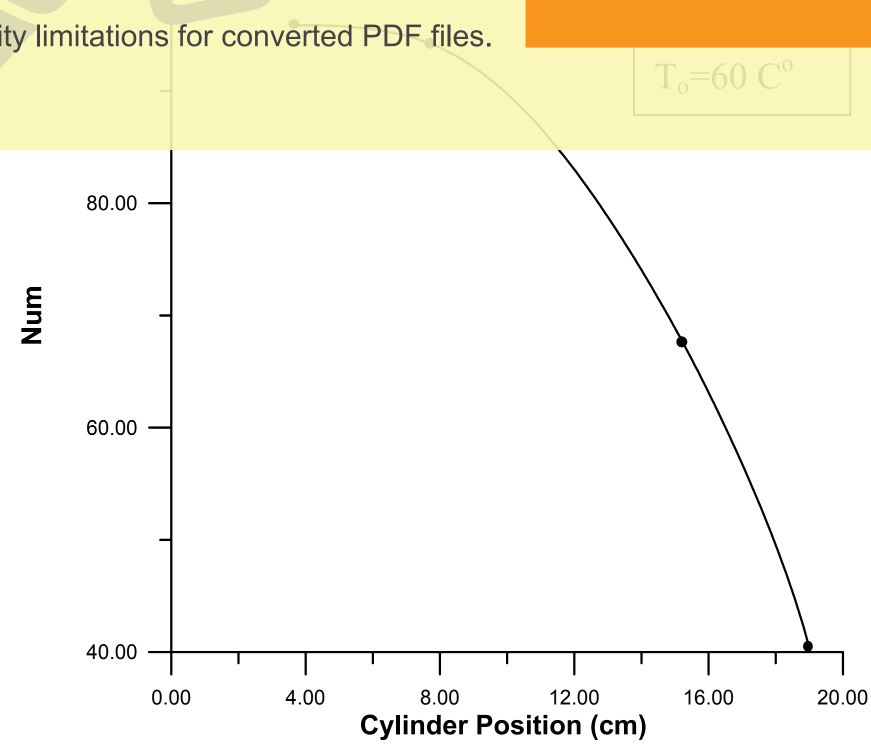

Figure (5.103): The variation of mean Nusselt number to attain temperature of 50 C^o against position of cylinder.

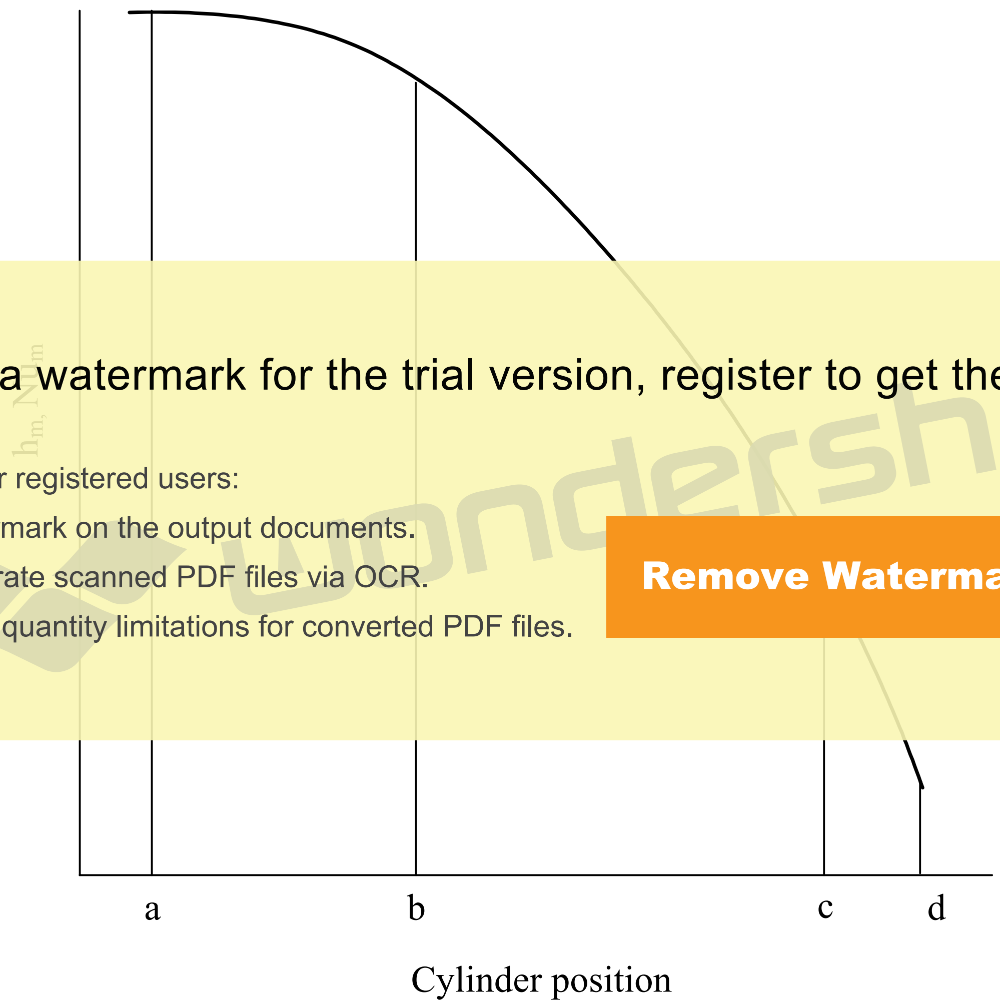

Figure (5.104): General shape of mean heat transfer coefficient and Nusselt number.

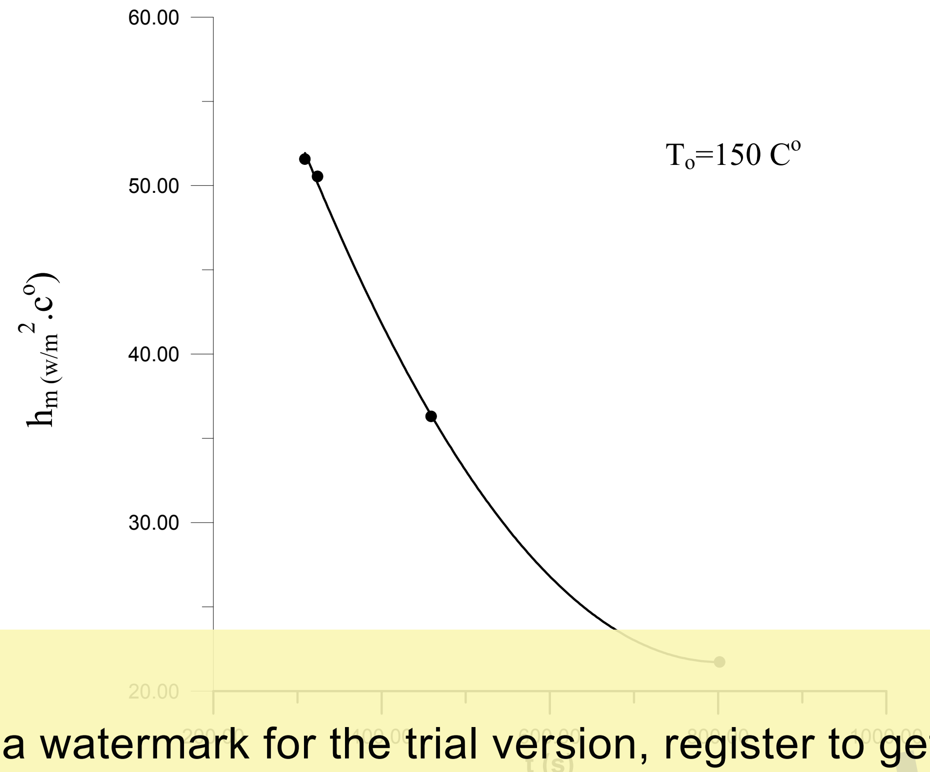

Figure (5.105) the variation of mean heat transfer coefficient against time to attain temperature of 50 C$^{o.}$ (position of cylinder=3.7, 7.75, 15.25, 19).

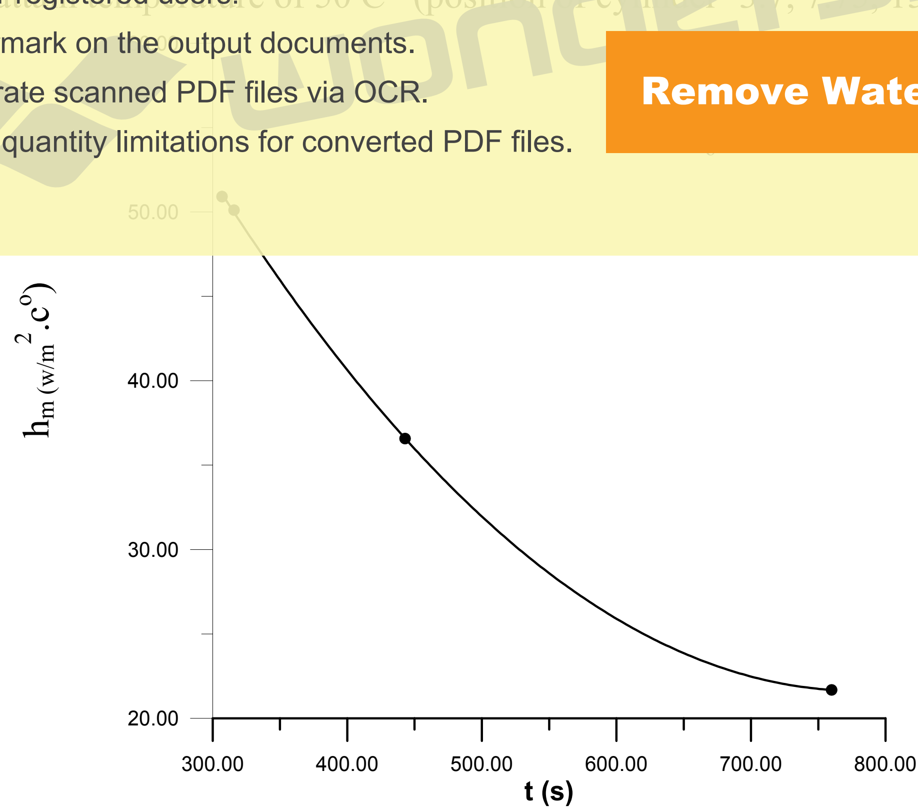

Figure (5.106) the variation of mean heat transfer coefficient against time to attain temperature of 50 C$^{o.}$ (position of cylinder=3.7, 7.75, 15.25, 19).

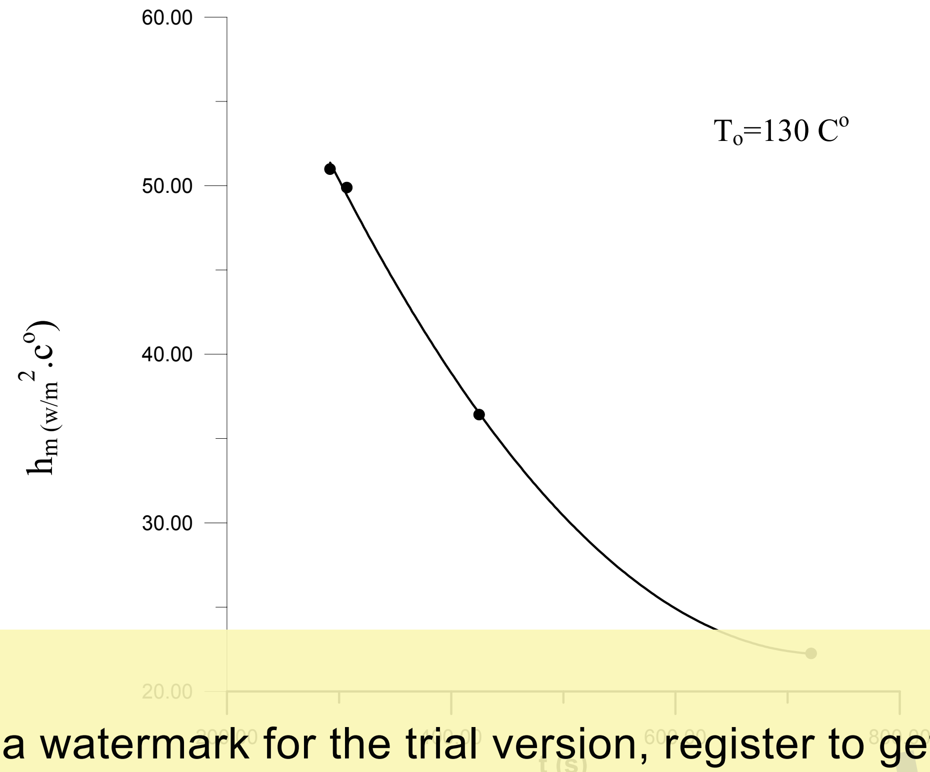

Figure (5.107) the variation of mean heat transfer coefficient against time to attain temperature of 50 $C^{o.}$ (position of cylinder=3.7, 7.75, 15.25, 19).

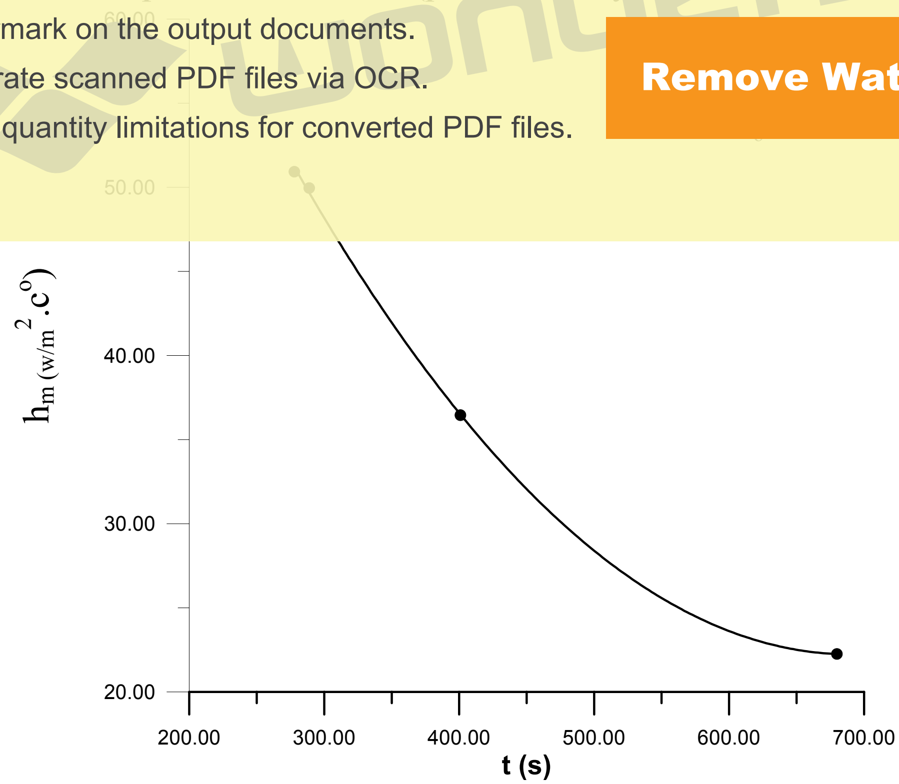

Figure (5.108) the variation of mean heat transfer coefficient against time to attain temperature of 50 $C^{o.}$ (position of cylinder=3.7, 7.75, 15.25, 19).

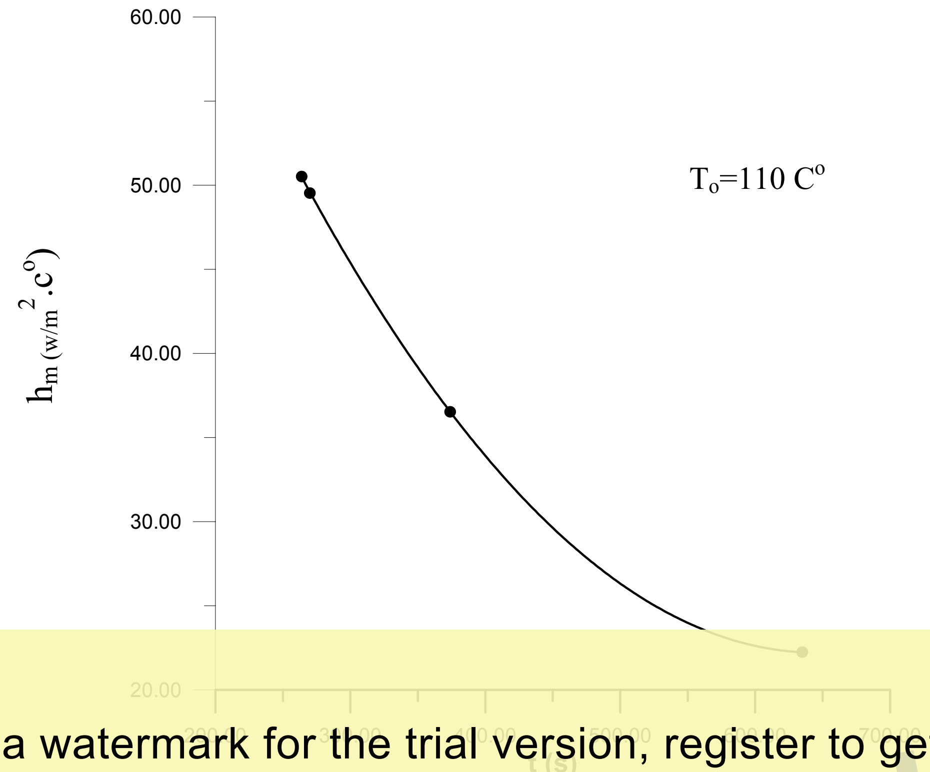

Figure (5.109) the variation of mean heat transfer coefficient against time to attain temperature of 50 $C^{o.}$ (position of cylinder=3.7, 7.75, 15.25, 19).

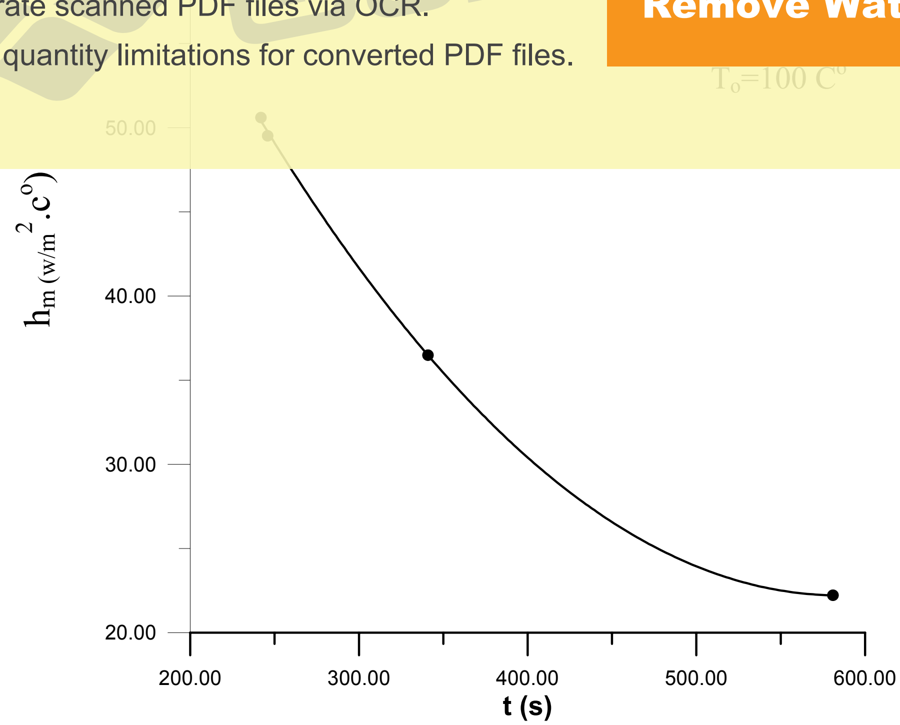

Figure (5.110) the variation of mean heat transfer coefficient against time to attain temperature of 50 $C^{o.}$ (position of cylinder=3.7, 7.75, 15.25, 19).

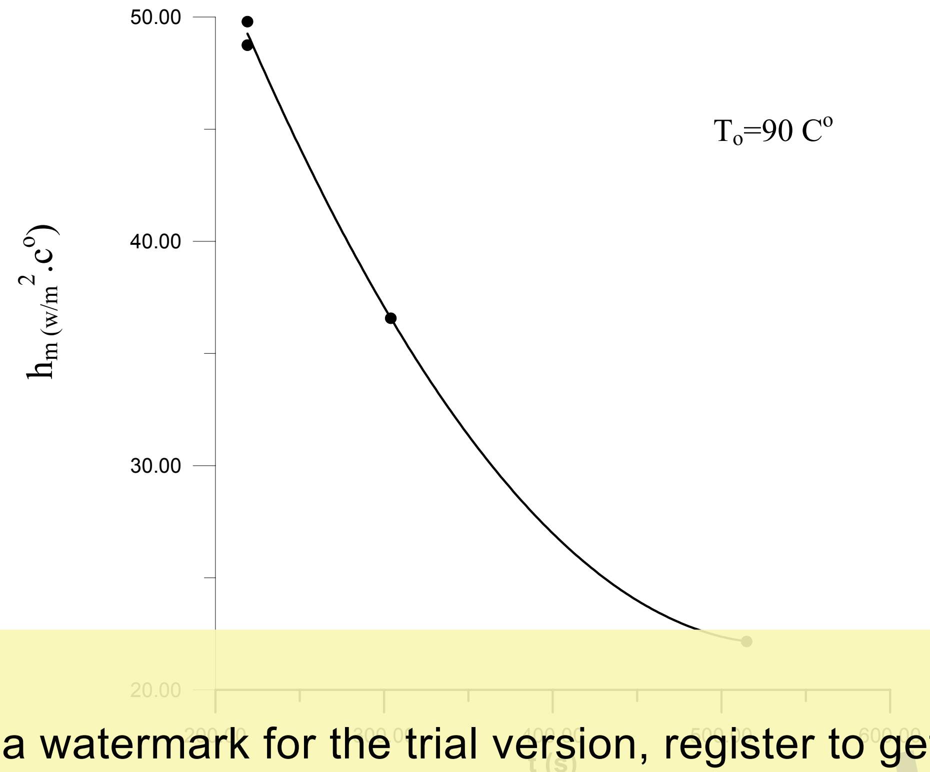

Figure (5.111) the variation of mean heat transfer coefficient against time to attain temperature of 50 C$^{o.}$ (position of cylinder=3.7, 7.75, 15.25, 19).

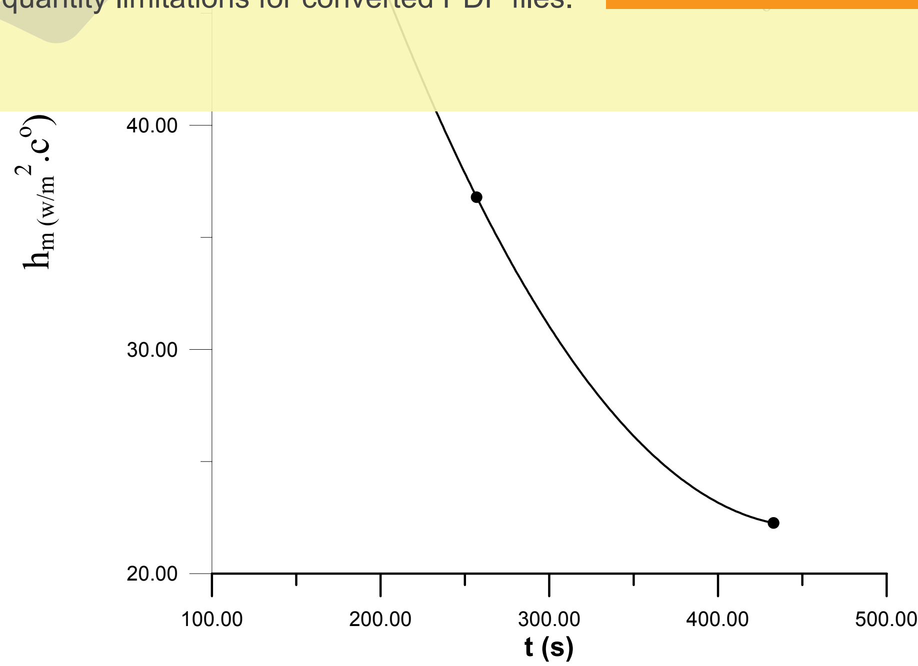

Figure (5.112) the variation of mean heat transfer coefficient against time to attain temperature of 50 C$^{o.}$ (position of cylinder=3.7, 7.75, 15.25, 19).

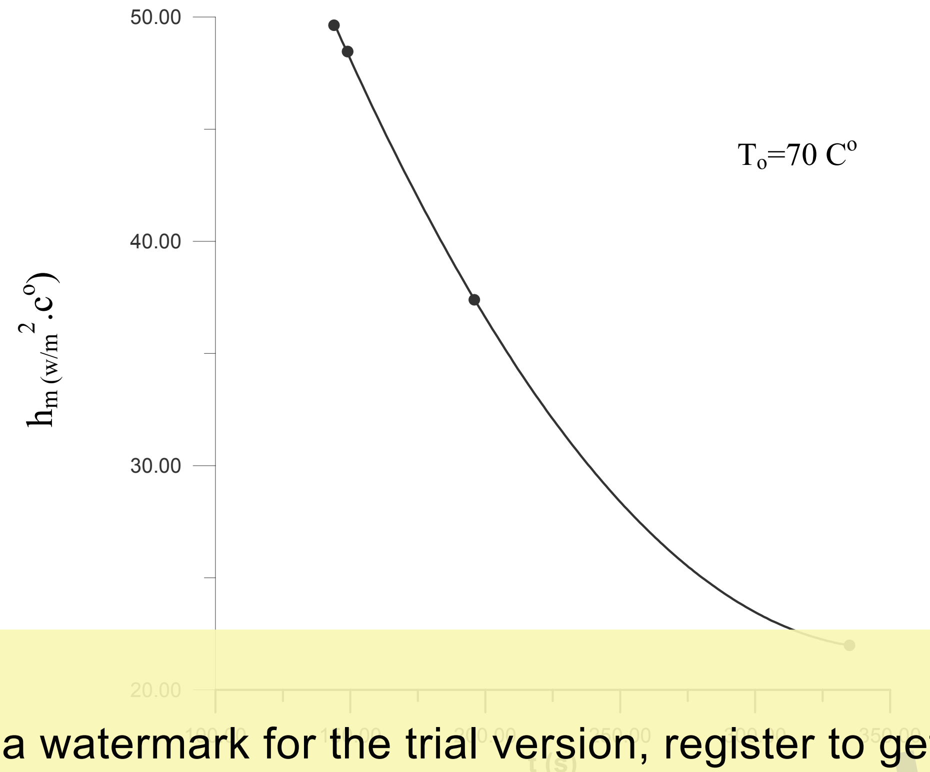

Figure (5.113) the variation of mean heat transfer coefficient against time to attain temperature of 50 C$^{o.}$ (position of cylinder=3.7, 7.75, 11.25, 19).

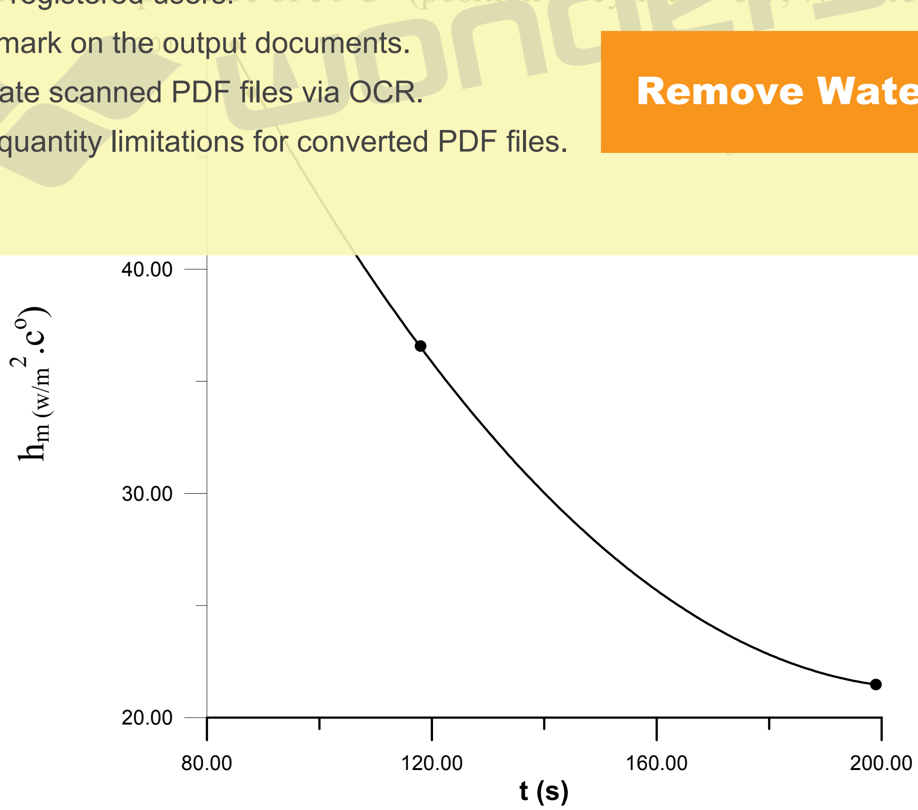

Figure (5.114) the variation of mean heat transfer coefficient against time to attain temperature of 50 C$^{o.}$ (position of cylinder=3.7, 7.75, 15.25, 19).

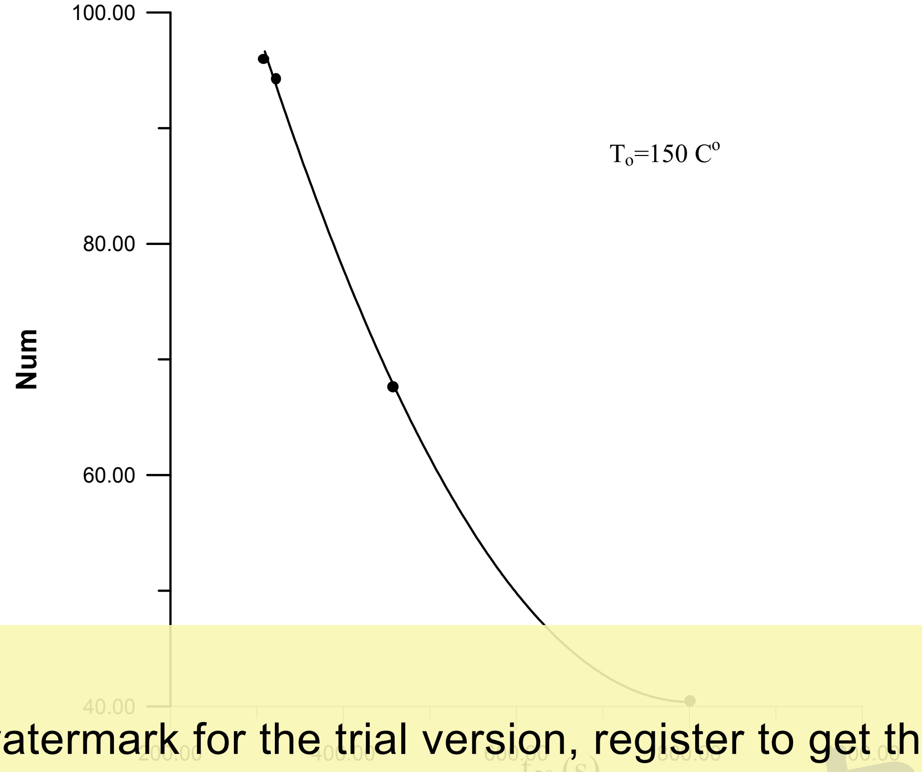

Figure (5.115) the variation of mean Nusselt number against time to attain temperature of 50 C°. (position of cylinder=3.7, 7.75, 11.5, 15.25, 19).

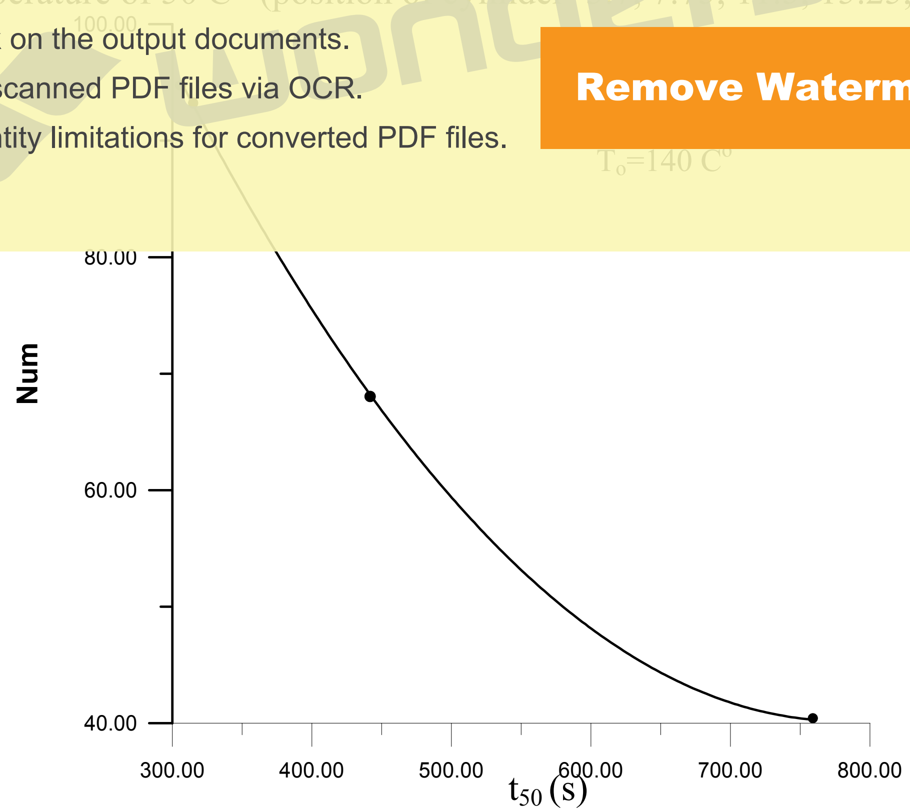

Figure (5.116) the variation of mean Nusselt number against time to attain temperature of 50 C°. (position of cylinder=3.7, 7.75, 11.5, 15.25, 19).

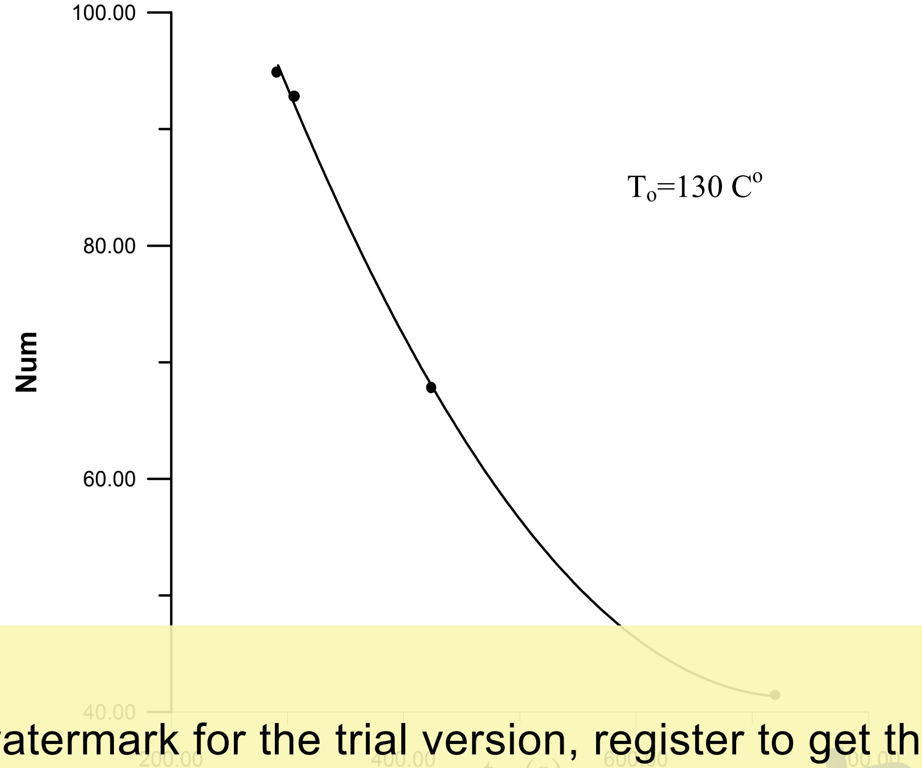

Figure (5.117) the variation of mean Nusselt number against time to attain temperature of 50 C°. (position of cylinder=3.7, 7.75, 11.5, 15.25, 19).

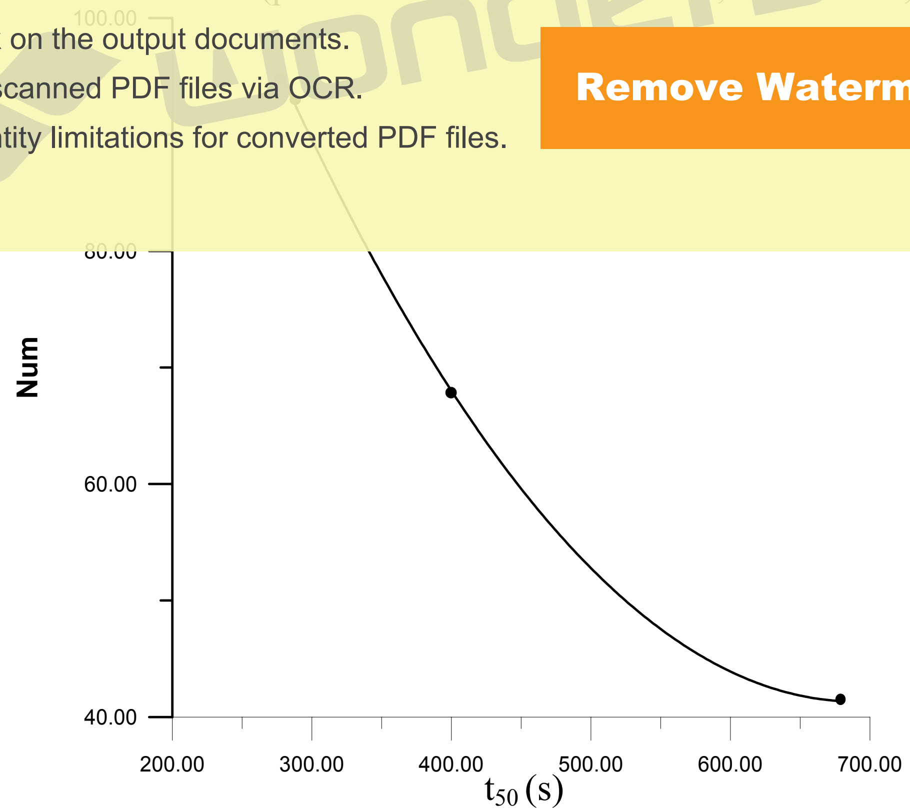

Figure (5.118) the variation of mean Nusselt number against time to attain temperature of 50 C°. (position of cylinder=3.7, 7.75, 11.5, 15.25, 19).

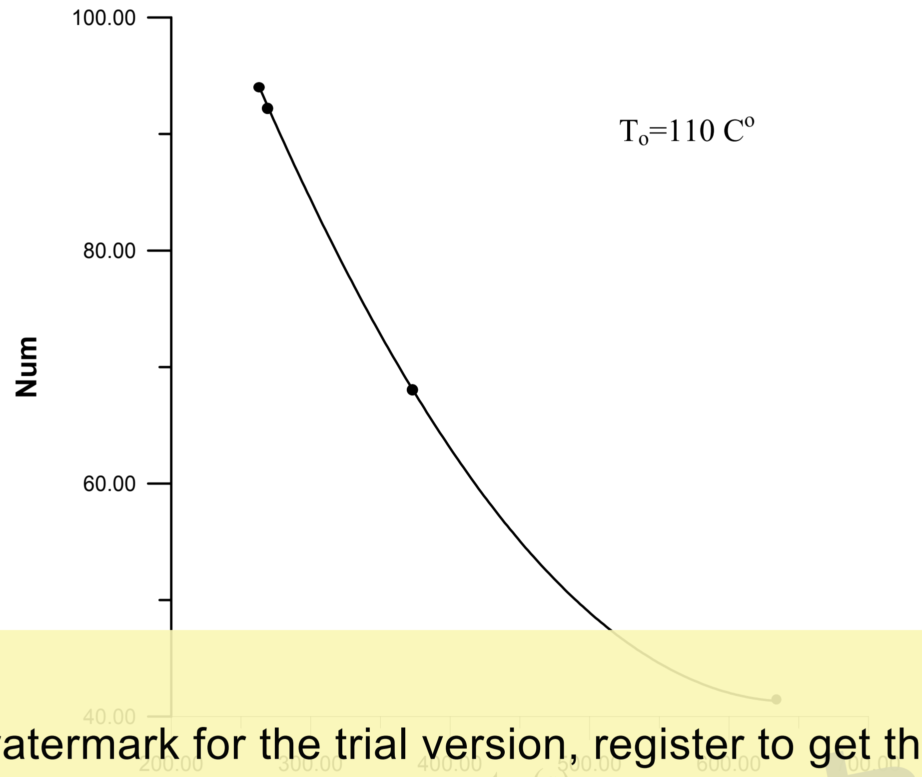

Figure (5.119) the variation of mean Nusselt number against time to attain temperature of 50 $C^{o.}$ (position of cylinder=3.7, 7.75, 11.5, 15.25, 19).

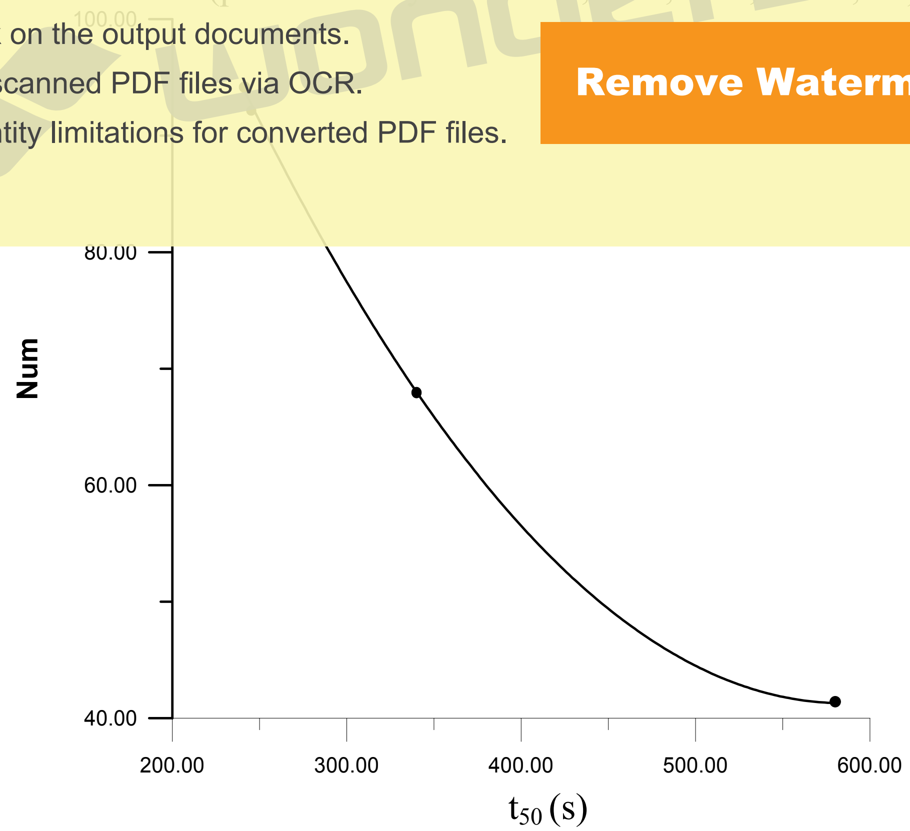

Figure (5.120) the variation of mean Nusselt number against time to attain temperature of 50 $C^{o.}$ (position of cylinder=3.7, 7.75, 11.5, 15.25, 19).

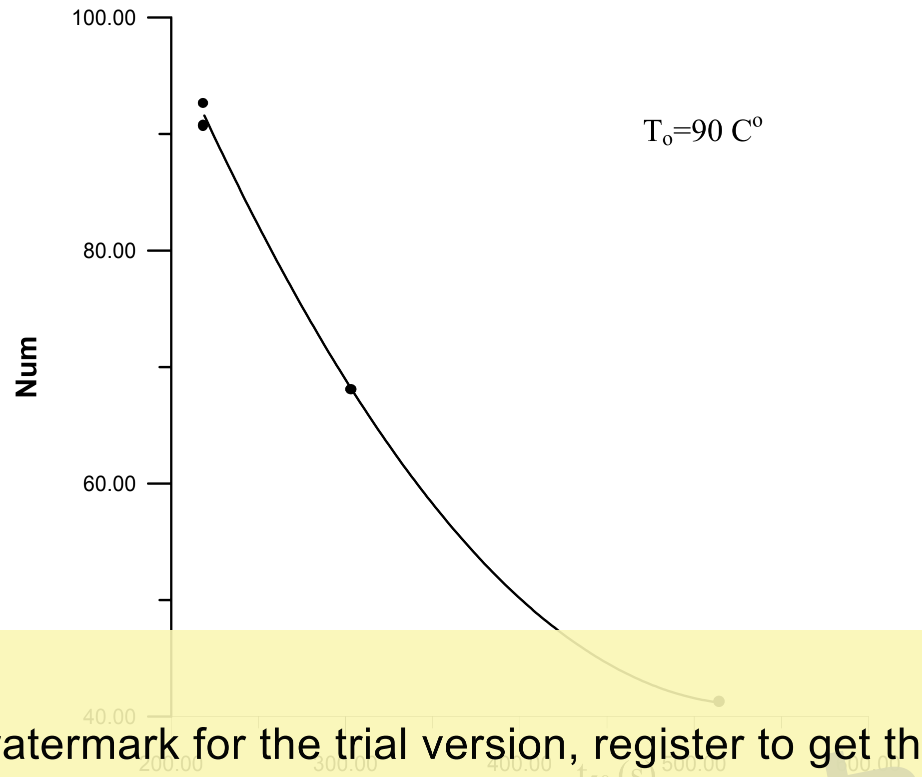

Figure (5.121) the variation of mean Nusselt number against time to attain temperature of 50 $C^{o.}$ (position of cylinder=3.7, 7.75, 11.5, 15.25, 19).

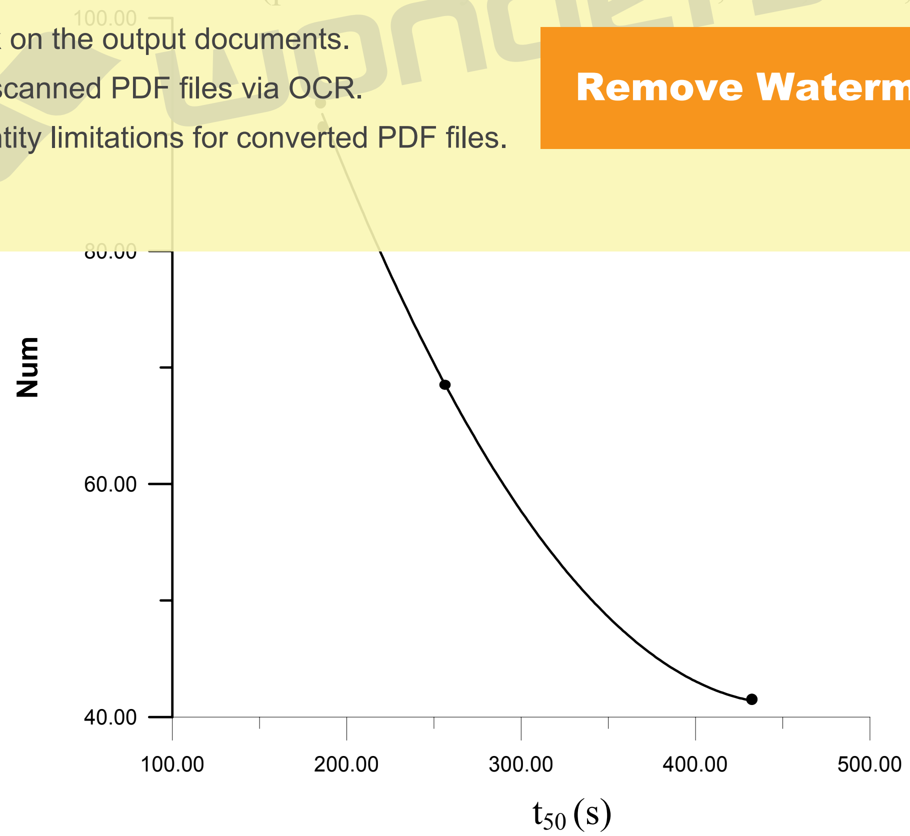

Figure (5.122) the variation of mean Nusselt number against time to attain temperature of 50 $C^{o.}$ (position of cylinder=3.7, 7.75, 11.5, 15.25, 19).

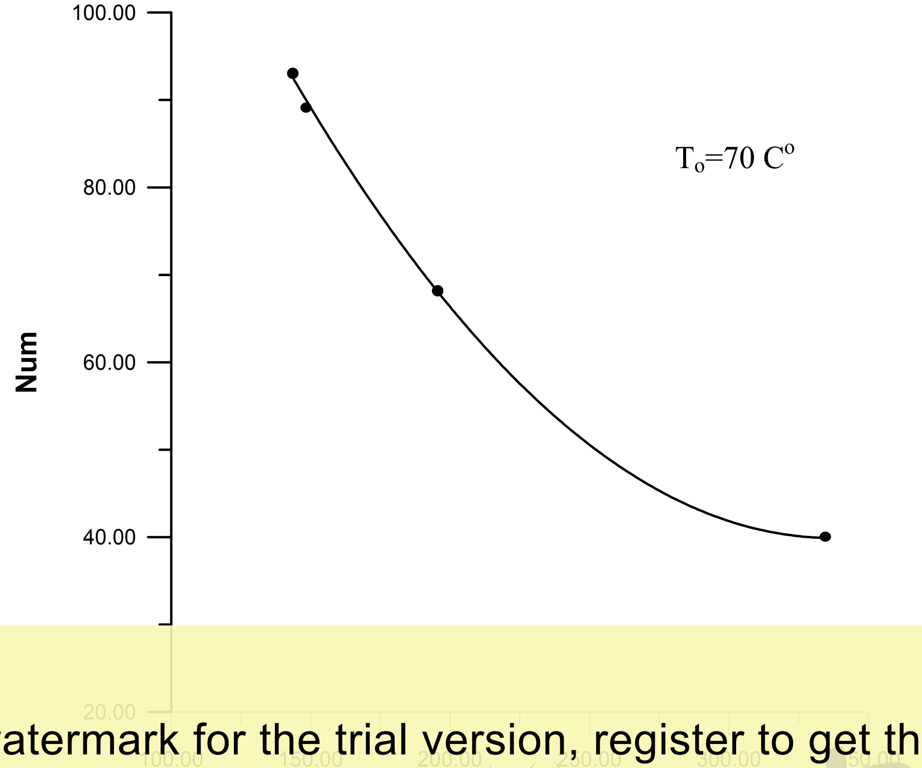

Figure (5.123) the variation of mean Nusselt number against time to attain temperature of 50 C°. (position of cylinder=3.7, 7.75, 11.5, 15.25, 19).

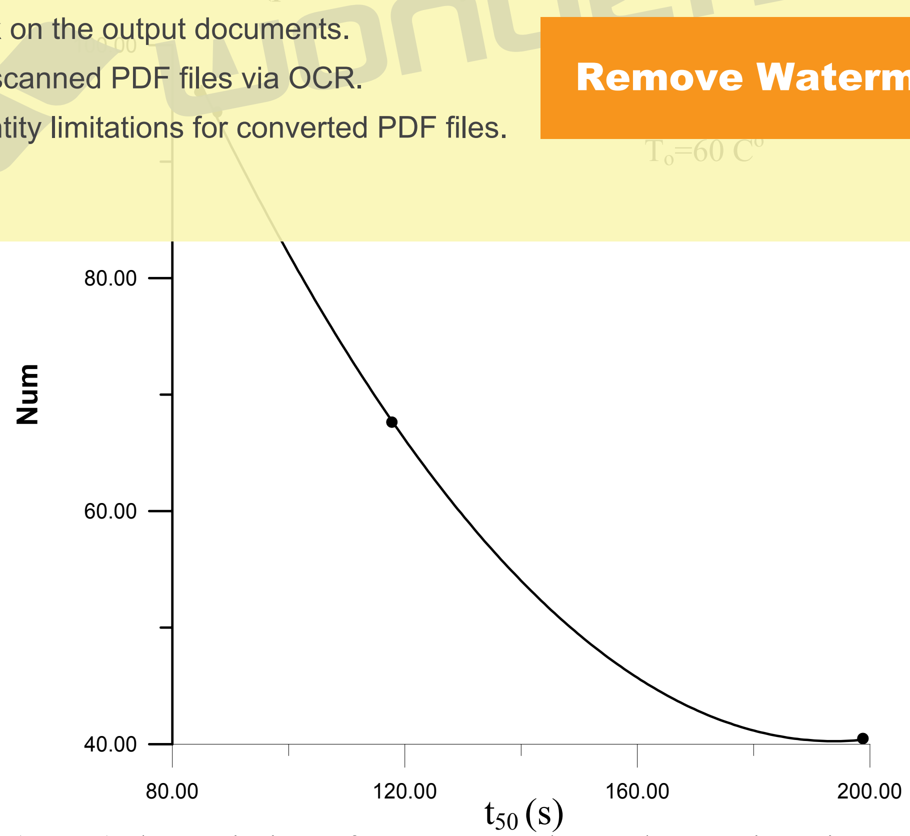

Figure (5.124) the variation of mean Nusselt number against time to attain temperature of 50 C°. (position of cylinder=3.7, 7.75, 11.5, 15.25, 19).

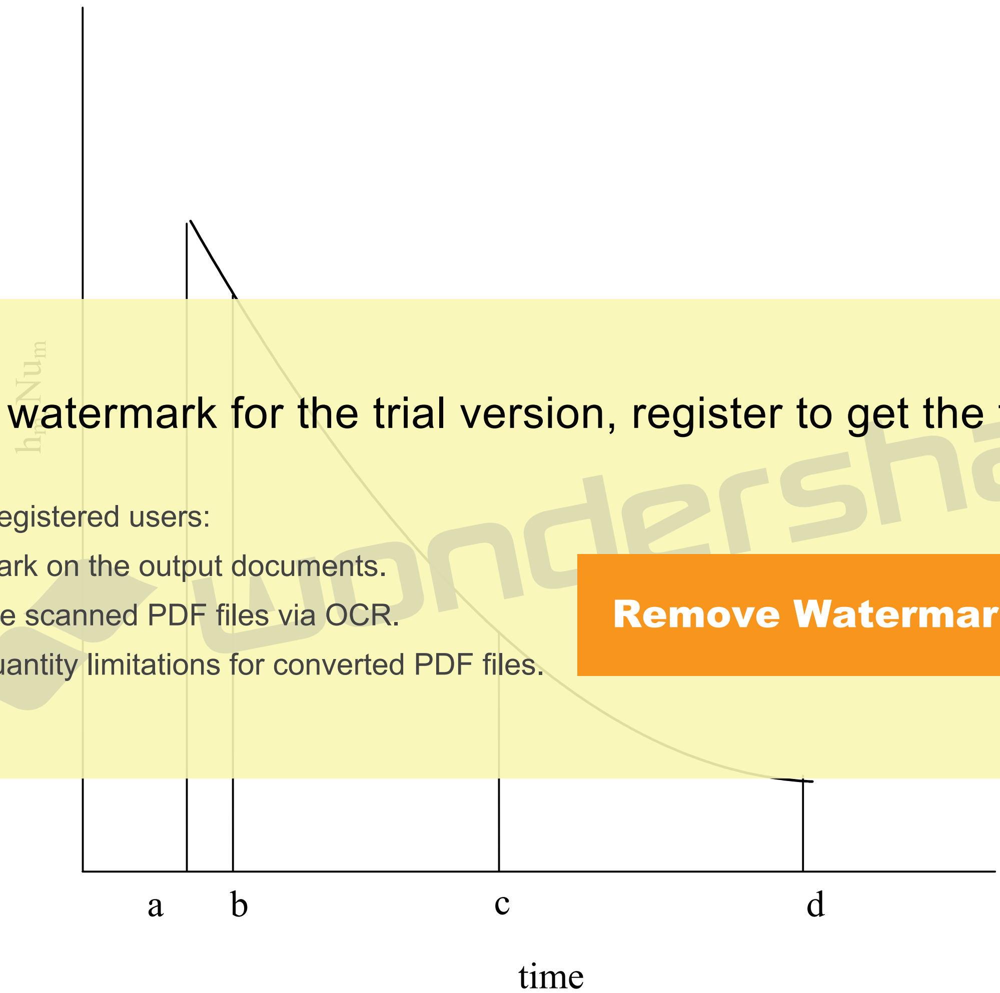

Figure (5.125): General shape of mean heat transfer coefficient and Nusselt number.

5.3.3 Varuation of (h_m) and (Nu_m) with temperature ratio (T/T_{max}).

From each curve in figures (5.64-5.83) , the mean heat transfer coefficient and Nusselt number will be obtained at temperature of 50 c^o, then it is plotted against temperature ratio of (T/T_{max}) shown in figure (5.126-5.127).As mentioned before about the pattern flow on each cylinder position that means the rate of heat transfer will be increased as cylinder position is decreased then the rate of increasing in mean heat transfer coefficient and Nusselt number with temperature ratio of (T/T_{max}) will be increased as cylinder position is decreased. When the temperature difference is decreased depend on convection equation ($q = h\ A\ \Delta T$), the mean heat transfer coefficient and Nusselt number will be increased along the curve in each figures (5.126-5.127) and when the heat capacity of the material of cylinder is increased the mean heat transfer coefficient and Nusselt number will be increased along the curve.

5.3.4 Variation of (h_{are}) and (Nu_{are}) with cylinder position.

The average of heat transfer coefficient and Nusselt number from each Appendix (C-1, C-2, C-3, C-4) will be obtained and it is plotted against cylinder position as shown (5.128-5.129). The average heat transfer coefficient and Nusselt number will be decreased as cylinder position is increased because of the pattern flow on each cylinder that it will be affected on the rate of heat transfer from each cylinder that means, the rate of heat transfer will be decreased as cylinder position is increased then the average heat transfer coefficient and Nusselt number will be decreased as the rate of heat transfer is decreased depend on convection equation ($q=h\ A\ \Delta T$).

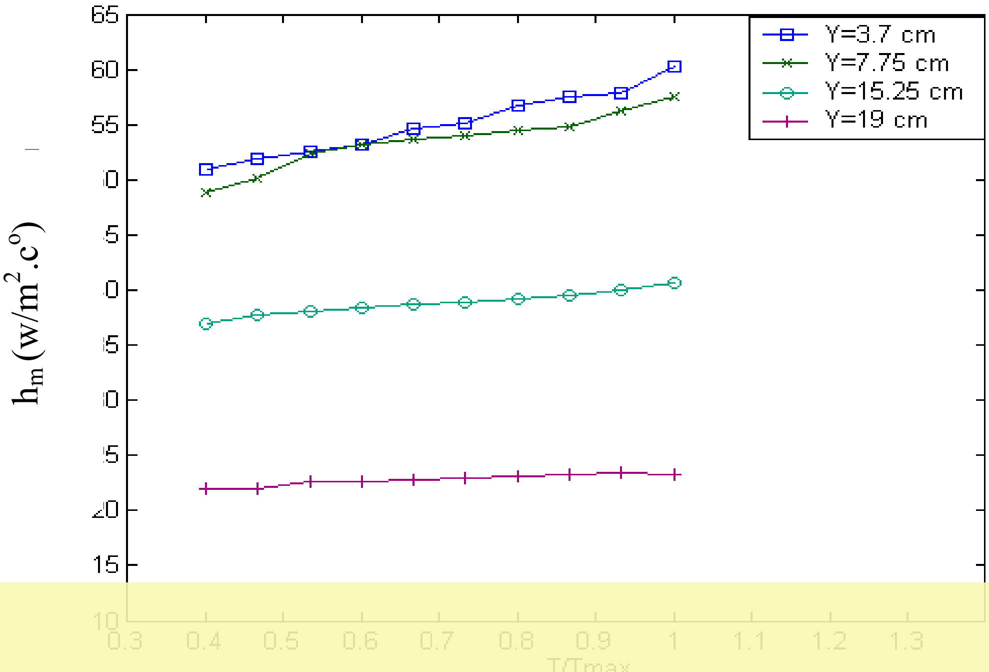

Figure (5.126) the variation of mean heat transfer coefficient at temperature of 50 C^o against temperature ratio of (T/T_{max}).
(T_{max}=150, T=150, 140, 130, 120, 110, 100, 90, 80, 70, 60).

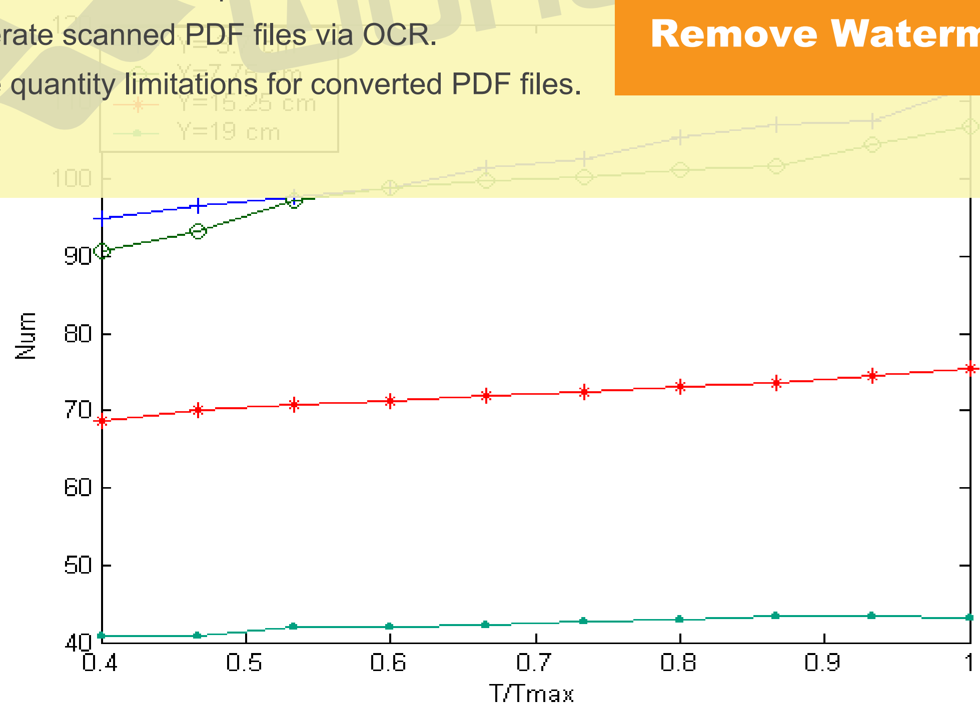

Figure (5.127) the variation of mean Nusselt number at temperature of 50 C^o against temperature ratio of (T/T_{max}).
(T_{max}=150, T=150, 140, 130, 120, 110, 100, 90, 80, 70, 60).

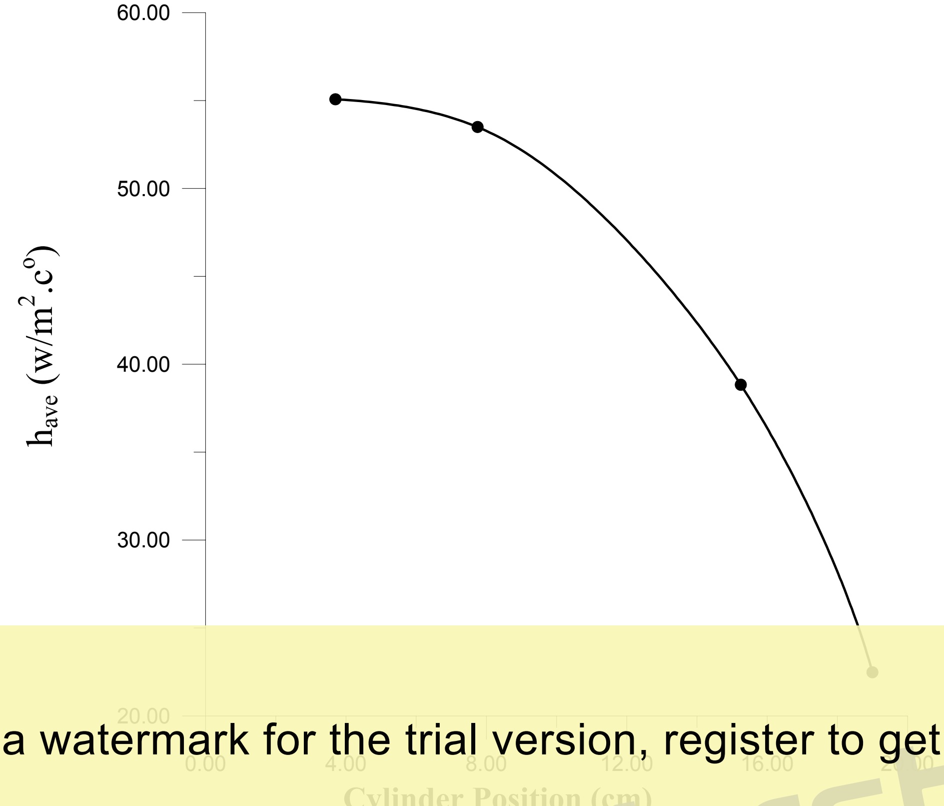

Figure (5.128) the variation of average heat transfer coefficient at temperature

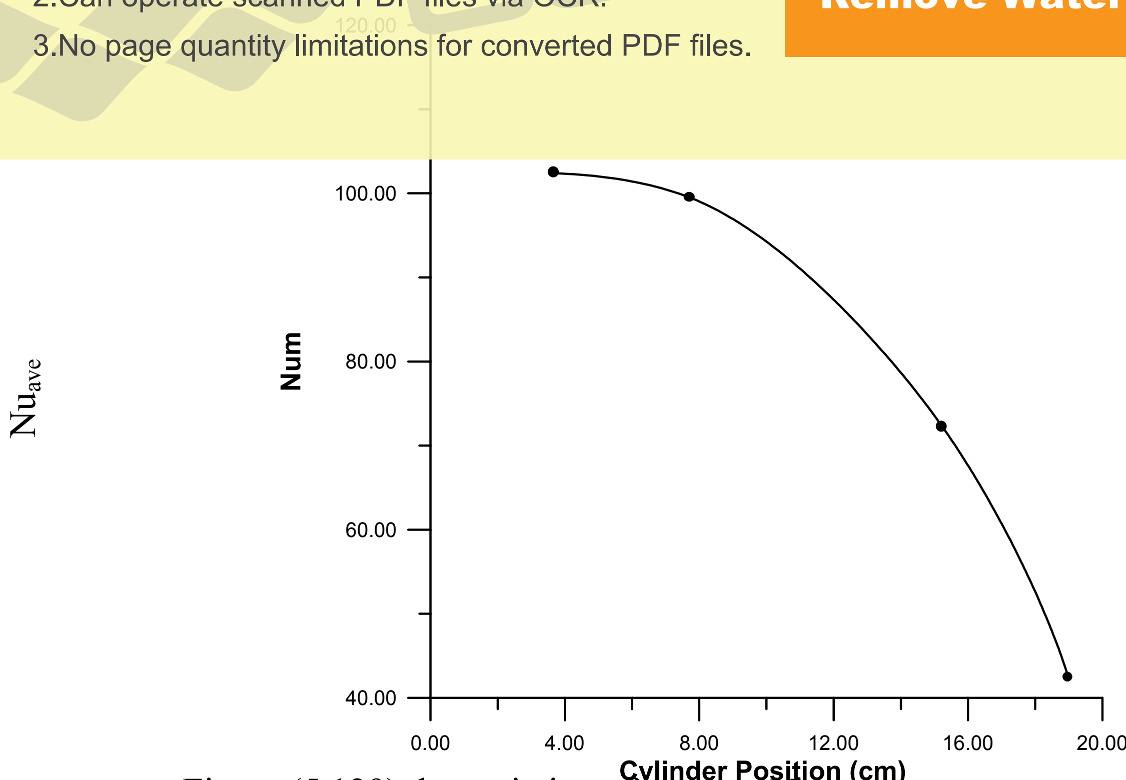

Figure (5.129) the variation of average Nusselt at temperature of 50 C^o from each appendix (C-1, C-2, C-3, C-4) against position of cylinder.

Chapter Six

Conclusions and Recommendations for Future Work

6.1 Conclusions

As results of the experimental investigation carried out to study force convection heat transfer as unsteady state conduction ((i.e. lumped-capacitance system)) from the out side surface of uniformly heated cylinder of 4.96 cm diameter, 6.7 cm length and 5 mm thickness to air in a duct . The following conclusion can be made: -

1. At some reference temperature (T_o =150, 140, 130, 120, 110, 100, 90, 80, 70, 60 C^o), the rate of decreasing in temperature (T) with time interval (t) will be increased as cylinder position [illegible] 15.25, 19 cm) is increased.

2. The rate of increasing in heat tr[illegible] number at [illegible] reference tempera[illegible] [illegible]0, 100, 90, 80, 70, 60 C^o) with time interval (t) will be increased as cylinder position (Y=3.7, 7.75, 15.25, 19 cm) is decreased.
3. At some reference temperature (T_o =150, 140, 130, 120, 110, 100, 90, 80, 70, 60 C^o) and cylinder position (Y=3.7, 7.75, 15.25, 19 cm), the heat transfer coefficient and Nusselt number will be increase with time interval (t) as temperature difference (T-50) is decreased.
4. The surface temperature of cylinder (T) will be decreased with time interval (t) as temperature different (T-50) is decreased.
5. At some cylinder position (Y=3.7, 7.75, 15.25, 19 cm), the rate of decreasing in temperature (T) with time interval (t) will be

increased as reference temperature (T_o =150, 140, 130, 120, 110, 100, 90, 80, 70, 60 C^o) is increased.

6.2 Recommendations for Future Work

During the course of this research, there appear some aspects that can be further developed to enhance this work. The following suggestion could serve as further topics of research with in the same field of this thesis: -

1. The present cylinder in a two-dimensional wind tunnel can be used for testing the effect of different aerodynamics shapes on heat transfer coefficient from cylinder wall by transient conduction, then repeating the experimental procedure of this thesis in order to obtain a well examination.

2. [illegible] cylinder position where the [illegible] streamline of air in duct will be steady in order to obtain a well examination for the parameters which are investigated in the present study.
3. Introducing a new study includes the effects of air velocity in the duct on heat transfer coefficient from cylinder wall, which another parameter will be affected.
4. Introducing a new study includes the effects of another size of cylinder on heat transfer coefficient from cylinder wall, which another parameter will be affected.

References

1. J.P.Hollman, “Heat Transfer”, English edition, McGraw-Hill, 1997.
2. Noor.Y Al-Ubaidy “The effect of adverse pressure on the flow dynamic characteristics and heat transfer coefficient, Nahreen University, 2002.
3. R.S.Khurmi “Fliud Mechanics” 1989.
4. Remn-Min Guo,”Two-Dimensional transient thermal behavior of work rolls in rolling process”,Department of Automation Technology,Ohio.
5. M. Raudenský, M. Pohanka & J. Horsky,”Combined inverse conduction method for highly transient processes”, Bron University of Technology.
6. A. F. Emery, ”Transient and steady state free convection from a horizontal cylinder”, University of [illegible]
7. [illegible] heat transfer [illegible] rod simulation using heaters”, GEAP-13259, January 1972, general Electric Company, and San Jose, California Atomic power Department.
8. Fernando R. Sousa, R.C.S.Freier, G.S.Deep, E.K.Melcher and I.S.S.Silva,”Response time Evulation of constant temperature circuits”, Paris.
9. Donea J.,” On the Accuracy of the Finite Element Solution to the Transient Heat Conduction Equation”, Int.J.Num.Meth.Eng. V8, pp103-110, (1978).
10. Bruch Jr. J. C. & Zyroloski G., “Conduction Problems Solved by Finite Element Method”, Int. J. Num. Meth. Eng., V8, pp481-494, (1974)

11.Sparrow E. m., Haji-Shelikh A. & Lundgren T.S. “The Inverse Problem in Transient Heat Conduction”, J. Appl., Mech., 85E, 369-375, (1964).

12.Imber M. 7 Khan J., “Prediction of Transient Temperature Distribution with Embedded Thermocouples”, AlAA J., v. 10, pp784-789 (1972).

13.Burggraf O.R. “An Exact Solution of the Inverse Problem in Heat Conduction Theory and Applications”, Journal of HEAT transfer, Trans. OF ASME, series C, V. 83, pp 373-381, (1964).

14.Osman A. M. & Beck J. V., “Non-linear Inverse Problem for the Estimation of the Time-and-Space Dependent Heat Transfer Coefficient”, J. Thermo physics & Heat Transfer, 3, pp146-152, (1989).

15.Beck J. V., “Non-linear Estimation Applied to the Non-linear Inverse Heat Conduction Problems”, Int. J. Heat Transfer, 13, 703-716 (1970).

16.Beck J. V., “Function Specification [illegible] Heat Conduction Problems”, a proof paper (1994).

17.Majeed M. H., “Finite Element technique for Heat Transfer problem and Inverse Heat Conduction Problems”, a Ph.D thesis submitted to Baghdad University, 1999.

18.Martin T. J. & Dulikravich G. S., “Inverse Determination of Steady Heat Convection Coefficient distribution”, J. of Heat Transfer, v.120, pp 328-334 (1998).

19.Jafar M.H,”transient heat transfer with phase changes”, FEB thesis submitted to Baghdad University, (1978).

20.Nabras.H.G,”Finite element and boundary element study of conduction heat transfer with special application to the rocket engine shell”, thesis submitted to Baghdad University, (2001).

21.Poots. 1962, “An Approximate Treatment solidification Front”, J.Heat Mass Transfer, Vol. 5, pp. 339-348.

22.Richard T. Beauboueuf and Alan J. Champman, 1967, “Freezing of Fluid in Forced Flow”, J. Heat Mass Transfer, Vol. 10, pp. 1581-1587.

23.K. Stephen, 1969, “Influence of Heat Transfer on Melting and solidification in Forced Flow”, J. Heat Mass Transfer, Vol. 12, pp. 199-214.

24.C. Bekermann and R. Viskanta, “Effect of Solid Sub cooling on Natural Convection Melting of a Pure Metal”, J. Heat Mass Transfer, Vol. 111, pp. 416-424.

25.Nazar.F.A, “Analysis of Multi-Dimensional Transient heat transfer with phase change using B. E. C”, thesis submitted to Technology University,(2001)

26.B. Vick, D. J. Nelson and X. Yu, 1998, “Freezing and melting with Multiple phase Front along t [illegible] Mass Transfer, Vol. 120, pp. 422-4[illegible]

27.Al-Arabi, M.A.Heat transfer data, university of Technology Baghdad, 1977.

28.Ede.A.J.An introduction to heat transfer, London, 1967.

29.Welty.J.R. Engineering heat transfer, John Wiley&Sons, New York, 1974.

30.Arpaci, V. S., “Conduction Heat Transfer”, Addison-Welsley Publishing Co., 1966, pp 336-412.

31.Guo, Remn-Min, “Heat Transfer of a Finite Length Roll Subject to Multiple Zone Cooling and Surface Heating Boundary Conditions”, ASME paper, HTD-Vol. 261, 1993a, pp 9-19

32.Guo, Remn-Min, “Transient Temperature Distribution of Work Rolls Subject to Asymmetric Multiple Zone Cooling”, 5th

International Symposium on Transport Phenomena Dynamics of Rotating Machinery, Mauli, Hawaii, May, 1994b

33. Myers, G. E., “Analytical Methods in Conduction Heat Transfer”, pp122-125

34. Pallone, G. T., "Transient Temperature Distribution in Work Rolls During Hot Rolling of Sheet and Strip", Vol. 60, No. 12, 1983, pp. 21-26

35. Parke, D. M., and Baker, J. L., "Temperature Effects of Cooling Work Rolls", Iron and Steel Eng., vol. 49, 1972, pp 675-680

36. Patula, E. P., "Steady-State Temperature Distribution in a Rotating Roll Subject to Surface Heat Fluxes and Convective Cooling", ASME Journal of Heat Transfer, Vol. 103, pp 36-41, 1981

37. Poplawski, J. V., and Seccombe, D. A., "Mathematical Modeling of Cold Rolling in Tandem Mills", Presented at AISE Annual Convention, Sept. 1979

38. [illegible] J. V., Blackwell, B. & [illegible] Conduction, Wiley, New York, 1985.

39. Raudensk, M. Heat Transfer Coefficient Estimation by Inverse Conduction Algorithm, Int. J. Num. Meth. Heat Fluid Flow, vol 3, pp. 257-266, and 1993.

40. Blanc,G.,Beck,J..,Raynaud,M.,solution of the Inverse Heat Conduction Problem with a Time-Variable Number of Future Temperatures,” Numerical Heat Transfer, B, pp437:451,1997.

41. Attasak Jaree, Peter L. Silveston R Hudgins, Hector Budman and Michael Menzinger,”Temerature response to reactant concentration perturbation in a near-Adiabatic packed-Bed reactor

Configuration of the system used in the experimental work

1. Sets of U-tube manometers.
2. Entrance region (first region).
3. Second region.
4. Diffuser.
5. Main switchboard
6. Control gate valve.
7. Location of test section.
8. Base. Plant.

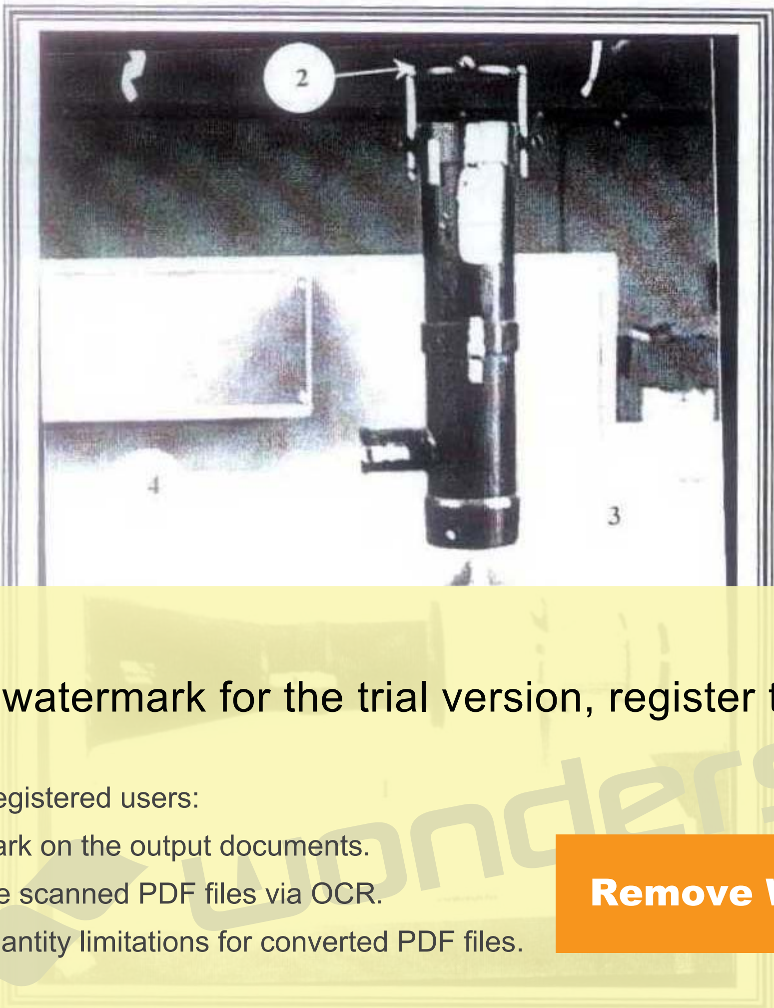

Induced airflow system
1: Centrifugal impeller fan.
2: Control gate valve.
3: Electrical motor
4: Nozzle.

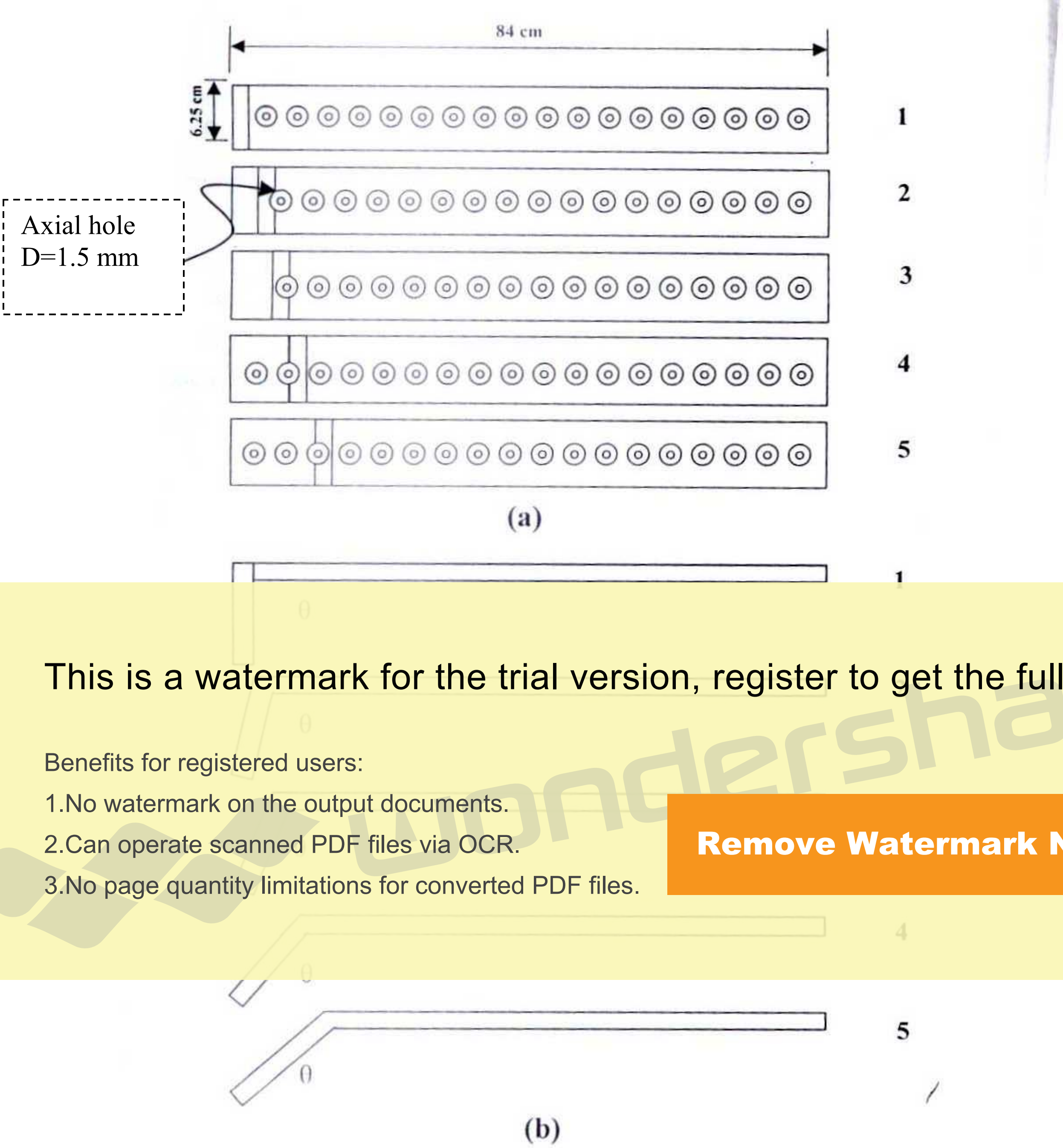

Configuration of five test section; 1) $\theta=90^\circ$ 2) $\theta=75^\circ$ 3) $\theta=60$ 4) $\theta=45^\circ$ 5) $\theta=30^\circ$ a) Top view, b) side View.

Schematic illustration for the experimental system.
((Description for the numbers is shown next page))

A-1

Number	Description
1	Test Rig
2	U-tube-Manometer
3	Scale Board
4	Pitot-tube
5	Control Panel
6	Position of test section
7	[illegible]
8	Cent[illegible]
9	El[illegible]
[illegible]	Control Gate Valve

Table for the Description of the number

4.4 Calibration of Thermocouples

The thermocouples were calibrated against the melting point of ice made from distilled water and the boiling points of the following four substances:-

1. Aceton (CH_3 Co CH_3) BP=56.5 C
2. Ethanol (C_2 H_5 OH) BP=78.5 C
3. Distilled water (H_2O) BP=100 C
4. Naphtaline ($C_{10}H_8$) BP=217.96 C

A schematic diagram of the apparatus used for the calibration is shown in fig (4.4). It consists essentially of a glass flask which contains the boiling substance and a glass tube in which the th [illegible]. The vapor in the space between the flask and th [illegible] the vapor in the glass tube.

The same potentiometer used with the main experiments was also used in the calibration experiments.

The results of calibration are listed in table (4-3), the calibration curve is shown in fig (4.5).

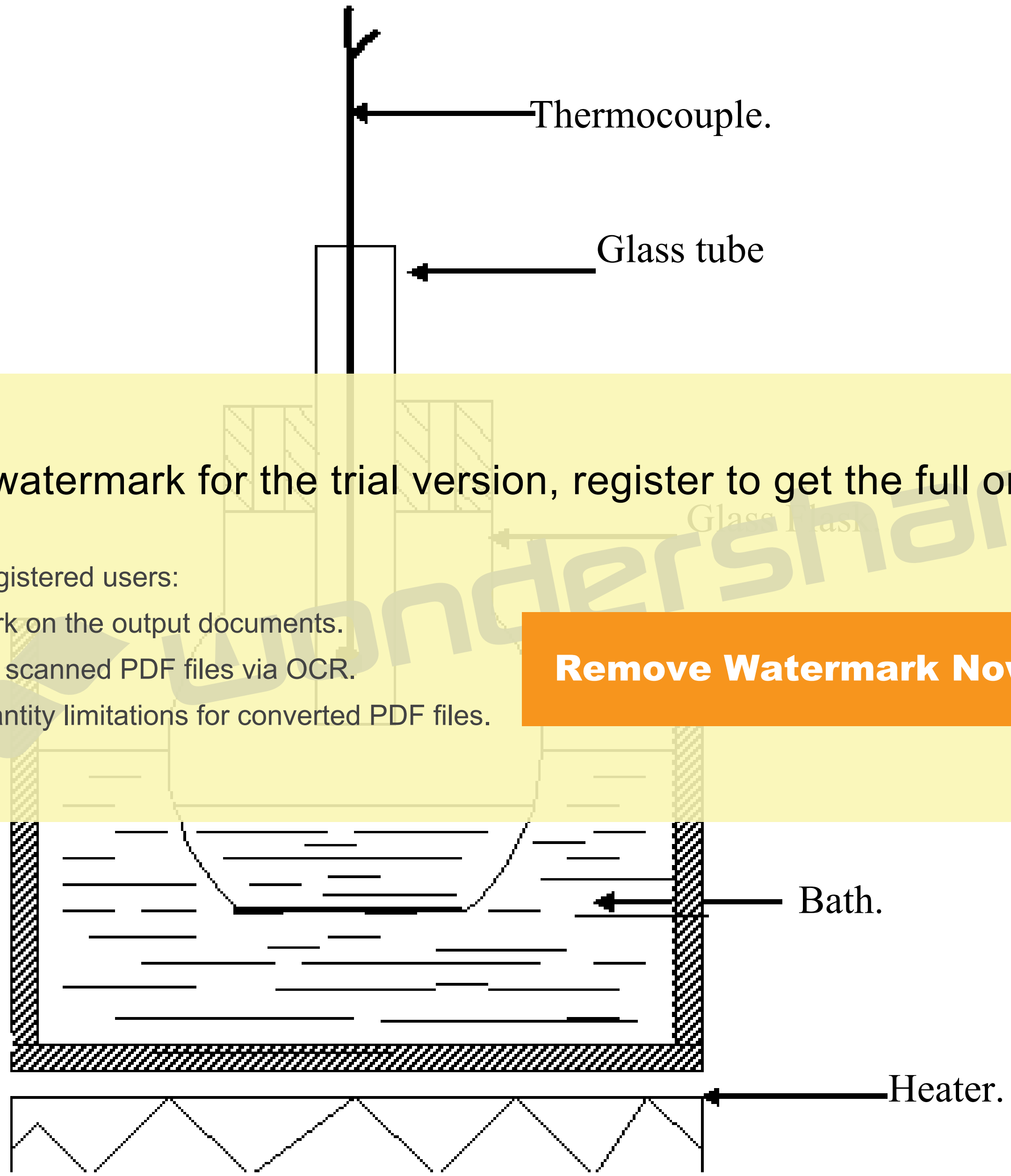

Fig (4.4) Thermocouples Calibration Apparatus.

Table (4.3) Results of thermocouples calibration

Substance	Boiling (C)	e.m.f. (mV)
Aceton	56.5	2.5
Ethanol	78.5	3.38
Distilled water	100	4.275
Nephtaline	217.96	10.15

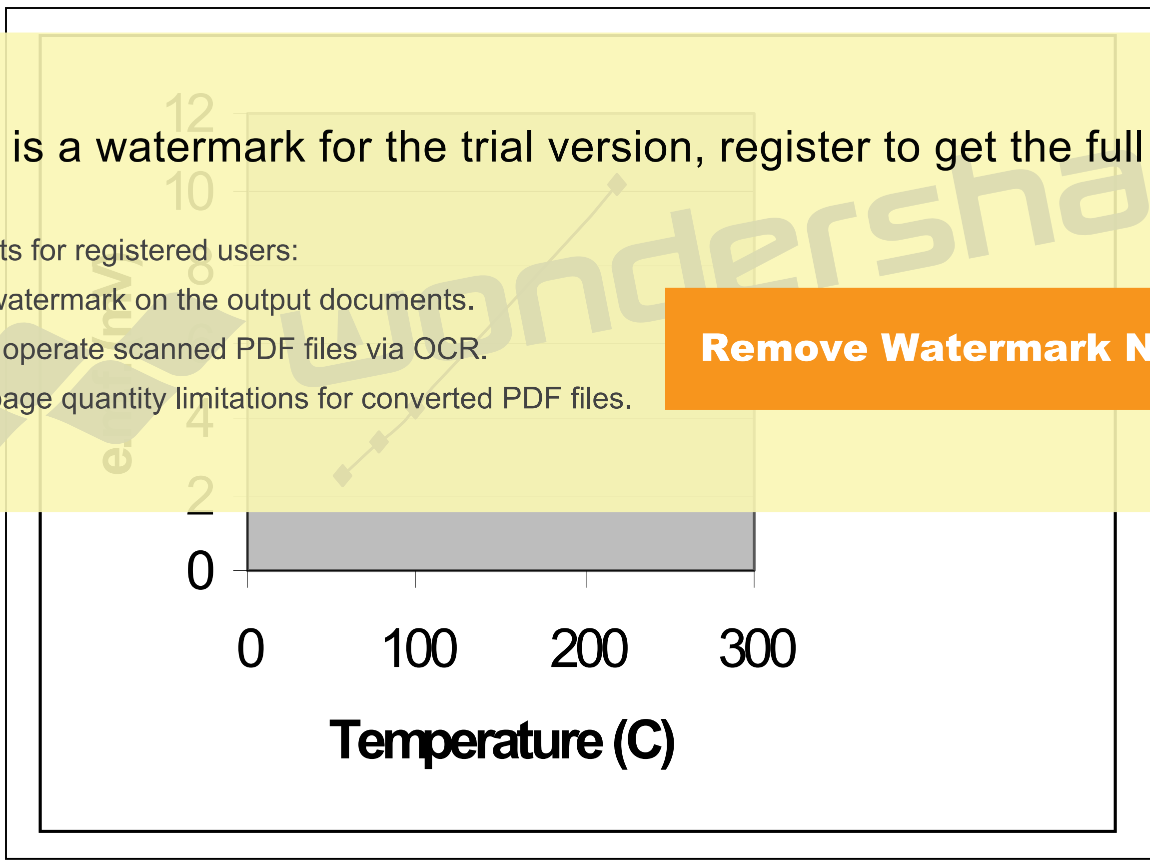

Fig (4.5) Thermocouples Calibration curve

Contents

Nomenclature

Symbol	Definition	Units
A	Surface area	m^2
Bi	Biot number	-
c	Specific heat of cylinder	kJ/kg.c^o
d	Diameter of thermocouple position	m
D_{in}	Inside diameter of cylinder	m
D_o	Outside diameter of cylinder	m
E_{in}	Internal energy	W
E_{stored}	Stored energy	W
Fo	Forier number	-
h	Heat transfer coefficient	w/m2.co
h_{ave}	Average heat transfer coefficient	w/m2.co
h_{local}	Local heat transfer coefficient	w/m2.co
h_m	Mean heat transfer coefficient	[illegible]
K	Conductivity of cylinder	w/m.c
L	Cylinder length	M
[illegible]	[illegible] the cylinder [illegible]	[illegible]
[illegible]	Nusselt nu[illegible]	[illegible]
Nu_{ave}	Average Nusse[illegible]	[illegible]
Nu_{local}	Local Nusselt number	-
Nu_m	Mean Nusselt number	-
q	Rate of heat	W
t	Time	s
T	Attainting temperature	c^o
T_∞	Air temperature	c^o
t_c	Thickness of cylinder	m
T_{max}	Maximum temperature	c^o
t_{max}	Maximum time	s
$\mathbf{T_o}$	Initial temperature	$\mathbf{c^o}$
T_s	Surface temperature	c^o
u_∞	Air velocity	m/s
V	Cylinder Volume	m^3
Y	Cylinder position	cm

ϑ	Angle of thermocouple position	Degree
τ	Time constant	-
α	Thermal diffusivity	m^2/s
θ	Attainting temperature difference $(T\text{-}T_\infty)$	c^o
θ_o	Initial temperature difference $(T_o\text{-}T_\infty)$	c^o
ρ	Density of cylinder	Kg/m^3
ℓ	Depth of thermocouple position in cylinder	mm
ρ_∞	Air density	Kg/m^3

APPENDIX (A)

Configuration of the system used in the experimental

APPENDIX G

Material and Ai